Double parton scattering
- a tale of two partons

Dissertation zur Erlangung des Doktorgrades
des Department Physik der Universität Hamburg

vorgelegt von

Tomas Kasemets

aus *Solna, Sweden*

Hamburg
2013

Gutachter der Dissertation:	Dr. Markus Diehl
	Prof. Dr. Sven-Olaf Moch
Gutachter der Disputation:	Dr. Markus Diehl
	Prof. Dr. Joachim Bartels
Datum der Disputation:	12. Juni 2013
Vorsitzender des Prüfungsausschusses:	Prof. Dr. Günter Sigl
Vorsitzender des Promotionsausschusses:	Prof. Dr. Peter Hauschildt
Dekan der Fakultät für Mathematik, Informatik und Naturwissenschaften:	Prof. Dr. Heinrich Graener

A joy that is shared, is a joy made double

Abstract

Double parton scattering in proton-proton collisions can give sizable contributions to final states in parts of phase space. We investigate the correlations between the partons participating in the two hard interactions of double parton scattering. With a detailed calculation of the differential cross section for the double Drell-Yan process we demonstrate how initial state correlations between the partons affect the rate and distribution of final state particles. We present our results with focus on correlations between the polarizations of the partons. In particular transversely polarized quarks lead to a dependence of the cross section on angles between final state particles of the two hard interactions, and thereby on the invariant mass of particle pairs. The size of the spin correlations, and therewith the degree to which the final state particles are correlated, depends on unknown double parton distributions. We derive positivity bounds on the double parton distributions that follow from their interpretation as probability densities, taking into account all possible spin correlations between two partons in an unpolarized proton. We show that the bounds are stable under homogeneous leading-order DGLAP evolution to higher scales. We make direct use of the positivity bounds in numerical investigations on the double DGLAP evolution for two linearly polarized gluons and for two transversely polarized quarks. We find that the linearly polarized gluons are likely to be negligible at high scales but that transversely polarized quarks can still play a significant role. We examine the dependence of the double parton distributions on the transverse distance between the two partons, and therewith between the two hard interactions. We further study the interplay between transverse and longitudinal variables of the distributions, as well as the impact of the differences in integration limits between the evolution equations for single and double parton distributions.

vi

Zusammenfassung

Der Mechanismus der Doppel-Parton Streuung in Proton-Proton Kollisionen kann zu großen Beiträgen zu den Endzuständen in Teilen des Phasenraums führen. Wir untersuchen die Korrelationen zwischen den an den harten Streuprozessen teilnehmenden Partonen der Doppel-Partonen Streuung. Mit einer ausführlichen Berechnung des differentiellen Wirkungsquerschnitts des Doppel-Drell-Yan-Prozess zeigen wir, wie die Korrelationen zwischen den Anfangszuständen der Partonen die Ereignistate und Verteilung der Teilchen im Endzustand beeinflussen. Wir präsentieren unsere Ergebnisse mit Schwerpunkt auf Korrelationen zwischen den Polarisationen der Partonen. Insbesondere Quarks mit transversaler Polarisation führen zu einer Abhängigkeit des Wirkungsquerschnitts von den Winkeln zwischen den Teilchen im Endzustand und damit von der invarianten Masse der Teilchenpaare. Die Größe der Spinkorrelationen, und damit das Ausmaß mit dem die Teilchen im Endzustand korreliert sind, ist abhängig von den unbekannten Doppel-Partonverteilungsfunktionen. Wir leiten Positivitätsgrenzen an die Doppel-Partonverteilungsfunktionen her aus deren Wahrscheinlichkeitsinterpretation, wobei wir alle möglichen Spinkorrelationen zwischen zwei Partonen in einem unpolarisierten Proton berücksichtigen. Wir zeigen, dass die Grenzen stabil unter der DGLAP Evolution führender Ordnung zu höheren Skalen sind. Wir benutzen die Positivitätsgrenzen daraufhin in der numerischen Untersuchung der Doppel-DGLAP Evolution für zwei linear polarisierte Gluonen und für zwei transversal polarisierte Quarks. Wir finden, dass die linear polarisierten Gluonen vermutlich bei hohen Skalen vernachlässbar sind, aber dass die transversal polarisierten Quarks noch eine signifikante Rolle spielen können. Wir untersuchen die Abhängigkeit der Doppel-Partonverteilungsfunktionen vom transversalen Abstand zwischen den zwei Partonen, und damit von Abstand zwischen den zwei harten Streuprozessen. Wir studieren das Zusammenspiel zwischen den longitudinalen und transversalen Variablen in den Verteilungen und den Einfluss des Unterschieds der Integrationsgrenzen zwischen den Evolutionsgleichungen für Einzel- und Doppel-Partonverteilungen.

Acknowledgements

For the opportunity to work with him, for always taking the time to explain and point me in the right direction, for teaching me the required patience and precision, I want to thank my supervisor Markus Diehl. I further want to thank Joachim Bartels for his guidance in the beginning of my time as a PhD. I am thankful to Torbjörn Sjöstrand for introducing me to research in high-energy particle physics, to Andreas Schäfer for useful discussions towards the end of my PhD and to Daniel Boer for early correspondence. I am grateful to Aoife Bharucha, Jonathan Gaunt and Lisa Zeune for useful discussions and feedback on the manuscript.

For her support and for putting up with me I want to thank my office mate during all my three years at DESY, Julia Harz. For interesting and useful discussions I want to thank Andreas Goudelis, Frank Tackmann and Simon Plätzer, Oscar Stål and Moritz McGarrie. I am thankful to the theory group for the inspiring atmosphere and in particular to the rest of building 1b.

I want to thank my close friends Andreas, Nicklas and Victor for all the good stuff over the years, and the players in the floorball team for taking my mind off physics. I want to thank my family; my parents Sten and Marianne, my sister Sanne, my brothers Jonathan and Daniel for making me who I am. Finally I want to thank Lisa for making life great.

Contents

Chapter 1

Introduction

Matter, as we know it from everyday life, mainly consists of protons, neutrons and electrons. Out of these, only the electrons are believed to be fundamental particles, particles without substructure. Protons and neutrons have since the seventies been known to consist of quarks, antiquarks and gluons - collectively dubbed partons. All of the partons carry color, the quantum number of the strong interaction. The strong force keeps the colored partons bound in color neutral hadrons - such as protons and neutrons. The quantum dynamics of the colored particles are described by the theory of the strong interaction, Quantum Chromodynamics (QCD).

What distinguishes the strong interaction from the other fundamental forces, is that its strength increases with distance. Increasing the strength of an interaction is synonymous to increasing its coupling, and at large distances the coupling of QCD grows. The growth with distance provides a major challenge for theorists and experimentalists alike, since the partons cannot be studied on their own but only in color neutral bound states. The size of the coupling at large distances prevents us from using the powerful method of perturbative QCD - which is based on an expansion in the small coupling constant. In high energy collisions, theorists are saved by the reverse phenomena. At small distances the coupling constant of QCD decreases. Since the length scale probed is inversely proportional to the energy of the probe, small distances are equivalent to high energies and we can treat the partons as approximately free particles.

This already suggests a way to treat high-energy proton-proton collisions. The high-energy interaction between one parton in each proton is factorized from the low-energy physics binding partons inside each proton. To formalize such a factorization has proven to be one of the greatest challenges in theoretical particle physics, and for many processes, calculations are based on the assumption that the factorization holds at least approximately. The strategy is to construct experiments to measure the universal low-energy description of protons, so called parton distribution functions, and combine them with calculations of the hard interactions to predict the outcome of new experimental studies. These can in turn be used to further improve the measurement of the parton distributions and the loop is closed.

At hadron colliders the treatment of QCD affects everything. In attempts to find new particles, even ones whose creation is described by the electroweak interaction,

the treatment of the proton in the initial state, the underlying event, final and initial state interactions are all dominated by QCD. Therefore, in the era of the LHC, a thorough understanding of the strong-interaction in proton-proton collisions is indispensable. While the dynamics of the strong-interaction is moving towards the domain of precision physics, there are still aspects that are under poor theoretical and experimental control. One such aspect is multiparton interactions, processes where in a single proton-proton collision more than one parton in each proton take part in a hard scattering. Multiparton interactions can give significant contributions to both signal and background processes, such as Higgs production [1], electroweak processes [2–10], multijet production [11–18] and SUSY searches [19]. Resent studies have demonstrated an enhancement of double parton scattering in proton-nucleus and nucleus-nucleus collisions [20, 21]. The concept of multiparton interactions has close connections to Monte-Carlo generators and substantial efforts has been made in modeling and implementing them [22–28]. A mini-review on earlier developments is given in [25], and an overview of current developments is given in the conference proceedings [29, 30].

The concept of multiparton interactions is easy: when two protons collide, two showers of partons pass by each other. If two of the partons in the showers can have a hard interaction with one another, then why not two additional ones, or yet another two, or more. And although the theory for describing such effects is well known (QCD), the development of a systematic treatment within QCD is far from mature.

The simplest realization of multiparton interactions is double parton scattering, when in a single proton-proton collision, two partons from each proton participate in separate hard interactions. Double parton scattering holds the answer to fundamental questions about the nature of the proton, in particular on correlations between its constituents. Experimental evidence for double parton scattering was first found at the ISR [31], followed by measurements at the SPS [32] and the Tevatron [33–37].

Due to the rapid increase of the partonic densities at small momentum fractions, one expects double and multiparton interactions to become increasingly relevant with collider energy, and thus be more prominent at the LHC than ever before. First results have indeed been reported [38,39], with more studies expected in the future [40]. The expected increase has inspired an upsurge in interest to understand the theoretical foundations of multiple hard scatterings [41–51], and many issues still need to be clarified or worked out.

The simplest possible approach to double parton scattering, is to assume that there are no correlations between the two partons. This leads to easy and compact results, but the validity of such an approach is certainly not to be taken for granted. The range of validity as well as the limitations need to be investigated. In this spirit, several recent studies on the correlations between the two hard interactions have been conducted [17,27,52–57]. Alternatively, one can approach double parton scattering via a systematic treatment in QCD. Significant progress towards a complete QCD description has recently been made [44,50], with proper treatment of the different correlation effects.

The two approaches have different strengths and weaknesses. Therefore, they are both important and can provide complementary information. Whilst the simple treat-

ment allows for quick predictions that can be tested against experimental result, it suffers from a lack of reliability and even the possibility of oversimplification - pointing experimentalists in the wrong direction when searching for DPS signals. The second approach, with a rigorous treatment of double parton scattering in QCD, instead suffers from theoretical difficulties making it hard to make quantitative predictions and thus lacking in contact with the experimental reality.

The present thesis aims at taking the treatment of double parton scattering in perturbative QCD closer to being able to make experimental and testable predictions. We focus on the correlations between the two partons and their observable consequences - in particular due to their *polarization*.

The structure of the thesis is as follows. In chapter 2 we briefly remind the reader of the essentials of QCD, particularly emphasizing aspects that will be of importance in the following, and give references where those interested can find a detailed background to the topic. Thereafter, the focus will be on the theoretical description of double parton scattering. Starting from a tree level description, we introduce the concepts of double parton distributions (DPDs) - describing the distribution of two partons inside the proton. We derive an expression for the cross section in terms of partonic cross sections, encoding the hard interaction between the colliding partons, and the double parton distributions. We further summarize some important parts of the theory of double parton scattering beyond the tree level treatment, and give account of some model calculations of DPDs as well as the experimental status of double parton scattering.

In chapter 3, we investigate the double Drell-Yan process, where two electroweak gauge bosons are produced in two independent quark-antiquark annihilation processes. We calculate the cross section and present our results with particular attention to how correlations between the initial state partons propagate into observable consequences at the level of the double parton cross section.

The size of the correlation effects depends on unknown double parton distributions which are the focus in chapter 4. We construct spin-density matrices for all combinations of partons, revealing the entire helicity structure of two partons in an unpolarized proton and put constraints on the polarized distributions from a probability interpretation. We show that these bounds are stable under leading order double DGLAP evolution.

In chapter 5 we investigate the numerical impact of double DGLAP evolution on double parton distributions. We examine how the evolution affects a Gaussian ansatz for the transverse distance dependence of the DPDs and the rate at which evolution leads to a convergence between the transverse dependencies of different parton spices. We investigate the impact of evolution on the importance of linearly polarized gluons and transversely polarized quarks, and study the impact of the integration limit differences between the single and double parton evolution equations. In a simple model of the proton we study the interplay between transverse position and longitudinal momentum fractions of the two partons.

The results in chapter 3 have been published in [58] but we expand them here, providing additional details and explanations. The bulk of chapter 4 was published in [59] but further details have been added. Chapter 5 mainly contains new, previously

unpublished results, with the exception of section 5.6 which was published in [58].

The figures in this thesis were produced with JaxoDraw [60] and Matplotlib [61], parts of the calculations were done with FORM [62] and Mathematica [63].

Chapter 2

Theory of double parton scattering

2.1 QCD and single parton scattering

Before diving into the theory of double parton scattering, let us dwell for a moment on some features of QCD and single parton scattering which will play important roles in the rest of the thesis. For a more thorough introduction to the topic see for example [64], and for a more in depth treatment see [65].

QCD describes the interactions of the colored particles, i.e. quarks, antiquarks and gluons. It is a so called standard non-Abelian Yang-Mills theory with gauge group SU(3) [65]. The quarks (antiquarks) transform under the fundamental (anti-fundamental) representation while the gluons transform under the adjoint representation. The quark field $\psi_{\alpha j f}$ carry three indices, a Dirac index α, a color index j which takes three values and a flavor index f. The gluon field A_μ^a carries a Lorentz vector index μ and a color index a which takes eight different values, for the eight generators of the gauge group.

As discussed already in the introduction, key features of the strong force are confinement of colored particles inside hadrons and asymptotic freedom of the partons at high energies. Both are related to the negative sign of the β-function in QCD

$$\beta(\alpha_s) = -\frac{11C_A - 2n_f}{12\pi}\alpha_s^2 + \mathcal{O}(\alpha_s^3) , \tag{2.1}$$

describing the evolution of the strong coupling α_s with the energy scale μ

$$\frac{\partial}{\partial \log \mu^2}\alpha_s = \beta(\alpha_s), \tag{2.2}$$

and thus of the strength of QCD. $C_A = N_c = 3$ where N_c is the number of colors of QCD and n_f is the number of active quark flavors. Note that this expression for the β function loses its accuracy when the coupling gets large at long distances (low energies) and is hence at most an indication of confinement.

The property of asymptotic freedom is essential for the connection between QCD and the parton model - in which the partons are treated as free particles - and its success in describing high energy collisions. In the parton model the collision between two protons

(a)   (b)
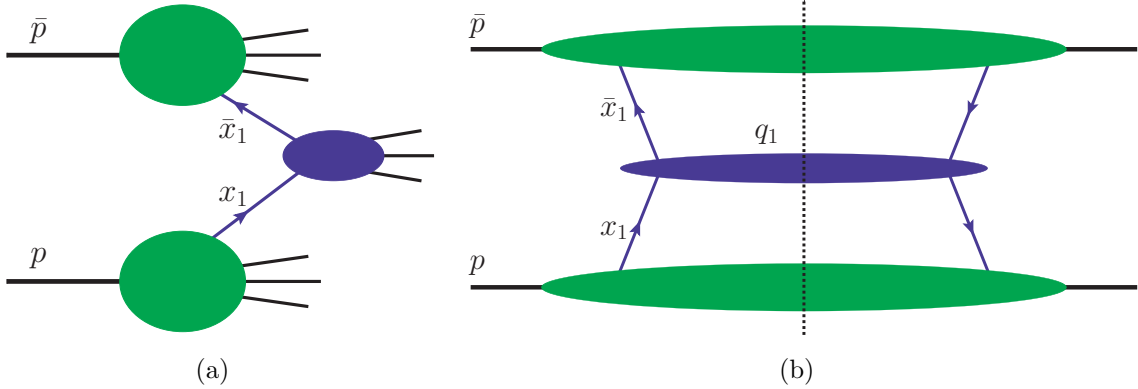
Figure 2.1: Illustration of single parton scattering (a) and a diagrammatic representation of the single parton cross section (b). The dotted vertical line denotes the final state cut.

is viewed as a passing of two bunches of free partons. Most of the partons in each bunch pass by without noticing the presence of the other, but one parton from each bunch collide. The cross section can then be calculated from the cross section of the partonic interaction, times a probability of finding the interacting partons inside their parent protons.

Let us now make the factorization of long and short distance scales in the calculation of scattering cross sections quantitative. Consider the two proton scattering graph in figure 2.1(a) where two partons with momentum fractions x_1 and $\bar{x}_1$ interact in one hard interaction. Completing this picture with the complex conjugated amplitude, figure 2.1(b) represents the cross section which can be expressed as

$$\sigma = \sum_{ij} \int dx_1 \int d\bar{x}_1 f_i(x_1) f_j(\bar{x}_1) \hat{\sigma}_{ij}. \tag{2.3}$$

The short distance, high energy part of the interaction between the two partons i and j is given by the partonic cross section $\hat{\sigma}_{ij}$. In the parton model, the functions f_i describe the probability of finding parton i with a fraction x_1 of the longitudinal momentum of the proton. In full QCD however, the probability interpretation is complicated by renormalization. The factorization of hard and soft parts in (2.3) is a highly non-trivial task in a complete treatment of QCD. It requires taking care of the exchange of additional particles, in particular the exchange of collinear and soft gluons [65]. It has strictly only been demonstrated for hard processes producing color neutral states, such as gauge bosons (γ, Z, $W^{\pm}$) and Higgs bosons. The factorization of hard and soft parts takes place at a scale μ. The hard cross section as well as the parton distribution functions thereby develop a dependence on the factorization scale:

$$f_i(x) \rightarrow f_i(x; \mu). \tag{2.4}$$

A natural choice of the factorization scale in a cross section calculation is the scale of the hard interaction Q. The change of f_i with μ is described by the DGLAP evolution

equations [66–69], which for the parton distribution of a single quark reads

$$\frac{\partial}{\partial \log \mu^2} f_q(x, \mu) = \frac{\alpha_s}{2\pi} \int_x^1 \frac{d\xi}{\xi} \left[P_{qq}\left(\frac{x}{\xi}\right) f_q(\xi, \mu) + P_{qg}\left(\frac{x}{\xi}\right) f_g(\xi, \mu) \right]. \qquad (2.5)$$

P_{qq} and P_{qg} are the Altarelli-Parisi splitting kernels [66], given in appendix B, respectively describing a quark radiating off a gluon and the transition of a gluon into a quark by radiating an antiquark. The factorization formula (2.3) can be generalized to the case when the transverse momentum of the hard interaction $\boldsymbol{q}_1$ is measured:

$$\frac{d\sigma}{dx_1 d\bar{x}_1 d^2\boldsymbol{q}_1} = \sum_{ij} \int d^2\boldsymbol{k}_1 d^2\bar{\boldsymbol{k}}_1 \delta^{(2)}(\boldsymbol{q}_1 - \boldsymbol{k}_1 - \bar{\boldsymbol{k}}_1) f_i(x_1, \boldsymbol{k}_1) f_j(\bar{x}_1, \bar{\boldsymbol{k}}_1) \hat{\sigma}_{ij}. \qquad (2.6)$$

The parton distribution functions $f_i(x_1)$ have been promoted to transverse momentum distributions $f_i(x_1, \boldsymbol{k}_1)$, where $\boldsymbol{k}_1$ ($\bar{\boldsymbol{k}}_1$) is the transverse momentum of parton i (j). The two functions require different regularization and subtractions of divergences and therefore depend in different ways on an renormalization scale and a rapidity parameter, polluting a simple relationship between them. In addition, depending on the definition used for the transverse momentum dependent distributions, (2.6) might have to be complemented by a soft factor [65]. It should also be mentioned that for transverse momentum dependent factorization in proton-proton collisions with jets in the final state, issues has been identified [70].

2.2 Introduction to DPS

Analogously to the separation of the single parton cross section we want to decompose the cross section of double parton scattering into different pieces describing the long and short distance physics, as illustrated in figure 2.2(a). An intuitive generalization of (2.3) would be a separation into two hard partonic cross sections and two functions describing the distributions of two partons inside each proton depending on the longitudinal momentum fractions of both partons, x_1 and x_2. However, the two colliding partons in each hard interaction have to be at the same transverse position and a closer examination reveals the additional dependence of the double parton distributions on the vector $\boldsymbol{y}$ between the two hard collisions, as illustrated in figure 2.2(b). We can then write the double parton cross section as

$$\sigma_{DPS} \sim \sum_{ijkl} \int dx_1 dx_2 \int d\bar{x}_1 d\bar{x}_2 \int d^2\boldsymbol{y} \, f_{ij}(x_1, x_2, \boldsymbol{y}) f_{kl}(\bar{x}_1, \bar{x}_2, \boldsymbol{y}) \hat{\sigma}_{ik} \hat{\sigma}_{jl}. \qquad (2.7)$$

However, this formula needs to be modified due to correlations between the two partons in the same hadron, leading to several features not present in single parton scattering. In the next section we will derive a cross section formula at leading order for double parton scattering taking these correlations into account. Here we will continue our less formal but more intuitive discussion of double parton scattering and the different correlation effects.
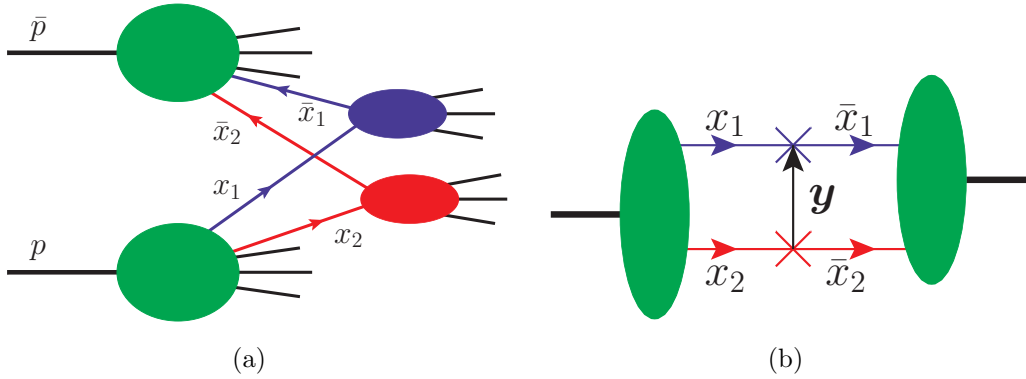
Figure 2.2: Illustration of double parton scattering (a) and geometrical interpretation of $\boldsymbol{y}$ as the vector between the two interactions points (b).

In single parton scattering, the momentum and quantum numbers of an interacting parton in the amplitude have to be equal to those of its partner in the conjugate amplitude. In double parton scattering the situation is different: Only the sum over the two partons in the amplitude has to be equal to the sum in the conjugate amplitude. This allows for a difference in momentum between a parton in the amplitude and its partner in the conjugate amplitude. The imbalance in one of the hard interactions has to be compensated by the partons in the other interaction. In transverse position, this results in the dependence of the double parton distributions on the distance $\boldsymbol{y}$ between the two hard interactions. Further, the color of the partons can either, as in single parton scattering, be balanced inside each hard interaction, or as an interference effect between them. In the same spirit, there can be interference in parton flavor (between for example up- and down-type quarks), in fermion number (between quarks and antiquarks) and for processes with color in the final state also in parton type (between quarks and gluons). In addition, the two partons with the same parent proton can have correlated polarizations. All these effects combine into a bewildering number of different double parton distributions. Although as we will see, not all of them have to be taken into account at all times.

In the remainder of this chapter we will review parts of the theory developed for double parton scattering. We start with a tree level analysis in section 2.3, deriving the double parton cross section in terms of double parton distributions. This will be done taking proper care of the different correlation effects between the quantum numbers of the partons - described by the correlation functions for two partons in a proton and resulting in a multitude of different double parton distributions. Thereafter we discuss some of the properties which go beyond the leading order analysis in section 2.4, such as the evolution of the double parton distributions, Sudakov logarithms and the status of factorization. Finally we summarize some recent studies modeling the double parton distribution and review the experimental status of double parton scattering.

2.3   Tree level analysis

We now derive a double parton scattering cross section formula in terms of hard partonic cross sections and double parton distributions. The derivation closely follows [44] and we try to keep the notation as similar as possible. We choose, however, to directly consider quarks and antiquarks rather than scalar partons. In the process we will explicitly treat the different types of correlations and interferences possible in double parton scattering. The aim and final outcome of this derivation is (2.59).

Here as well as in remaining parts of the thesis we use light-cone coordinates, with plus and minus components of a vector v equal to $v^{\pm} = (v^0 \pm v^3)/\sqrt{2}$ and bold font indicating a transverse vector $\boldsymbol{v} = (v^1, v^2)$. We work in a reference frame where the proton with momentum p ($\bar{p}$) moves fast to the right (left), and the transverse momenta of the protons are zero $\boldsymbol{p} = \bar{\boldsymbol{p}} = 0$. We consider the case where the scale of the two hard interactions q_i^2 are large compared to their transverse momentum $|\boldsymbol{q}_i|$, and neglect the mass of the proton. For simplicity, we do not assume any specific hierarchy between the two scales, $q_1^2 \sim q_2^2 \sim Q^2$. The center of mass energy of the proton collision is

$$s = (p + \bar{p})^2 \approx 2p\bar{p} = 2p^+\bar{p}^-. \tag{2.8}$$

We define the longitudinal momentum fractions $x_i = q_i^+/p^+$ for the partons in the right moving proton and $\bar{x}_i = q_i^-/\bar{p}_i^-$ for the partons in the left moving proton. These are related to the square of the hard momenta and the rapidity as

$$q_i^2 \approx 2q_i^+ q_i^- \approx x_i \bar{x}_i s \,, \qquad\qquad Y_i = \tfrac{1}{2} \log \frac{q_i^+}{q_i^-} = \tfrac{1}{2} \log \frac{x_i \bar{p}^-}{\bar{x}_i p^+}. \tag{2.9}$$

Typical momentum fractions for processes at the 8 TeV LHC are, $x_1 = \bar{x}_1 \approx 0.011$ for the production of a Z boson at $Q = 91$ GeV with zero rapidity. If the Z boson is instead produced with $Y = 2.0$, the momentum fractions are $x_1 \approx 0.084$ and $\bar{x}_1 \approx 0.0015$. For the production of a Higgs boson with zero rapidity at $Q = 125$ GeV the longitudinal momentum fractions are $x_1 = \bar{x}_1 \approx 0.016$.

2.3.1   Double parton cross section

We consider the double parton scattering in figure 2.3, where two quarks from the right moving proton interact with two anti-quarks from the left moving proton in two separate hard interactions. For the full double parton cross section, also the graphs where one or both anti-quarks come from the right moving proton must be included.

The momentum variables are defined as in figure 2.3. Barred labels refer to quantities associated with the left moving proton and primed labels to quantities in the conjugate amplitude. In this section, we will keep the indices for the quantum numbers of the quark and antiquark fields implicit and restore them in section 2.3.2. The double parton
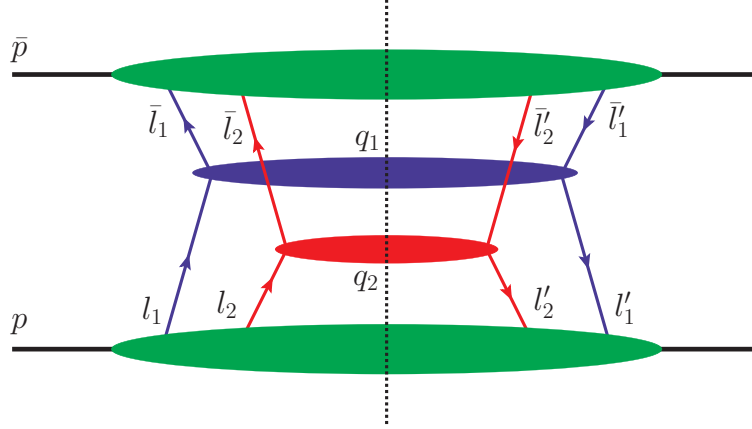
Figure 2.3: A graph for the double parton scattering process, where two quarks in the right-moving proton interact with two antiquarks in the left-moving proton. The figure shows the assignment of four-momenta $(p, \bar{p}, q_i, l_i. \bar{l}_i, l'_i, \bar{l}'_i)$.

cross-section of figure 2.3 is

$$
\begin{aligned}
d\sigma = {}& \frac{1}{C}\frac{1}{4p\bar{p}} \left[\prod_{i=1}^{2} \frac{d^4 q_i}{(2\pi)^4}\right] \left[\prod_{i=1}^{2} \int \frac{d^4 l_i}{(2\pi)^4} \frac{d^4 l'_i}{(2\pi)^4} \frac{d^4 \bar{l}_i}{(2\pi)^4} \frac{d^4 \bar{l}'_i}{(2\pi)^4}\right] \\
& \times (2\pi)^4 \delta^{(4)}(q_1 - l_1 - \bar{l}_1)(2\pi)^4 \delta^{(4)}(q_1 - l'_1 - \bar{l}'_1) \\
& \times \sum_{X,\bar{X}} \Big[\sum_{j=1}^{m} \int \frac{d^3 p_{X,j}}{(2\pi)^3 2p^0_{X,j}}\Big]\Big[\sum_{j=1}^{\bar{m}} \int \frac{d^3 p_{\bar{X},j}}{(2\pi)^3 2p^0_{\bar{X},j}}\Big] \\
& \times H_1(q_1, l_1, l'_1, \bar{l}_1, \bar{l}'_1) H_2(q_2, l_2, l'_2, \bar{l}_2, \bar{l}'_2) \\
& \times (2\pi)^4 \delta^{(4)}(p + \bar{p} - \sum_{j=1}^{m} p_{X,j} - \sum_{j=1}^{\bar{m}} p_{\bar{X},j} - q_1 - q_2) \\
& \times \left[\prod_{i=1}^{2} \int d^4\xi_i d^4\xi'_i d^4\bar{\xi}_i d^4\bar{\xi}'_i e^{i(\xi_i l_i - \xi'_i l'_i) + i(\bar{\xi}_i \bar{l}_i - \bar{\xi}'_i \bar{l}'_i)}\right] \\
& \times \langle p| \bar{T}\Big[\bar{\psi}(\xi'_1)\bar{\psi}(\xi'_2)\Big] |X\rangle \langle X| T\Big[\psi(\xi_2)\psi(\xi_1)\Big] |p\rangle \\
& \times \langle \bar{p}| \bar{T}\Big[\psi(\bar{\xi}'_1)\psi(\bar{\xi}'_2)\Big] |\bar{X}\rangle \langle \bar{X}| T\Big[\bar{\psi}(\bar{\xi}_2)\bar{\psi}(\bar{\xi}_1)\Big] |\bar{p}\rangle .
\end{aligned}
\tag{2.10}
$$

The combinatorial factor C equals 2 if the final states of the two hard interactions are identical, and otherwise equals 1. The flux factor is $1/(4p\bar{p})$ and all internal momenta are integrated over with δ-functions enforcing momentum conservation. $p_{j,X}$ $(p_{j,\bar{X}})$ is the momenta of particle j in the proton remnants $|X\rangle$ $(|\bar{X}\rangle)$ of the right (left) moving proton. The sums runs over all possible remnants X and all particles j in X. H_1 (H_2) represents the first (second) hard interaction. In case the hard interaction produces a stable particle, then H_i includes the δ-function $\delta(q_i^2 - m_i^2)$ which combines with the

integration over the momentum q_i to give the correct final state phase-space $\int \frac{d^3 q_i}{(2\pi)^3 2q_i^0}$.
The matrix element $\langle X | T [\psi(\xi_2)\psi(\xi_1)] | p \rangle$ represents the transition from the initial proton
state to the remnants by removing two quarks from the proton. T denotes time ordering
while $\bar{T}$ denotes anti-time ordering. We only consider unpolarized protons and a sum
over the proton spin is implied.

Translation of the matrix element to $\xi'_2 = 0$,

$$
\int d^4\xi'_1 d^4\xi'_2 e^{-i\xi'_1 l'_1 - i\xi'_2 l'_2} \langle p | \bar{T} [\bar{\psi}(\xi'_1)\bar{\psi}(\xi'_2)] | X \rangle
$$

$$
= \int d^4\xi'_1 d^4\xi'_2 e^{-i\xi'_1 l'_1} e^{-i\xi'_2 (l'_1 + l'_2 + \sum_{j=1}^m p_{X,j} - p)} \langle p | \bar{T} [\bar{\psi}(\xi'_1)\bar{\psi}(0)] | X \rangle
$$

$$
= \int d^4\xi'_1 e^{-i\xi'_1 l'_1} (2\pi)^4 \delta^{(4)}(l'_1 + l'_2 + \sum_{j=1}^m p_{X,j} - p) \langle p | \bar{T} [\bar{\psi}(\xi'_1)\bar{\psi}(0)] | X \rangle , \qquad (2.11)
$$

allows us to extract a δ-function for momentum conservation in the proton. With the
equivalent operation for the left moving proton we can eliminate the X and $\bar{X}$ dependence
in the δ-function for over-all momentum conservation,

$$
\sum_{X,\bar{X}} \Big[\sum_{j=1}^m \int \frac{d^3 p_{X,j}}{(2\pi)^3 2p^0_{X,j}} \Big] \Big[\sum_{j=1}^{\bar{m}} \int \frac{d^3 p_{\bar{X},j}}{(2\pi)^3 2p^0_{\bar{X},j}} \Big]
$$

$$
\times (2\pi)^4 \delta^{(4)}(p + \bar{p} - \sum_{j=1}^m p_{X,j} - \sum_{j=1}^{\bar{m}} p_{\bar{X},j} - q_1 - q_2)
$$

$$
\times \Big[\prod_{i=1}^2 \int d^4\xi_i d^4\xi'_i d^4\bar{\xi}_i d^4\bar{\xi}'_i e^{i(\xi_i l_i - \xi'_i l'_i) + i(\bar{\xi}_i \bar{l}_i - \bar{\xi}'_i \bar{l}'_i)} \Big]
$$

$$
\times \langle p | \bar{T} [\bar{\psi}(\xi'_1)\bar{\psi}(\xi'_2)] | X \rangle \langle X | T [\psi(\xi_2)\psi(\xi_1)] | p \rangle
$$

$$
\times \langle \bar{p} | \bar{T} [\psi(\bar{\xi}'_1)\psi(\bar{\xi}'_2)] | \bar{X} \rangle \langle \bar{X} | T [\bar{\psi}(\bar{\xi}_2)\bar{\psi}(\bar{\xi}_1)] | \bar{p} \rangle
$$

$$
= \sum_{X,\bar{X}} \Big[\sum_{j=1}^m \int \frac{d^3 p_{X,j}}{(2\pi)^3 2p^0_{X,j}} \Big] \Big[\sum_{j=1}^{\bar{m}} \int \frac{d^3 p_{\bar{X},j}}{(2\pi)^3 2p^0_{\bar{X},j}} \Big]
$$

$$
\times (2\pi)^4 \delta^{(4)}(p + \bar{p} - \sum_{j=1}^m p_{X,j} - \sum_{j=1}^{\bar{m}} p_{\bar{X},j} - q_1 - q_2)
$$

$$
\times \Big[\prod_{i=1}^2 \int d^4\xi_i d^4\bar{\xi}_i e^{i\xi_i l_i + i\bar{\xi}_i \bar{l}_i} \Big] \int d^4\xi'_1 d^4\bar{\xi}'_1 e^{-i\xi'_1 l'_1 - i\bar{\xi}'_1 \bar{l}'_1}
$$

$$
\times (2\pi)^4 \delta^{(4)}(l'_1 + l'_2 + \sum_{j=1}^m p_{X,j} - p)(2\pi)^4 \delta^{(4)}(\bar{l}'_1 + \bar{l}'_2 + \sum_{j=1}^{\bar{m}} p_{\bar{X},j} - \bar{p})
$$

$$
\times \langle p | \bar{T} [\bar{\psi}(\xi'_1)\bar{\psi}(0)] | X \rangle \langle X | T [\psi(\xi_2)\psi(\xi_1)] | p \rangle
$$

$$
\times \langle \bar{p} | \bar{T} [\psi(\bar{\xi}'_1)\psi(0)] | \bar{X} \rangle \langle \bar{X} | T [\bar{\psi}(\bar{\xi}_2)\bar{\psi}(\bar{\xi}_1)] | \bar{p} \rangle
$$

$$
\begin{aligned}
&= \sum_{X,\bar{X}} \Big[\sum_{j=1}^{m} \int \frac{d^3 p_{X,j}}{(2\pi)^3 2p_{X,j}^0} \Big] \Big[\sum_{j=1}^{\bar{m}} \int \frac{d^3 p_{\bar{X},j}}{(2\pi)^3 2p_{\bar{X},j}^0} \Big] \\
&\quad \times (2\pi)^4 \delta^{(4)}(l_1' + l_2' + \bar{l}_1' + \bar{l}_2' - q_1 - q_2) \\
&\quad \times \Big[\prod_{i=1}^{2} \int d^4\xi_i d^4\xi_i' d^4\bar{\xi}_i d^4\bar{\xi}_i' e^{i(\xi_i l_i - \xi_i' l_i') + i(\bar{\xi}_i \bar{l}_i - \bar{\xi}_i' \bar{l}_i')} \Big] \\
&\quad \times \langle p| \bar{T} \left[\bar{\psi}(\xi_1') \bar{\psi}(\xi_2') \right] |X\rangle \langle X| T \left[\psi(\xi_2) \psi(\xi_1) \right] |p\rangle \\
&\quad \times \langle \bar{p}| \bar{T} \left[\psi(\bar{\xi}_1') \psi(\bar{\xi}_2') \right] |\bar{X}\rangle \langle \bar{X}| T \left[\bar{\psi}(\bar{\xi}_2) \bar{\psi}(\bar{\xi}_1) \right] |\bar{p}\rangle \\
&= (2\pi)^4 \delta^{(4)}(l_1' + l_2' + \bar{l}_1' + \bar{l}_2' - q_1 - q_2) \\
&\quad \times \Big[\prod_{i=1}^{2} \int d^4\xi_i d^4\xi_i' d^4\bar{\xi}_i d^4\bar{\xi}_i' e^{i(\xi_i l_i - \xi_i' l_i') + i(\bar{\xi}_i \bar{l}_i - \bar{\xi}_i' \bar{l}_i')} \Big] \\
&\quad \times \langle p| \bar{T} \left[\bar{\psi}(\xi_1') \bar{\psi}(\xi_2') \right] T \left[\psi(\xi_2) \psi(\xi_1) \right] |p\rangle \\
&\quad \times \langle \bar{p}| \bar{T} \left[\psi(\bar{\xi}_1') \psi(\bar{\xi}_2') \right] T \left[\bar{\psi}(\bar{\xi}_2) \bar{\psi}(\bar{\xi}_1) \right] |\bar{p}\rangle \,.
\end{aligned}
\tag{2.12}
$$

Without the δ-function constraining $p_{X,j}$ $(p_{\bar{X},j})$ we could in the final step eliminate the complete sets of states (X and $\bar{X}$)

$$
\sum_X \prod_{j=1}^{m} \int \frac{d^3 p_{X,j}}{(2\pi)^3 2p_{X,j}^0} |X\rangle \langle X| = 1.
\tag{2.13}
$$

The cross section (2.10) therewith takes the form

$$
\begin{aligned}
d\sigma &= \frac{1}{C} \frac{1}{4p\bar{p}} \Big[\prod_{i=1}^{2} \frac{d^4 q_i}{(2\pi)^4} \Big] \Big[\prod_{i=1}^{2} \int \frac{d^4 l_i}{(2\pi)^4} \frac{d^4 l_i'}{(2\pi)^4} \frac{d^4 \bar{l}_i}{(2\pi)^4} \frac{d^4 \bar{l}_i'}{(2\pi)^4} \Big] \\
&\quad \times (2\pi)^4 \delta^{(4)}(q_1 - l_1 - \bar{l}_1)(2\pi)^4 \delta^{(4)}(q_1 - l_1' - \bar{l}_1') \\
&\quad \times H_1(q_1, l_1, l_1', \bar{l}_1, \bar{l}_1') H_2(q_2, l_2, l_2', \bar{l}_2, \bar{l}_2') \\
&\quad \times (2\pi)^4 \delta^{(4)}(l_1' + l_2' + \bar{l}_1' + \bar{l}_2' - q_1 - q_2) \\
&\quad \times \Big[\prod_{i=1}^{2} \int d^4\xi_i d^4\xi_i' d^4\bar{\xi}_i d^4\bar{\xi}_i' e^{i(\xi_i l_i - \xi_i' l_i') + i(\bar{\xi}_i \bar{l}_i - \bar{\xi}_i' \bar{l}_i')} \Big] \\
&\quad \times \langle p| \bar{T} \left[\bar{\psi}(\xi_1') \bar{\psi}(\xi_2') \right] T \left[\psi(\xi_2) \psi(\xi_1) \right] |p\rangle \\
&\quad \times \langle \bar{p}| \bar{T} \left[\psi(\bar{\xi}_1') \psi(\bar{\xi}_2') \right] T \left[\bar{\psi}(\bar{\xi}_2) \bar{\psi}(\bar{\xi}_1) \right] |\bar{p}\rangle \,.
\end{aligned}
\tag{2.14}
$$

Translational invariance of the proton matrix elements and integration over ξ_2' and $\bar{\xi}_2'$ allows us to write the cross section in terms of correlation functions for two (anti)quarks in the right(left)-moving proton, Φ ($\bar{\Phi}$):

$$
d\sigma = \frac{1}{C} \frac{1}{4p\bar{p}} \Big[\prod_{i=1}^{2} \frac{d^4 q_i}{(2\pi)^4} \Big] \Big[\prod_{i=1}^{2} \int \frac{d^4 l_i}{(2\pi)^4} \frac{d^4 l_i'}{(2\pi)^4} \frac{d^4 \bar{l}_i}{(2\pi)^4} \frac{d^4 \bar{l}_i'}{(2\pi)^4} \Big]
$$

$$
\begin{aligned}
&\times (2\pi)^4 \delta^{(4)}(q_1 - l_1 - \bar{l}_1)(2\pi)^4 \delta^{(4)}(q_1 - l_1' - \bar{l}_1') \\
&\times H_1(q_1, l_1, l_1', \bar{l}_1, \bar{l}_1') H_2(q_2, l_2, l_2', \bar{l}_2, \bar{l}_2') \\
&\times (2\pi)^4 \delta^{(4)}(l_1' + l_2' + \bar{l}_1' + \bar{l}_2' - q_1 - q_2) \\
&\times (2\pi)^4 \delta^{(4)}(l_1 + l_2 - l_1' - l_2')(2\pi)^4 \delta^{(4)}(\bar{l}_1 + \bar{l}_2 - \bar{l}_1' - \bar{l}_2') \\
&\times \left[\prod_{i=1}^{2} \int d^4\xi_i d^4\bar{\xi}_i e^{i\xi_i l_i + i\bar{\xi}_i \bar{l}_i} \right] \int d^4\xi_1' d^4\bar{\xi}_1' e^{-i\xi_1' l_1' - i\bar{\xi}_1' \bar{l}_1'} \\
&\times \langle p| \bar{T}\left[\bar{\psi}(\xi_1')\bar{\psi}(0) \right] T\left[\psi(\xi_2)\psi(\xi_1) \right] |p\rangle \\
&\times \langle \bar{p}| \bar{T}\left[\psi(\bar{\xi}_1')\psi(0) \right] T\left[\bar{\psi}(\bar{\xi}_2)\bar{\psi}(\bar{\xi}_1) \right] |\bar{p}\rangle \\
=\; &\frac{1}{C}\frac{1}{2p\bar{p}} \left[\prod_{i=1}^{2} \frac{d^4 q_i}{(2\pi)^4} \right] \left[\prod_{i=1}^{2} \int \frac{d^4 l_i}{(2\pi)^4} \frac{d^4 l_i'}{(2\pi)^4} \frac{d^4 \bar{l}_i}{(2\pi)^4} \frac{d^4 \bar{l}_i'}{(2\pi)^4} \right] \\
&\times (2\pi)^4 \delta^{(4)}(q_1 - l_1 - \bar{l}_1)(2\pi)^4 \delta^{(4)}(q_1 - l_1' - \bar{l}_1') \\
&\times H_1(q_1, l_1, l_1', \bar{l}_1, \bar{l}_1') H_2(q_2, l_2, l_2', \bar{l}_2, \bar{l}_2') \\
&\times (2\pi)^4 \delta^{(4)}(l_1' + l_2' + \bar{l}_1' + \bar{l}_2' - q_1 - q_2) \\
&\times (2\pi)^4 \delta^{(4)}(l_1 + l_2 - l_1' - l_2')(2\pi)^4 \delta^{(4)}(\bar{l}_1 + \bar{l}_2 - \bar{l}_1' - \bar{l}_2') \\
&\times \Phi(l_1, l_2, l_1', l_2')\bar{\Phi}(\bar{l}_1, \bar{l}_2, \bar{l}_1', \bar{l}_2').
\end{aligned}
\tag{2.15}
$$

Two quark correlation function

The two quark correlation function is given by

$$
\begin{aligned}
\Phi(l_1, l_2, l_1', l_2') = \int &\frac{d^4\xi_1}{(2\pi)^4} \frac{d^4\xi_1'}{(2\pi)^4} \frac{d^4\xi_2}{(2\pi)^4} e^{i\xi_1 l_1 + i\xi_2 l_2 - i\xi_1' l_1'} \\
&\times \langle p| \bar{T}\left[\bar{\psi}(\xi_1')\bar{\psi}(0) \right] T\left[\psi(\xi_2)\psi(\xi_1) \right] |p\rangle \Big|_{l_1 + l_2 = l_1' + l_2'}
\end{aligned}
\tag{2.16}
$$

and analogously for two anti-quarks in the left-moving proton. With a change of momentum variables

$$
\begin{array}{ll}
l_1 = k_1 - \dfrac{r_1}{2}\,, & \qquad l_1' = k_1 + \dfrac{r_1}{2}\,, \\[2mm]
l_2 = k_2 - \dfrac{r_2}{2}\,, & \qquad l_2' = k_2 + \dfrac{r_2}{2}
\end{array}
\tag{2.17}
$$

together with a translation, the correlation function takes the form

$$
\begin{aligned}
\Phi(k_1, k_2, r_1, r_2) = \int &\frac{d^4\xi_1}{(2\pi)^4} \frac{d^4\xi_1'}{(2\pi)^4} \frac{d^4\xi_2}{(2\pi)^4} e^{i(\xi_1 - \xi_1')k_1 - (\xi_1 + \xi_1')r_1/2 + i\xi_2 k_2 - i\xi_2 r_2/2'} \\
&\times \langle p| \bar{T}\left[\bar{\psi}(\xi_1' - \tfrac{1}{2}\xi_2)\bar{\psi}(-\tfrac{1}{2}\xi_2) \right] T\left[\psi(\tfrac{1}{2}\xi_2)\psi(\xi_1 - \tfrac{1}{2}\xi_2) \right] |p\rangle \Big|_{r_1 + r_2 = 0}.
\end{aligned}
\tag{2.18}
$$

We set $r = r_1 = -r_2$ and change integration variables according to

$$
y + \tfrac{1}{2}z_1 = \xi_1 - \tfrac{1}{2}\xi_2\,, \qquad y - \tfrac{1}{2}z_1 = \xi_1' - \tfrac{1}{2}\xi_2\,, \qquad z_2 = \xi_2\,,
\tag{2.19}
$$

the two quark correlation function can be expressed as

$$\Phi(k_1, k_2, r) = \int \frac{d^4z_1}{(2\pi)^4} \frac{d^4z_2}{(2\pi)^4} \frac{d^4y}{(2\pi)^4} \mathrm{e}^{iz_1k_1+iz_2k_2-iyr}$$
$$\times \langle p| \bar{T} \left[\bar{\psi}(y - \tfrac{1}{2}z_1)\bar{\psi}(-\tfrac{1}{2}z_2) \right] T \left[\psi(\tfrac{1}{2}z_2)\psi(y + \tfrac{1}{2}z_1) \right] |p\rangle. \tag{2.20}$$

With the equivalent substitutions in the two antiquark correlation function for the left-moving proton, we can write the cross section in terms of the correlation functions as

$$d\sigma = \frac{1}{C} \frac{1}{4p\bar{p}} \left[\prod_{i=1}^{2} \frac{d^4q_i}{(2\pi)^4} \right] \left[\prod_{i=1}^{2} \int d^4k_i d^4\bar{k}_i (2\pi)^4 \delta^{(4)}(q_i - k_i - \bar{k}_i) \right]$$
$$\times \int d^4r d^4\bar{r} (2\pi)^4 \delta^{(4)}(r + \bar{r})$$
$$\times H_1(q_1, k_1, \bar{k}_1, r, \bar{r}) H_2(q_2, k_2, \bar{k}_2, -r, -\bar{r})$$
$$\times \Phi(k_1, k_2, r) \bar{\Phi}(\bar{k}_1, \bar{k}_2, \bar{r}). \tag{2.21}$$

Hard scattering approximation

The parton level interactions (H_1 and H_2) involve the hard scales $q_1^2 \sim Q^2$ and $q_2^2 \sim Q^2$. In figure 2.3 it is implicit that the parton lines originating in the protons have virtualities much smaller than the hard scale. For the right and left moving protons respectively, the momentum variables scale as

$$p^+ \sim k_i^+ \sim q_i^+ \sim Q, \qquad\qquad \bar{p}^- \sim \bar{k}_i^- \sim q_i^- \sim Q,$$
$$p^- \sim k_i^- \sim r^- \sim \Lambda^2/Q, \qquad\qquad \bar{p}^+ \sim \bar{k}_i^+ \sim \bar{r}^+ \sim \Lambda^2/Q. \tag{2.22}$$

r^+ and $\bar{r}^-$ could by scaling arguments be of order Q, but momentum conservation forces $r + \bar{r} = 0$ and thus

$$r^+ \sim \bar{r}^- \sim \Lambda^2/Q. \tag{2.23}$$

All transverse momentum vectors are of the hadronic scale,

$$|\boldsymbol{k}_i| \sim |\bar{\boldsymbol{k}}_i| \sim |\boldsymbol{r}| \sim |\bar{\boldsymbol{r}}| \sim |\boldsymbol{q}_i| \sim \Lambda. \tag{2.24}$$

In the hard scattering we can neglect transverse momenta and quantities of order Λ^2/Q. This leads to the great simplification that the hard function H_i only depend on q_i, which due to invariance under a Lorentz boost along the $\hat{z}$-axis only occurs in the combination $2q_i^+ q_i^- \approx q_i^2$, and

$$H(q_i, k_i, \bar{k}_i, r_i) \approx H(q_i^2). \tag{2.25}$$

The simplification is a virtue of the momentum variables chosen, where there are no kinematic constraints relating r and $\bar{r}$ to the final state momenta q_1 and q_2. In the correlation functions we neglect momenta of order Λ^2/Q such that

$$k_i^+ = q_i^+ - \bar{k}_i^+ \approx q_i^+, \qquad\qquad r^+ = -\bar{r}^+ \approx 0,$$
$$\bar{k}_i^- = q_i^- - k_i^- \approx q_i^-, \qquad\qquad \bar{r}^- = -r^- \approx 0, \tag{2.26}$$

with the result that the longitudinal momenta of the partons in the amplitude and conjugate amplitude have to be equal. Expressing the integrals over momenta in light-cone coordinates, we get

$$
\left[\prod_{i=1}^{2} \int dk_i^+ d\bar{k}_i^+ \delta(q_i^+ - k_i^+ - \bar{k}_i^+) \int dk_i^- d\bar{k}_i^- \delta(q_i^- - k_i^- - \bar{k}_i^-) \right]
$$

$$
\times \int dr^+ d\bar{r}^+ \delta(r^+ + \bar{r}^+) \int dr^- d\bar{r}^- \delta(r^- + \bar{r}^-)
$$

$$
\times H_1(q_1, k_1, \bar{k}_1, r, \bar{r}) H_2(q_2, k_2, \bar{k}_2, r, \bar{r})
$$

$$
\times \Phi(k_1, k_2, r) \bar{\Phi}(\bar{k}_1, \bar{k}_2, \bar{r})
$$

$$
\approx H_1(q_1^2) H_2(q_2^2) \int dk_1^- dk_2^- \int dr^- \Phi(k_1, k_2, r)
$$

$$
\times \int d\bar{k}_1^+ d\bar{k}_2^+ \int d\bar{r}^+ \bar{\Phi}(\bar{k}_1, \bar{k}_2, \bar{r}) \Big|_{\substack{k_i^+ = q_i^+,\, \bar{k}_i^- = q_i^-, \\ r^+ = \bar{r}^- = 0}} . \tag{2.27}
$$

Rewriting $d^4 q_i = (p^+ \bar{p}^-) dx_i d\bar{x}_i d^2 \boldsymbol{q}_i$, we can write the cross section (2.21) as

$$
d\sigma = \frac{1}{C} \left[\prod_{i=1}^{2} dx_i d\bar{x}_i d^2 \boldsymbol{q}_i \frac{k_i^+ \bar{k}_i^-}{2 q_i^2} H_i(q_i^2) \int d^2 \boldsymbol{k}_i d^2 \bar{\boldsymbol{k}}_i \delta^{(2)}(\boldsymbol{q}_i - \boldsymbol{k}_i - \bar{\boldsymbol{k}}_i) \right]
$$

$$
\times \int \frac{d^2 \boldsymbol{r} d^2 \bar{\boldsymbol{r}}}{(2\pi)^2} \delta^{(2)}(\boldsymbol{r} + \bar{\boldsymbol{r}})
$$

$$
\times \int dk_1^- dk_2^- (2\pi)^3 2p^+ \int dr^- \Phi(k_1, k_2, r)
$$

$$
\times \int d\bar{k}_1^+ d\bar{k}_2^+ (2\pi)^3 2\bar{p}^- \int d\bar{r}^+ \bar{\Phi}(\bar{k}_1, \bar{k}_2, \bar{r}) \Big|_{\substack{k_i^+ = q_i^+,\, \bar{k}_i^- = q_i^-, \\ r^+ = \bar{r}^- = 0}} . \tag{2.28}
$$

Let us now define double parton distributions in terms of the correlation function

$$
F(x_1, x_2, \boldsymbol{k}_1, \boldsymbol{k}_2, \boldsymbol{r}) = \int dk_1^- dk_2^- (2\pi)^3 2p^+ \int dr^- \Phi(k_1, k_2, r) \Big|_{\substack{k_i^+ = x_i p^+, \\ r^+ = 0}} . \tag{2.29}
$$

Integrating the correlation function over minus momenta forces $z_i^+ = 0$ and $y^+ = 0$. The fields in the correlation function are thus evaluated at equal light-cone time, and we can drop the (anti-)time ordering. The fields are spatially separated and therefore anti-commute and we can, with an even number of commutations, reorder the fields as

$$
F(x_1, x_2, \boldsymbol{k}_1, \boldsymbol{k}_2, \boldsymbol{r}) = \left[\prod_{i=1}^{2} \int \frac{dz_i^- d^2 \boldsymbol{z}_i}{(2\pi)^3} e^{i x_i z_i^- p^+ - i \boldsymbol{z}_i \boldsymbol{k}_i} \right] 2p^+ \int dy^- d^2 \boldsymbol{y} e^{i \boldsymbol{y} \boldsymbol{r}}
$$

$$
\times \langle p | \bar{\psi}(-\tfrac{1}{2} z_2) \psi(\tfrac{1}{2} z_2) \bar{\psi}(y - \tfrac{1}{2} z_1) \psi(y + \tfrac{1}{2} z_1) | p \rangle \Big|_{z_i^+ = y^+ = 0} . \tag{2.30}
$$

Expressing the cross section in the double parton distributions

$$d\sigma = \frac{1}{C}\left[\prod_{i=1}^{2} dx_i d\bar{x}_i d^2\boldsymbol{q}_i \frac{k_i^+ \bar{k}_i^-}{2q_i^2} H_i(q_i^2) \int d^2\boldsymbol{k}_i d^2\bar{\boldsymbol{k}}_i \delta^{(2)}(\boldsymbol{q}_i - \boldsymbol{k}_i - \bar{\boldsymbol{k}}_i)\right]$$

$$\times \int \frac{d^2\boldsymbol{r}}{(2\pi)^2} F(x_1, x_2, \boldsymbol{k}_1, \boldsymbol{k}_2, \boldsymbol{r}) \bar{F}(\bar{x}_1, \bar{x}_2, \bar{\boldsymbol{k}}_1, \bar{\boldsymbol{k}}_2, -\boldsymbol{r}) \qquad (2.31)$$

completes the first part of our cross section derivation. The piece with the hard functions in (2.31),

$$\frac{k_i^+ \bar{k}_i^-}{2q_i^2} H_i(q_i^2) \qquad (2.32)$$

is related to the partonic cross-section ($\hat{\sigma}_i$) in a way which we will make precise after discussing the spin structure. The cross section can then be written as

$$\frac{d\sigma}{\prod_{i=1}^{2} dx_i\, d\bar{x}_i\, d^2\boldsymbol{q}_i} = \frac{1}{C}\hat{\sigma}_1\,\hat{\sigma}_2 \int d^2\boldsymbol{k}_i d^2\bar{\boldsymbol{k}}_1 \delta^{(2)}(\boldsymbol{q}_1 - \boldsymbol{k}_1 - \bar{\boldsymbol{k}}_1)$$

$$\times \int d^2\boldsymbol{k}_2 d^2\bar{\boldsymbol{k}}_2 \delta^{(2)}(\boldsymbol{q}_2 - \boldsymbol{k}_2 - \bar{\boldsymbol{k}}_2) \int \frac{d^2\boldsymbol{r}}{(2\pi)^2}$$

$$\times F(x_1, x_2, \boldsymbol{k}_1, \boldsymbol{k}_2, \boldsymbol{r}) \bar{F}(\bar{x}_1, \bar{x}_2, \bar{\boldsymbol{k}}_1, \bar{\boldsymbol{k}}_2, -\boldsymbol{r}). \qquad (2.33)$$

The vector $\boldsymbol{k}_i$ ($\bar{\boldsymbol{k}}_i$) is the average transverse momentum of the parton from the right (left) moving proton participating in interaction i, while $\boldsymbol{r}$ is the difference in transverse momentum between the parton in the amplitude and its partner in the conjugate amplitude.

Transverse position

Fourier transforming the DPDs into transverse position space, gives

$$F(x_1, x_2, \boldsymbol{z}_1, \boldsymbol{z}_2, \boldsymbol{y}) = \int \frac{d^2\boldsymbol{r}}{(2\pi)^2} e^{-i\boldsymbol{y}\boldsymbol{r}} \int d^2\boldsymbol{k}_1 d^2\boldsymbol{k}_2 e^{i\boldsymbol{z}_1\boldsymbol{k}_1 + i\boldsymbol{z}_2\boldsymbol{k}_2} F(x_1, x_2, \boldsymbol{k}_1, \boldsymbol{k}_2, \boldsymbol{r}) \qquad (2.34)$$

where $\boldsymbol{z}_i$ ($\bar{\boldsymbol{z}}_i$) is the conjugate variable of the average transverse momentum of parton i $\boldsymbol{k}_i$ ($\bar{\boldsymbol{k}}_i$) and $\boldsymbol{y}$ of $\boldsymbol{r}$. The cross section can be expressed as

$$\frac{d\sigma}{\prod_{i=1}^{2} dx_i\, d\bar{x}_i\, d^2\boldsymbol{q}_i} = \frac{1}{C}\,\hat{\sigma}_1\,\hat{\sigma}_2 \int \frac{d^2\boldsymbol{z}_1}{(2\pi)^2} \frac{d^2\boldsymbol{z}_2}{(2\pi)^2}\, e^{-i\boldsymbol{z}_1\boldsymbol{q}_1 - i\boldsymbol{z}_2\boldsymbol{q}_2}$$

$$\times \int d^2\boldsymbol{y}\; F(x_1, x_2, \boldsymbol{z}_1, \boldsymbol{z}_2, \boldsymbol{y})\, \bar{F}(\bar{x}_1, \bar{x}_2, \boldsymbol{z}_1, \boldsymbol{z}_2, \boldsymbol{y}), \qquad (2.35)$$

with transverse position and longitudinal momentum fractions as in figure 2.4. The arguments $\boldsymbol{z}_i$ and $\boldsymbol{y}$ of the distributions determine where the hard-scattering processes take place in transverse configuration space. As indicated in figure 2.4, $\boldsymbol{y}$ is the transverse distance between the two scattering partons in a proton (and hence between the two annihilation processes) if one takes the average position between the scattering amplitude and its conjugate.
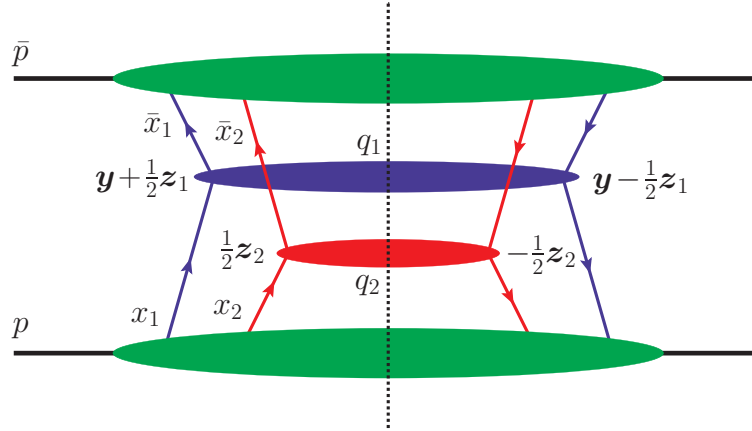
Figure 2.4: A graph for the double parton scattering process, where two quarks in the right-moving proton interact with two antiquarks in the left-moving proton. The figure shows the assignment of light-cone momentum fractions $(x_i, \bar{x}_i)$ and of transverse position arguments as explained in the text.

Transverse momentum integrated cross section

Integrating (2.35) over the transverse boson momenta $\boldsymbol{q}_1$ and $\boldsymbol{q}_2$ sets $\boldsymbol{z}_i = \bar{\boldsymbol{z}}_i = 0$ and we obtain

$$\frac{d\sigma}{\prod_{i=1}^{2} dx_i \, d\bar{x}_i} = \frac{1}{C} \, \hat{\sigma}_1 \hat{\sigma}_2 \int d^2\boldsymbol{y} \, F(x_1, x_2, \boldsymbol{y}) \, \bar{F}(\bar{x}_1, \bar{x}_2, \boldsymbol{y}) \,. \tag{2.36}$$

Here $F(x_1, x_2, \boldsymbol{y})$ and $\bar{F}(\bar{x}_1, \bar{x}_2, \boldsymbol{y})$ are transverse-momentum integrated (also called collinear) DPDs, which were introduced long ago in [71, 72]. We recognize the vector $\boldsymbol{y}$ and its geometrical interpretation from the DPS introduction and its illustration in figure 2.2(b), as the vector from the second to the first hard interaction. The collinear double parton distributions are naively obtained by setting $\boldsymbol{z}_1 = \boldsymbol{z}_2 = \boldsymbol{0}$ in the distributions of (2.35). However, just as for their single parton counterparts in section 2.1 the collinear and transverse-momentum dependent DPDs require different regularization and subtractions of divergences. As a result the distributions depend in different ways on an ultraviolet renormalization scale and (with the exception of specific distributions) also on a rapidity parameter related to Sudakov logarithms.

The cross section formulas so far have been schematic in that they omit labels and summations over the quantum numbers of the partons - to which we will now turn our attention.

2.3.2 Double parton distributions

Let us take a closer look at the double parton distributions. In particular, we want to study their spin, color and flavor structure. We therefore need to restore the labels on
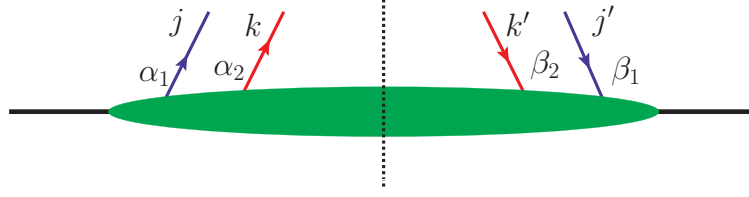
Figure 2.5: A graph for the spin and color labels in the double parton distributions. α_i's are the spin labels of the quarks in the amplitude and β_i's for their partners in the conjugate amplitude.

the quark fields in the two quark correlation function (2.20)

$$
\Phi_{\Sigma_1, \Sigma'_1, \Sigma_2, \Sigma'_2,}(k_1, k_2, r) = \int \frac{d^4 z_1}{(2\pi)^4} e^{iz_1 k_1} \frac{d^4 z_2}{(2\pi)^4} e^{iz_2 k_2} \frac{d^4 y}{(2\pi)^4} e^{-iyr}
$$
$$
\times \langle p | \bar{T} \left[\bar{\psi}_{\Sigma'_1}(y - \tfrac{1}{2} z_1) \bar{\psi}_{\Sigma'_2}(-\tfrac{1}{2} z_2) \right] T \left[\psi_{\Sigma_2}(\tfrac{1}{2} z_2) \psi_{\Sigma_1}(y + \tfrac{1}{2} z_1) \right] | p \rangle , \quad (2.37)
$$

where Σ_i collectively labels the flavor, color and spin of the quark participation in hard interaction i. This dependence is transferred to the double parton distributions (2.30) and after the Fourier transform in (2.34) yields

$$
F_{\Sigma_1, \Sigma'_1, \Sigma_2, \Sigma'_2,}(x_1, x_2, \boldsymbol{z}_1, \boldsymbol{z}_2, \boldsymbol{y}) = 2p^+ \int \frac{dz_1^-}{2\pi} \frac{dz_2^-}{2\pi} dy^- \; e^{ix_1 z_1^- p^+ + ix_2 z_2^- p^+}
$$
$$
\times \langle p | \bar{\psi}_{\Sigma'_2}(-\tfrac{1}{2} z_2) \psi_{\Sigma_2}(\tfrac{1}{2} z_2) \bar{\psi}_{\Sigma'_1}(y - \tfrac{1}{2} z_1) \psi_{\Sigma_1}(y + \tfrac{1}{2} z_1) | p \rangle \Big|_{z_i^+ = y^+ = 0}. \quad (2.38)
$$

Next, we treat the different quantum numbers one by one and see how they give rise to a rich spectra of different double parton distributions.

Spin

Defining the spin labels of the partons as in figure 2.5 and restoring the spin labels on the hard interactions, results in the contraction

$$
\Phi_{\alpha_1 \beta_1, \alpha_2 \beta_2} \bar{\Phi}_{\bar{\alpha}_1 \bar{\beta}_1, \bar{\alpha}_2 \bar{\beta}_2} H_{1, \beta_1 \alpha_1, \bar{\beta}_1 \bar{\alpha}_1} H_{2, \beta_2 \alpha_2, \bar{\beta}_2 \bar{\alpha}_2} \quad (2.39)
$$

between the spin labels of hard functions and correlation functions. $\bar{\alpha}_i$ and $\bar{\beta}_i$ correspond to partons in the left moving proton. For notational simplicity, we focus on one of the index pairs and drop the subscripts on the spin labels. It is understood that the equivalent transformations are made for all indices. With a Fierz transform, see for example [73], on the spin labels the correlation function can be expressed as

$$
\Phi_{\alpha \beta} = \text{tr}(\tfrac{1}{2} \Phi) \tfrac{1}{2} \delta_{\alpha \beta} + \text{tr}(\tfrac{1}{2} \gamma_5 \Phi) \tfrac{1}{2} (\gamma_5)_{\alpha \beta} + \text{tr}(\tfrac{1}{2} \gamma_\mu \Phi) \tfrac{1}{2} (\gamma^\mu)_{\alpha \beta}
$$
$$
+ \text{tr}(\tfrac{1}{2} \gamma_5 \gamma_\mu \Phi) \tfrac{1}{2} (\gamma^\mu \gamma_5)_{\beta \alpha} + \text{tr}(\tfrac{1}{2} i \sigma_{\nu \mu} \gamma_5 \Phi) \tfrac{1}{4} i (\sigma^{\mu \nu} \gamma_5)_{\alpha \beta}. \quad (2.40)
$$

The dominant terms are those with the maximum number of plus-components in the correlation functions, since they are proportional to the large momentum p^+. To leading power we thus get

$$\Phi_{\alpha\beta}H_{i,\beta\alpha} = \text{tr}(\tfrac{1}{2}\gamma^+\Phi)\text{tr}(\tfrac{1}{2}\gamma^- H_i) + \text{tr}(\tfrac{1}{2}\gamma^+\gamma_5\Phi)\text{tr}(\tfrac{1}{2}\gamma_5\gamma^- H_i)$$
$$+ \text{tr}(i\tfrac{1}{2}\sigma^{j+}\gamma_5\Phi)\text{tr}(i\tfrac{1}{2}\sigma^{j-}\gamma_5 H_i) \tag{2.41}$$

for the contraction of the spin indices between the correlation function and hard inter-action i.

We now define the collinear approximation k_c of the parton momentum k, where $k_c^+ = k^+$, $k_c^- = 0$ and $\boldsymbol{k}_c = \boldsymbol{0}$. Multiplying H_i with a factor k_i^+, we get for the first $(\tfrac{1}{2}\gamma^-)$ term in (2.41)

$$k_i^+\text{tr}\left(\tfrac{1}{2}\gamma^- H_i\right) = \text{tr}\left(\tfrac{1}{2}\slashed{k}_{i,c}H_i\right) = \tfrac{1}{2}\sum_s \bar{u}_s(k_{i,c})H_i u_s(k_{i,c}), \tag{2.42}$$

which is the spin averaged, squared amplitude for an on-shell quark. The terms in (2.41) give partonic cross sections

$$\hat{\sigma}_{i,a\bar{a}} = \frac{1}{2q_i^2}\left[P_a(k_{i,c})\right]_{\alpha\beta}\left[P_{\bar{a}}(\bar{k}_{i,c})\right]_{\bar{\beta}\bar{\alpha}}H_{i,\beta\alpha\bar{\alpha}\bar{\beta}}, \tag{2.43}$$

with the projections

$$P_q(k_c) = P_{\bar{q}}(k_c) = \tfrac{1}{2}\slashed{k}_c,$$
$$P_{\Delta q}(k_c) = -P_{\Delta\bar{q}}(k_c) = \tfrac{1}{2}\gamma_5\slashed{k}_c,$$
$$P_{\delta q}^j(k_c) = P_{\delta\bar{q}}^j(k_c) = \tfrac{1}{2}\gamma_5\slashed{k}_c\gamma^j. \tag{2.44}$$

The spin vector of a quark can be parameterized as

$$s^\mu = \lambda\left(\frac{p^\mu}{m} - mn^\mu\right) + s_T^\mu, \tag{2.45}$$

where m is the quark mass and λ (s_T) describes the degree of longitudinal (transverse) polarization. The operator

$$\frac{1 + \gamma_5\slashed{s}}{2} \tag{2.46}$$

projects onto quarks or antiquarks of different polarizations. The combination with the sum over spinors for quarks with different spin yields

$$(\slashed{k} \pm m)\frac{1 + \gamma_5\slashed{s}}{2} \xrightarrow{m\to 0} \slashed{k}\frac{1 \mp \lambda\gamma_5 + \gamma_5\slashed{s}_T}{2}. \tag{2.47}$$

Comparing to the projection operators in (2.44) we see that the different projections give the hard interactions of unpolarized, longitudinally polarized and transversely polarized

quarks and antiquarks. The Fierz transform for both the quarks in the correlation function, gives rise to nine different combinations, corresponding to the different polarizations of two quarks or antiquarks in an unpolarized proton.

For two quarks in an unpolarized right-moving proton we then write

$$F_{a_1 a_2}(x_1, x_2, \boldsymbol{z}_1, \boldsymbol{z}_2, \boldsymbol{y}) = 2p^+ \int \frac{dz_1^-}{2\pi} \frac{dz_2^-}{2\pi} \, dy^- \, e^{ix_1 z_1^- p^+ + ix_2 z_2^- p^+}$$
$$\times \langle p| \, \mathcal{O}_{a_2}(0, z_2) \, \mathcal{O}_{a_1}(y, z_1) \, |p\rangle \, , \tag{2.48}$$

where averaging over the proton polarizations is implied and where

$$\mathcal{O}_{a_i}(y, z_i) = \bar{q}_i(y - \tfrac{1}{2}z_i) \, \Gamma_{a_i} q_i(y + \tfrac{1}{2}z_i) \Big|_{z_i^+ = y^+ = 0} \tag{2.49}$$

is the operator for a quark. Notice that we have relabel here, and in the following, the quark field $\psi \to q$, where q_i will be used to indicate the quark flavor. The position arguments in (2.49) correspond to the assignments in figure 2.5. The Dirac matrices select quarks of the different polarizations in proton

$$\Gamma_q = \tfrac{1}{2}\gamma^+ \, , \qquad \Gamma_{\Delta q} = \tfrac{1}{2}\gamma^+\gamma_5 \, , \qquad \Gamma_{\delta q}^j = \tfrac{1}{2}i\sigma^{j+}\gamma_5 \quad (j = 1, 2) \, , \tag{2.50}$$

with the subscripts q for an unpolarized quark, Δq for a quark with longitudinal polarization and δq corresponding to a quark with polarization in the transverse direction j. The labels a_i in (2.48) specify both the flavor and the polarization of the quarks. In full analogy one can define DPDs $F_{\bar{a}_1, \bar{a}_2}$ for two antiquarks, as well as quark-antiquark distributions $F_{\bar{a}_1, a_2}$ and $F_{a_1, \bar{a}_2}$. For distributions with one or two gluons a similar decomposition can be made and we will return to this when dealing with gluon distributions in chapter 4.

Color

We now turn to the color structure of the double parton distributions. With color labels as in figure 2.5 we parameterize the DPDs in two terms. One term describing the case when the quark in the amplitude forms a color singlet with its partner in the conjugate amplitude, and one term describing the case when they couple to a color octet. We decompose the DPDs as [44]

$$F_{jj',kk'} = \frac{1}{N_c^2} \left({}^1\!F \delta_{jj'} \delta_{kk'} + \frac{N_c}{\sqrt{N_c^2 - 1}} \, {}^8\!F t_{jj'}^a t_{kk'}^a \right) . \tag{2.51}$$

The DPDs with the two color structures can be expressed as

$${}^c\!F_{a_1 a_2}(x_1, x_2, \boldsymbol{z}_1, \boldsymbol{z}_2, \boldsymbol{y}) = 2p^+ \int \frac{dz_1^-}{2\pi} \frac{dz_2^-}{2\pi} \, dy^- \, e^{ix_1 z_1^- p^+ + ix_2 z_2^- p^+}$$
$$\times \langle p| \, {}^c\!\mathcal{O}_{a_2}(0, z_2) \, {}^c\!\mathcal{O}_{a_1}(y, z_1) \, |p\rangle \, , \tag{2.52}$$

with $c = \{1, 8\}$ labeling the color representations. The operators of the singlet and octet distributions equals

$$
{}^{1}\mathcal{O}(y, z_i) = \bar{q}_{j'}(y - \tfrac{1}{2}z_i)\, \delta_{jj'} q_j(y + \tfrac{1}{2}z_i)\Big|_{z_i^+ = y^+ = 0}
\tag{2.53}
$$

$$
{}^{8}\mathcal{O}(y, z_i) = \bar{q}_{j'}(y - \tfrac{1}{2}z_i)\, t_{jj'}^a q_j(y + \tfrac{1}{2}z_i)\Big|_{z_i^+ = y^+ = 0}.
\tag{2.54}
$$

With the normalization factors in (2.51) the color singlet and octet distributions enter the cross section with equal weight

$$
\frac{1}{N_c^2} \left({}^{1}F^{1}\bar{F} + {}^{8}F^{8}\bar{F} \right),
\tag{2.55}
$$

in the production of color singlet states.

The distributions containing antiquarks are decomposed analogously. For distributions with one or two gluons a larger number of color combinations is possible, for the two gluon DPDs see equation 2.121 in [44], and for mixed quark-gluon DPDs see [43].

Flavor and fermion-number

There is one more index on the fields which we have yet to deal with. This is the flavor index, which gives rise to interference between quarks of different flavors.

The quark coupling to H_1 does not necessarily have the same flavor in the scattering amplitude and its complex conjugate, because a mismatch in flavor can be compensated by the quark coupling to H_2. For example, the quarks with transverse positions $\boldsymbol{y} + \tfrac{1}{2}\boldsymbol{z}_1$ and $-\tfrac{1}{2}\boldsymbol{z}_2$ in figure 2.4 can be u quarks if the quarks with transverse positions $\tfrac{1}{2}\boldsymbol{z}_2$ and $\boldsymbol{y} - \tfrac{1}{2}\boldsymbol{z}_1$ are d quarks, as in figure 2.6(a).

We label the flavor interference distributions as F^I (with a capital I as superscript) and they are given by [58]

$$
\begin{aligned}
F_{a_1 a_2}^{I}(x_1, x_2, \boldsymbol{z}_1, \boldsymbol{z}_2, \boldsymbol{y}) = 2p^+ \int \frac{dz_1^-}{2\pi} \frac{dz_2^-}{2\pi} \, dy^- \, e^{ix_1 z_1^- p^+ + ix_2 z_2^- p^+} \\
\times \langle p|\, \mathcal{O}_{a_2}^{I}(0, z_2)\, \mathcal{O}_{a_1}^{I}(y, z_1)\, |p\rangle
\end{aligned}
\tag{2.56}
$$

with the product of operators

$$
\mathcal{O}_{a_2}^{I}(0, z_2)\, \mathcal{O}_{a_1}^{I}(y, z_1) = \bar{q}_1(-\tfrac{1}{2}z_2)\, \Gamma_{a_2}\, q_2(\tfrac{1}{2}z_2)\, \bar{q}_2(y - \tfrac{1}{2}z_1)\, \Gamma_{a_1}\, q_1(y + \tfrac{1}{2}z_1)\Big|_{\substack{z_1^+ = z_2^+ = 0 \\ y^+ = 0}}.
\tag{2.57}
$$

These distributions are complex valued and their imaginary part changes sign when one interchanges the flavor (but not the spin) assignments and replaces $\boldsymbol{z}_i \to -\boldsymbol{z}_i$, e.g.

$$
F_{q_1 \Delta q_2}^{I}(x_1, x_2, \boldsymbol{z}_1, \boldsymbol{z}_2, \boldsymbol{y}) = \left[F_{q_2 \Delta q_1}^{I}(x_1, x_2, -\boldsymbol{z}_1, -\boldsymbol{z}_2, \boldsymbol{y}) \right]^{*}.
\tag{2.58}
$$
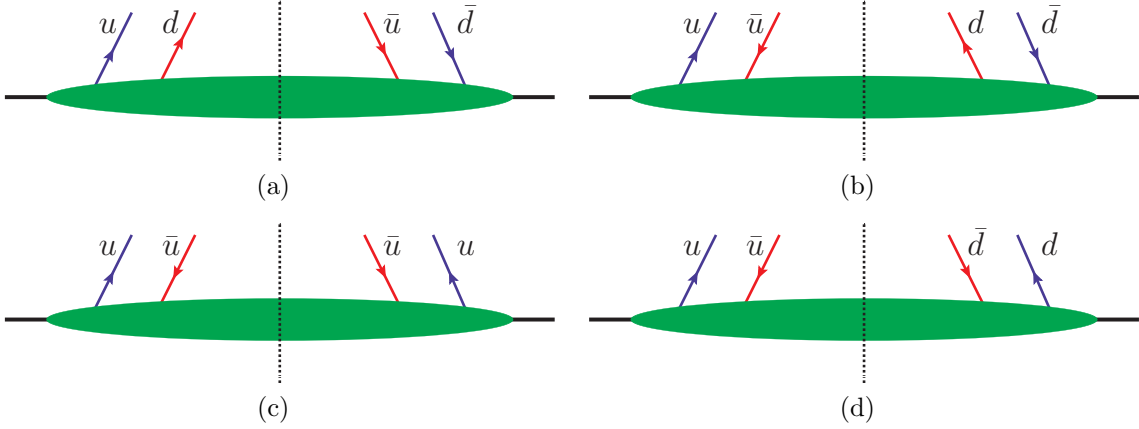
Figure 2.6: Example graphs for different interference double parton distributions. The $q,\bar{q}$ labels indicate whether a parton corresponds to a quark field or a conjugate quark field in the relevant DPD. The graphs illustrate flavor interference in (a) and (b), fermion number interference in (c) and combined flavor and fermion number interference in (d).

As we shall see in Chapter 3, this ensures that physical cross sections are real-valued.

For diagrams involving double parton distributions of one quark and one anti-quark there can in addition be interference in fermion number, between quarks and anti-quarks. Figure 2.6 shows a couple of different diagrams with flavor and fermion number interferences. It was argued in [44] that flavor number interference should be small at small x_i values.

2.3.3   DPS cross section with correlations

Taking all correlations into account, the double parton scattering cross section (2.35) in figure 2.3 takes the form

$$
\frac{d\sigma}{\prod_{i=1}^{2} dx_i \, d\bar{x}_i \, d^2\boldsymbol{q}_i} = \frac{1}{C} \sum_{a_1 a_2 a_3 a_4} \int \frac{d^2\boldsymbol{z}_1}{(2\pi)^2} \frac{d^2\boldsymbol{z}_2}{(2\pi)^2} \, e^{-i\boldsymbol{z}_1\boldsymbol{q}_1 - i\boldsymbol{z}_2\boldsymbol{q}_2} \int d^2\boldsymbol{y}
$$
$$
\times \left\{ d\hat{\sigma}_{a_1\bar{a}_3} \, d\hat{\sigma}_{a_2\bar{a}_4} \left[{}^1F_{a_1 a_2} \, {}^1\bar{F}_{\bar{a}_3\bar{a}_4} + c_8 \, {}^8F_{a_1 a_2} \, {}^8\bar{F}_{\bar{a}_3\bar{a}_4} \right] \right.
$$
$$
\left. + d\hat{\sigma}^I_{a_1\bar{a}_3} \, d\hat{\sigma}^I_{a_2\bar{a}_4} \left[{}^1F^I_{a_1 a_2} \, {}^1\bar{F}^I_{\bar{a}_3\bar{a}_4} + c_8 \, {}^8F^I_{a_1 a_2} \, {}^8\bar{F}^I_{\bar{a}_3\bar{a}_4} \right] \right\}. \qquad (2.59)
$$

The sum over a_i runs over the three different polarizations q_i, Δq_i and δq_i as well as over the different quark flavors q_i. The difference in color factor between the singlet and octet contributions are contained in c_8. For production of color singlet states, such as a γ, Z, W or Higgs bosons, $c_8 = 1$ with the prefactor in the definition (2.51) of the color octet.

To get the full DPS cross section, this formula has to be completed with the terms when the quarks and anti-quarks labels have been interchanged. For the cases involving mixed quark-antiquark DPDs the fermion number interference gives additional contributions, as discussed in the previous section. The mixed cases also give rise to other

$$\frac{s\,d\sigma}{\prod_{i=1}^{2} dx_i\,d\bar{x}_i\,d^2\boldsymbol{q}_i} \qquad \frac{s\,d\sigma}{\prod_{i=1}^{2} dx_i\,d\bar{x}_i}$$

For graph **a**: $\dfrac{1}{\Lambda^2 Q^2}$ and 1

For graph **b**: $\dfrac{1}{\Lambda^2 Q^2}$ and $\dfrac{\Lambda^2}{Q^2}$
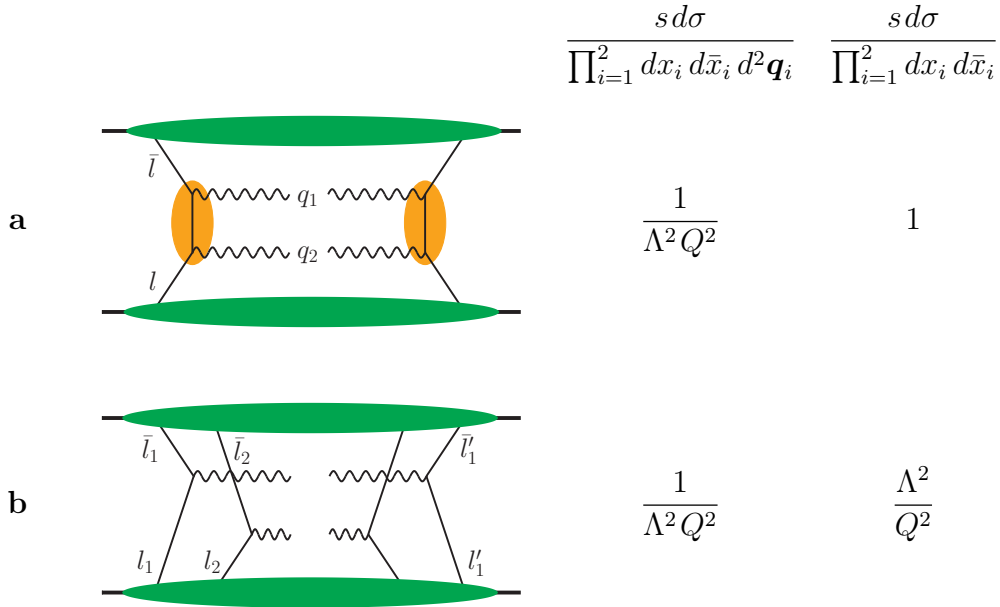
Figure 2.7: Example graphs for the production of a gauge boson pair via single and double parton scattering. Internal lines of the hard-scattering subgraphs are off shell by order Q^2 and partons emerging from the proton matrix elements are off shell by order Λ^2. Figure taken from [44].

types of flavor interferences, see figure 2.6(b). We will return to these flavor interference terms and discuss them in more detail when calculating the cross section for the double Drell-Yan process in chapter 3. For the full cross section the double parton scattering result has to be combined with the production of the same final state in a single hard interaction, as well as the interference between double and single parton scattering.

Power counting

For inclusive enough observables, such as the total cross section double parton scattering is power suppressed compared to single parton scattering

$$\frac{\sigma_{DPS}}{\sigma_{SPS}} \sim \frac{\Lambda^2}{Q^2}. \tag{2.60}$$

However, this is not the case for the cross section differential in the transverse momenta of the two hard interactions and in the region of small transverse momenta double and single parton scattering are of the same power. The power suppression arises when integrating over the transverse momenta due to the larger phase-space for the single parton scattering. In SPS $\boldsymbol{q}_1 + \boldsymbol{q}_2 \sim \Lambda$ but the difference can be of the order of the hard scale $\boldsymbol{q}_1 - \boldsymbol{q}_2 \sim Q$, while for DPS $\boldsymbol{q}_1 \sim \boldsymbol{q}_2 \sim \Lambda$. The power behavior of single and double parton graphs describing the production of gauge bosons are shown in figure 2.7.

2.3.4   Relation to single-parton distributions

The double parton distributions can be related to single-parton distributions. We will now discuss how to obtain such a relation and what kind of approximations are necessary. The decomposition of the DPDs in terms of single-parton distributions is only possible for the color singlet distributions of unpolarized partons and for simplicity we do not specify the flavor indices here.

   We insert a complete set of hadronic states between the two quark operators in (2.48). If one assumes that the proton state completely dominates this sum, the double parton distributions can be expressed as a product of two single-parton distributions [44]

$$F(x_1, x_2, \boldsymbol{z}_1, \boldsymbol{z}_2, \boldsymbol{y}) \approx \int d^2\boldsymbol{b} \; f\big(x_1, \boldsymbol{z}_1; \boldsymbol{b} + \boldsymbol{y} - \tfrac{1}{2}x_2\boldsymbol{z}_2\big) \, f\big(x_2, \boldsymbol{z}_2; \boldsymbol{b} + \tfrac{1}{2}x_1\boldsymbol{z}_1\big). \qquad (2.61)$$

The second argument of the single-parton distribution f is Fourier conjugate to the transverse quark momentum and the third argument gives the transverse position of the proton with respect to the quark, both averaged over the scattering amplitude and its conjugate. The shift of this argument by $\tfrac{1}{2}x_1\boldsymbol{z}_1$ or $-\tfrac{1}{2}x_2\boldsymbol{z}_2$ is a consequence of Lorentz invariance as explained in [43]. $\boldsymbol{b}$ is the vector from the proton's center of longitudinal momentum to the second hard interaction.

   For the collinear distributions the same approximations reduce to

$$F(x_1, x_2, \boldsymbol{y}) \approx \int d^2\boldsymbol{b} \; f\big(x_1; \boldsymbol{b} + \boldsymbol{y}\big) \, f\big(x_2; \boldsymbol{b}\big), \qquad (2.62)$$

where $f(x_1; \boldsymbol{b})$ is a generalized parton distribution. In the momentum representation (2.62) reads

$$F(x_1, x_2, \boldsymbol{r}) = f(x_1; \boldsymbol{r})f(x_2; \boldsymbol{r}), \qquad (2.63)$$

which we will use later for our investigation of the evolution of the transverse dependence of the double parton distributions in chapter 5.

2.4   Beyond tree level

2.4.1   Evolution of collinear double parton distributions

Deriving the evolution equations of the collinear DPDs in the transverse position ($\boldsymbol{y}$ dependent) representation, leads to evolution equations involving two independent DGLAP evolutions - one for each parton. The evolution equation for the DPD of two unpolarized quarks reads [44]

$$\frac{\partial f_{q_1 q_2}(x_1, x_2, y; \mu)}{\partial \log\mu^2} = \frac{\alpha_s}{2\pi} \bigg[P_{q_1 q_1} \otimes_1 f_{q_1 q_2} + P_{q_1 g} \otimes_1 f_{g q_2}$$
$$+ P_{q_2 q_2} \otimes_2 f_{q q_2} + P_{q_2 g} \otimes_2 f_{q_1 g} \bigg], \qquad (2.64)$$

where $\sum_q$ is a sum over the different quark flavors.

$$P_{ab}(\,.\,) \otimes_1 f_{bc}(\,.\,, x_2, y; \mu) = \int_{x_1}^{1-x_2} \frac{du_1}{u_1} P_{ab}\left(\frac{x_1}{u_1}\right) f_{bc}(u_1, x_2, y; \mu) \tag{2.65}$$

is a convolution in the first argument of the DPD, and analogously for $\otimes_2$, with the leading-order splitting function P_{ab} known from the DGLAP evolution of single parton distributions. The leading-order splitting functions are the same for quarks and anti-quarks, i.e. one has $P_{qq} = P_{\bar{q}\bar{q}}$, $P_{qg} = P_{\bar{q}g}$, $P_{gq} = P_{g\bar{q}}$ and there is no transition between quarks and antiquarks. We will discuss the evolution in more details in chapter 4.

If one derives the evolution equations in the r representation of the DPDs, some of the evolution equations contain an additional term with a single parton density, dubbed the single feed term. For example, the evolution of an unpolarized quark-antiquark distribution includes [44]

$$\frac{\alpha_s}{2\pi} \frac{1}{x_1 + x_2} P_{qg}\left(\frac{x_1}{x_1 + x_2}\right) f_g(x_1 + x_2), \tag{2.66}$$

describing the splitting of one gluon into the interacting quark-antiquark pair. The difference of the evolution equations between the r and y dependent DPDs can be understood as arising from an additional renormalization of $F_{q\bar{q}}(x_1, x_2, y)$ required at $y = 0$. This additional term has been discussed in [74–78] and is closely related to the separation between double and single parton scattering which will be discussed in the next section.

In the following chapters we will only make use of the homogeneous (y representation) evolution equation, for which we reserve the term double DGLAP evolution. We make this choice, because it is clear that the two independent evolutions will remain a part of the evolution of the DPDs, while at most parts of the single feed term should remain.

2.4.2   Double or single parton scattering?

Let us now touch upon a topic which has received much attention and invoked debate in the DPS community the last few years. The double parton scattering we have been dealing with so far, has been of the $2v2$ type as in figure 2.4 - where both partons are created non-perturbatively inside the proton. The two partons in the double scattering can however originate from a perturbative splitting described by the single feed term (2.66). This leads to $2v1$ ($1v2$) type of diagrams with a perturbative splitting in one of the protons and $1v1$ type of diagrams through perturbative splittings in both protons as shown in figure 2.8. The question arises if $1v1$ should be included in double partons scattering at all, or if it should be regarded as single parton scattering - leading to an issue of separation between single and double scattering. An intuitive answer to this question might be that it should be included as DPS only when the splitting occurs at a low enough scale. Implementing such a separation however turns out to be far from trivial.
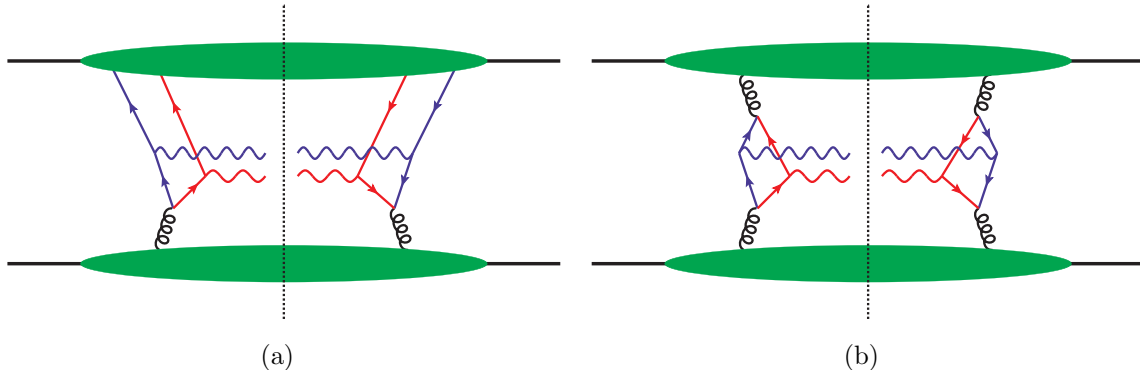
Figure 2.8: Example diagram for $2v1$ process (a) and the $1v1$ process (b).

The problem can be understood in the $\boldsymbol{y}$ representation. The double parton distributions for a quark and an antiquark behave as [44]

$$F_{q\bar{q}}(x_1, x_2, \boldsymbol{y}) \sim \frac{1}{\boldsymbol{y}^2} \tag{2.67}$$

for small $\boldsymbol{y}$. In the cross section this gives an integral over $\boldsymbol{y}$

$$\int d^2\boldsymbol{y} F_{q\bar{q}}(x_1, x_2, \boldsymbol{y}) \bar{F}_{q\bar{q}}(\bar{x}_1, \bar{x}_2, \boldsymbol{y}) \sim \int d^2\boldsymbol{y} \frac{1}{\boldsymbol{y}^4} \tag{2.68}$$

which has a quadratic divergence in $|\boldsymbol{y}|$. In the momentum representation the divergence originates in integrating an $\log(\boldsymbol{r}^2/\mu^2)$ dependent term which diverges at large $\boldsymbol{r}$.

The double parton scattering singularity has been extensively studied in [48], where it was shown that there is no power suppressed piece in the $1v1$ diagram which can be naturally included in DPS. Such a piece is however present in the $2v1$ diagrams [49].

Different solutions to the problem have been suggested in the literature. Invoking a cutoff of $\min(q_1^2, q_2^2)$ in the integral over $\boldsymbol{r}$ was advocated in [46]. [51] concluded that the two parton distributions have to be renormalized together at the level of the cross section to remove this ultraviolet divergency (since the two operators are evaluated at the same position when $\boldsymbol{y} = 0$). This leads to including the $2v2$ and $2v1$ diagrams as double parton scattering, but taking this literally might, strictly speaking, imply that one has to give up the concept of double parton distributions. Dropping the $1v1$ diagrams was also suggested by [42] with the statement that the $1v1$ diagram does not contain the low $\boldsymbol{q}_i$ enhancement characteristic for DPS. There are however concerns with such approaches, as discussed in [49] and alternative ways should still be investigated. These issues will not be further explored in this thesis, and we refer to the above references for more details on the topic.

2.4.3   Status of DPS factorization

The analysis of the tree level results above was concerned with the quark/antiquark initiated hard processes. The result can, at the tree level, be generalized to include

also processes which involves gluons in the initial state. As we now turn towards a discussion of factorization and effects of the exchange of additional gluons, we restrict our discussion to the case when the hard interactions produce color singlet states. For factorization involving the production of jets in hadron collisions, serious problems have been identified already in the case of a single hard scattering [70], and most likely these should be resolved before moving on to the more complicated case of two hard scatterings.

Although there exists no complete factorization proof for double parton scattering, important steps have been taken. For the production of color singlet states, [44] has shown that many elements of the factorization for single parton scattering [65, 79–81] can be applied also in the case of double parton scattering. In addition, some elements of a next-to-leading order factorization of the double Drell-Yan process have been given in [44]. For the transverse momentum integrated cross section, [50] showed that next-to-leading order factorization can be obtained in Soft Collinear Effective Theory (SCET), by means of the rapidity renormalization group introduced in [82, 83]. However, so far there have been no studies demonstrating a cancellation of soft gluons dominated by their transverse momenta, so called Glauber gluons, which was a substantial part of the proof of factorization in single Drell-Yan [65].

2.4.4 Gauge links

The operators defining the double parton distributions in our tree level analysis above are not gauge invariant. They need to be complemented by gauge links arising from collinear gluons. Collinear gluons, with polarization in the plus direction, exchanged between the right-moving proton and the hard interactions, are not power suppressed. Therefore an infinite number of such gluons have to be taken into account. Their leading-power contributions can be represented by gauge links (Wilson lines), which make the double parton distributions gauge invariant. The quark and antiquark fields in the DPDs are to be replaced by [43]

$$
\begin{aligned}
q_j(z) &\to [W(z,v)]_{jk}\, q_k(z)\,, \\
\bar{q}_j(z) &\to \bar{q}_k(z)\, \big[W^\dagger(z,v)\big]_{kj}
\end{aligned}
\tag{2.69}
$$

where the Wilson lines are defined as

$$
W(z,v) = P \exp\left[ig \int_0^\infty d\lambda v A^a(z - \lambda v) t^a \right].
\tag{2.70}
$$

P stands for path ordering while j and k are color indices. In order to avoid rapidity divergences in the parton distributions the direction v of the Wilson lines has to be tilted away from the light-cone [79, 81]. This gives rise to an additional parameter

$$
\zeta^2 = \frac{(2pv)^2}{|v^2|}
\tag{2.71}
$$

in the parton distributions. The choice of scale of this parameter is the hard scale Q. Complementing the DPDs with the Wilson lines changes the operators for two quarks in (2.48) into [44]

$$
[\bar{q}(-\tfrac{1}{2}z_2)W^\dagger(-\tfrac{1}{2}z_2;v)]_{k'}\Gamma_{a_2}[W(\tfrac{1}{2}z_2;v)q(\tfrac{1}{2}z_2)]_k
$$
$$
\times\, [\bar{q}(y-\tfrac{1}{2}z_1)W^\dagger(y-\tfrac{1}{2}z_1;v)]_{j'}\Gamma_{a_1}[W(y+\tfrac{1}{2}z_1;v)q(y+\tfrac{1}{2}z_1)]_j\Big|_{z_i^+=y^+=0}, \tag{2.72}
$$

for the color singlet DPDs. In addition to these Wilson lines from the collinear gluons, there can be exchanges of soft gluons between left and right moving partons. These give rise to a soft factor in the cross section, which is a vacuum expectation value of Wilson lines. Also the parton distributions include soft gluon momenta and one have to be careful no to double count the contributions [65, 80, 81].

2.4.5   Sudakov logarithms

Measured transverse momenta of the vector bosons $\boldsymbol{q}_i$ much smaller than the hard scale Q give rise to large Sudakov logarithms $\log|\boldsymbol{q}_i|/Q$. In order to obtain perturbatively stable results these logarithms have to be resummed to all order. In [44] the formalism for single gauge boson production [84] has been extended to double Drell-Yan. The dependence of the two quark distribution on the rapidity parameter ζ in (2.71) is given by [43]

$$
\frac{d}{d\log\zeta}\begin{pmatrix}{}^1F_{qq}\\{}^8F_{qq}\end{pmatrix} = [G(x_1\zeta,\mu)+G(x_2\zeta,\mu)+K(\boldsymbol{z}_1,\mu)+K(\boldsymbol{z}_2,\mu)]\begin{pmatrix}{}^1F_{qq}\\{}^8F_{qq}\end{pmatrix}
$$
$$
+\, \boldsymbol{M}(\boldsymbol{z}_1,\boldsymbol{z}_2,\boldsymbol{y})\begin{pmatrix}{}^1F_{qq}\\{}^8F_{qq}\end{pmatrix}, \tag{2.73}
$$

where the functions $G(x_i\zeta,\mu)$ and $K(\boldsymbol{z}_i,\mu)$ are known from the Collins-Soper equation of single parton scattering [79]. The matrix $\boldsymbol{M}$ couples the color singlet and color octet distributions and describes a dependence on ζ specific for double parton distributions. The general solution to this equation is

$$
\begin{pmatrix}{}^1F_{qq}(x_1,x_2,\boldsymbol{z}_1,\boldsymbol{z}_2,\boldsymbol{y};\zeta)\\{}^8F_{qq}(x_1,x_2,\boldsymbol{z}_1,\boldsymbol{z}_2,\boldsymbol{y};\zeta)\end{pmatrix} = \mathrm{e}^{-S(x_1\zeta,\boldsymbol{z}_1,\boldsymbol{z}_2)-S(x_2\zeta,\boldsymbol{z}_1,\boldsymbol{z}_2)}
$$
$$
\times\, \mathrm{e}^{\log\frac{\sqrt{x_1x_2}\zeta}{\mu_0}\boldsymbol{M}(\boldsymbol{z}_1,\boldsymbol{z}_2,\boldsymbol{y})}\begin{pmatrix}{}^1F_{qq}^{\mu_0}(x_1,x_2,\boldsymbol{z}_1,\boldsymbol{z}_2,\boldsymbol{y})\\{}^8F_{qq}^{\mu_0}(x_1,x_2,\boldsymbol{z}_1,\boldsymbol{z}_2,\boldsymbol{y})\end{pmatrix} \tag{2.74}
$$

with

$$
S(x\zeta,\boldsymbol{z}_1,\boldsymbol{z}_2) = -\tfrac{1}{2}\left[K(\boldsymbol{z}_1,\mu_0)+K(\boldsymbol{z}_2,\mu_0)\right]\log\frac{x\zeta}{\mu_0}
$$
$$
+ \int_{\mu_0}^{x\zeta}\frac{d\mu}{\mu}\left[\gamma_K(\alpha_s(\mu))\log\frac{x\zeta}{\mu}-G(\mu,\mu)\right]. \tag{2.75}
$$
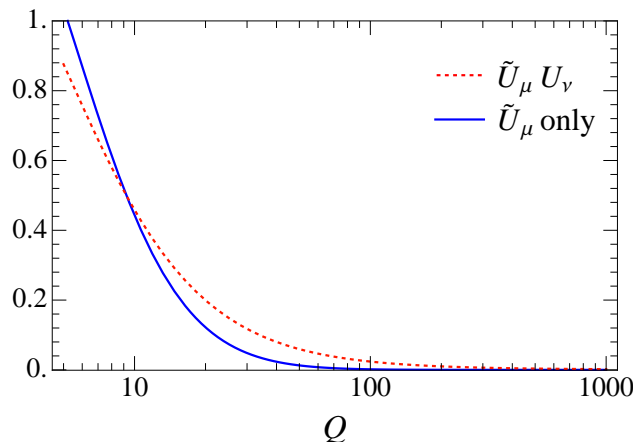
Figure 2.9: Sudakov suppression factor, with and without rapidity resummation, of the color interference in double Drell-Yan, where $C_V - C_R = N_c/2$. Figure taken from [50].

γ_K is the anomalous dimension from the renormalization group equation for K and G,

$$\gamma_K(\alpha_s(\mu)) = \frac{dG(x\zeta, \mu)}{d\log\mu} = -\frac{dK(\boldsymbol{z}, \mu)}{d\log\mu}. \tag{2.76}$$

The double logs, which come from the integral in (2.75) are the same as the double logs in single parton scattering. To double logarithmic accuracy, the Sudakov factors of double gauge boson production are thus a product of those for the single parton scattering production of a gauge boson.

For the DPDs including partons which do not couple to color singlets in each hard collision there is another type of Sudakov factor [44, 50, 85]

$$\tilde{U}_\mu = \exp\left[-\frac{\alpha_s}{2\pi}(C_V - C_R)\ln^2(\frac{Q^2}{\Lambda^2})\right]. \tag{2.77}$$

For color singlet distributions the color factors $C_V = C_R = C_F$ and (2.77) reduces to unity, but for distributions of other color configurations the different color factors for the emission of virtual and real gluons give $C_V - C_R \geq 0$. This leads to a Sudakov suppression of double parton scattering with color and fermion number interference. The suppression can be intuitively explained as arising due to a transportation of color over a long distance inside the proton [50]. For the production of bosons with large virtualities Q the color interference and fermion number interference can thus be neglected. The numerical size of the suppression is demonstrated in figure 2.9.

2.5 Model estimations

The double parton distributions has been examined in the MIT bag model [86], where sizable double parton correlations were found for spin, flavor and momentum fractions,
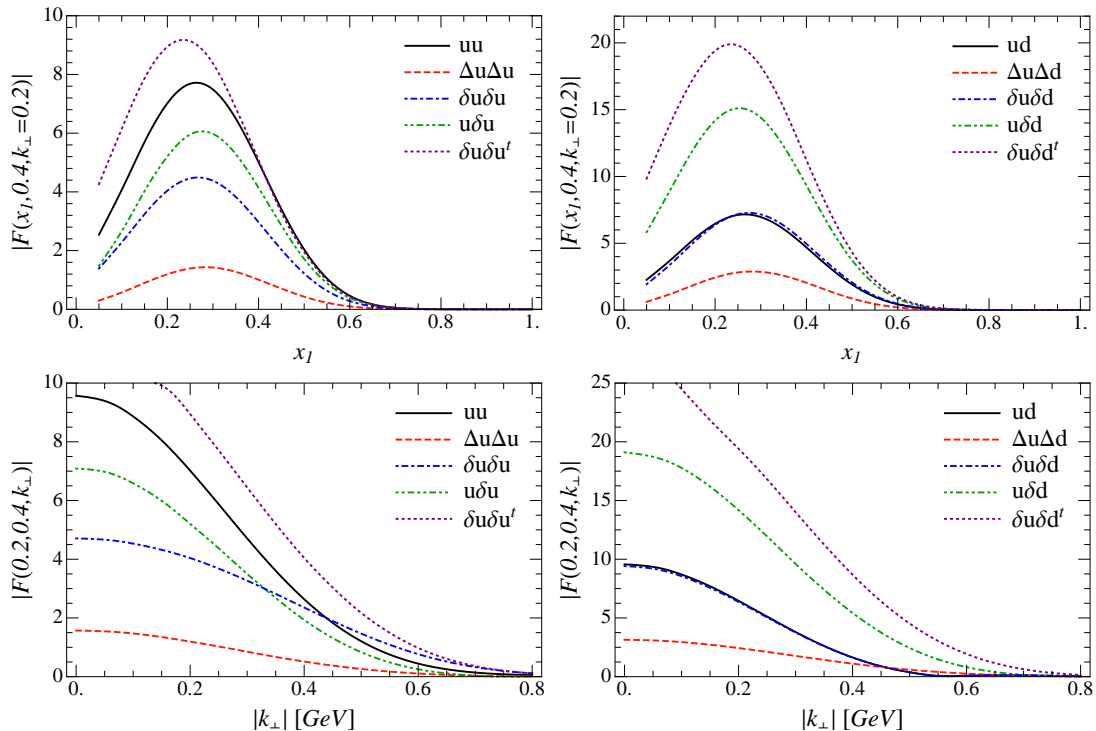
Figure 2.10: Double parton distributions in the MIT bag model. Figure taken from [86].

but only a weak interplay with transverse momenta. The double parton distributions obtained for different polarizations are shown in figure 2.10, demonstrating the large correlation between the polarizations of the partons. The unpolarized double parton distributions were also studied in two constituent quark models [57], one non-relativistic SU(6) symmetric model and one with a slight breaking of this symmetry. This study was not concerned with polarization effects, but for the unpolarized case strong correlations between longitudinal momentum fractions were found in both models - violating a factorization into one x_1 and one x_2 dependent function. Further, the correlation between momentum fractions and transverse momentum was found to be small, but model dependent. It was pointed out that the small correlation was a result of the dominance of the S-wave, and that models with larger contributions from wave functions with larger angular momentum would lead to stronger correlations.

2.6   Experimental status

Double parton scattering has a long experimental history. Experimental evidence for double parton interactions was first seen at the ISR [31]. Since then it has been seen at the SPS [32] and the Tevatron [33–37]. Due to the rapid increase of parton densities at small momentum fractions, one expects multiparton interactions to be even more prominent at the LHC, and first measurements have been made [38, 39].

Experiment	σ_{eff} [mb]	Process	Collider	$\sqrt{s}$ [TeV]
ATLAS [38]	$15 \pm 3^{+5}_{-3}$	Wjj	LHC	7
D0 [36]	$16.4 \pm 0.3 \pm 2.3$	$\gamma + 3 \times j$	Tevatron	1.96
CDF [35]	$14.5 \pm 1.7^{+1.7}_{-2.3}$	$\gamma/\pi^0 + 3 \times j$	Tevatron	1.8
CDF [33]	$12.1^{+10.7}_{-5.4}$	$4 \times j$	Tevatron	1.8

Table 2.1: Measured values of σ_{eff} at Tevatron and LHC.

Ignoring all spin, color, flavor and fermion number correlations effectively reduces the transverse momentum integrated cross section to (2.36). If one further assumes that the $\boldsymbol{y}$ dependence can be factorized from the x_i and $\bar{x}_i$ dependence and that it is the same for all partons, then $F(x_1, x_2, \boldsymbol{y})\bar{F}(\bar{x}_1, \bar{x}_2, \boldsymbol{y}) = F(x_1, x_2)\bar{F}(\bar{x}_1, \bar{x}_2)F(\boldsymbol{y})$. Making the additional assumptions that the longitudinal dependence on the two momentum fractions separate and that they separate into two normal parton distributions, then $F(x_1, x_2) = f(x_1)f(x_2)$. The double parton cross section can then be written in terms of single parton cross sections

$$\frac{d\sigma_{DPS}}{\prod_{i=1}^{2} dx_i d\bar{x}_i} = \frac{1}{C}\frac{d\sigma_1 d\sigma_2}{\sigma_{\text{eff}}} \tag{2.78}$$

where

$$\frac{1}{\sigma_{\text{eff}}} = \int d^2\boldsymbol{y} F(\boldsymbol{y}). \tag{2.79}$$

In past experiments, the focus has been on measuring σ_{eff}. Such measurement, although suffering from the difficulty to separate single and double parton scattering, are important. They can provide an estimate for the size of DPS cross sections and to some extent test the factorized ansatz (2.78). For example, a process dependence of σ_{eff} would indicate a breakdown of some of the approximations. A summary of the experimental status on σ_{eff} can be found in table 2.1 and figure 2.11 which shows the dependence of the measurements on the center of mass energy. The CDF measurement with γ/π^0+ three jets in uses a non-standard definition of σ_{eff} excluding events with 3 or more hard scatterings, as pointed out in [87]. Using instead an inclusive definition, [88] has obtained a new value for sigma effective $\sigma_{eff} = 12.0 \pm 1.4^{+1.3}_{-1.5}$ from the same measurement.

There are interesting measurements reported recently by LHCb for double charm production [39], which with a DPS interpretation, give a varying σ_{eff} depending on the produced hadrons. As an example the $D^0 D^0$ mode gives $\sigma_{\text{eff}} = 42 \pm 3 \pm 4$ mb while the $J/\Psi D^0$ mode gives $\sigma_{\text{eff}} = 14.9 \pm 0.4 \pm 1.1^{+2.3}_{-3.1}$ mb.
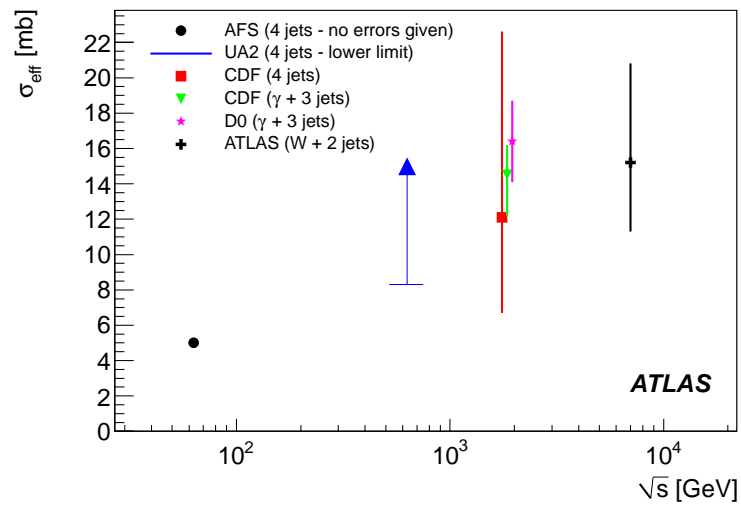
Figure 2.11: σ_{eff} as a function of center of mass energy. Figure taken from [38].

Chapter 3

The double Drell-Yan process

3.1 Introduction

Armed with the framework presented in the previous chapter, we now turn towards a detailed study of the correlations between the polarization of two partons in an unpolarized proton. We investigate how the correlations affect the overall rate and the final-state distributions in double hard scattering. We build on observations made in [44] and extend the results of [50]. The relevance of spin correlations in DPS was first pointed out in [72, 89] but not followed up until recently.

Our studying takes place at the stage set by the double Drell-Yan process, where each of the two hard interactions produce an electroweak gauge bosons (γ^*, Z, $W^\pm$) through quark-antiquark annihilation, followed by their leptonic decay. The Drell-Yan process has provided many insights in single parton scattering and the double Drell-Yan process has long been recognized as a prototype for double parton interactions [72, 90, 91]. Recent phenomenological studies have unfortunately shown that the rates expected for double Drell-Yan production at the LHC is likely too small to allow for detailed experimental analysis of the final-state distributions [9, 92]. However, we choose this process for our investigation, since it from a theoretical point of view is among the simplest double parton scattering processes but anyhow provides a wealth of nontrivial features. The results we obtain for the double Drell-Yan process will have analogs in other processes with higher rates. For example the production of a gauge boson associated with two jets or production of four jet final states. Note that the graph for the tree-level production of a gauge boson with subsequent decay only differs from the graph for $qq \rightarrow qq$ via an s-channel gluon by an overall color factor.

This chapter is organized as follows. In the next section we set the stage for the double Drell-Yan processes, decompose the double parton distributions involved and define the reference frames used. In section 3.4 we give our results for the cross section of the double Drell-Yan process. Section 3.5 summarizes our findings. In appendix A we list the coupling factors entering the cross section formula in section 3.4.

3.2   Setting the stage

Consider the production of two gauge bosons $V_1, V_2 = \gamma^*, Z, W$ in a pp collision, followed by the leptonic decays $\gamma^*, Z \to \ell^+\ell^-$ or $W \to \ell\nu$. Four-momenta are assigned as $p(p) + p(\bar{p}) \to V_1(q_1) + V_2(q_2) + X$. We are interested in the fully differential cross section of the four-lepton final state and restrict ourselves to the kinematic region where the transverse momenta $\boldsymbol{q}_1$ and $\boldsymbol{q}_2$ of the gauge bosons in the pp center-of-mass are much smaller than their invariant masses, i.e. we assume $\boldsymbol{q}_1^2, \boldsymbol{q}_2^2 \ll q_1^2, q_2^2$. As discussed in the previous chapter, for such kinematics the double parton scattering is not power suppressed compared to the production of the gauge boson pair by a single hard scattering. In the calculation of the cross section, the invariant mass $Q_i = (q_i^2)^{1/2}$ will serve as the hard scale necessary for the application of factorization. For simplicity we shall not assume any particular hierarchy in size between $\boldsymbol{q}_1$ and $\boldsymbol{q}_2$ or between Q_1 and Q_2.

We assume that the double hard scattering cross section factorizes as in (2.59) into the product of a double parton distribution in each proton and a parton-level cross section for each of the two hard scatters. Schematically, the double Drell-Yan cross section then reads

$$
\frac{d\sigma}{\prod_{i=1}^{2} dx_i\, d\bar{x}_i\, d^2\boldsymbol{q}_i\, d\Omega_i} \bigg|_{\mathrm{DDY}} = \frac{1}{C} \frac{d\hat{\sigma}_1}{d\Omega_1} \frac{d\hat{\sigma}_2}{d\Omega_2} \int \frac{d^2\boldsymbol{z}_1}{(2\pi)^2} \frac{d^2\boldsymbol{z}_2}{(2\pi)^2}\, e^{-i\boldsymbol{z}_1\boldsymbol{q}_1 - i\boldsymbol{z}_2\boldsymbol{q}_2}
$$

$$
\times \int d^2\boldsymbol{y}\, F(x_1, x_2, \boldsymbol{z}_1, \boldsymbol{z}_2, \boldsymbol{y})\, \bar{F}(\bar{x}_1, \bar{x}_2, \boldsymbol{z}_1, \boldsymbol{z}_2, \boldsymbol{y}) \qquad (3.1)
$$

with the cross section $d\hat{\sigma}_i/d\Omega_i$ for quark-antiquark annihilation into a lepton pair via the gauge boson V_i, taken differential w.r.t. the lepton angles in the appropriate boson rest frame (see section 3.2.2). In the pp center-of-mass we define the z axis to point into the direction of the proton momentum p. The factorization formula (3.1) generalizes the expression for single Drell-Yan production in terms of transverse-momentum dependent single parton densities [65, 79].

Integrating (3.1) over the transverse boson momenta $\boldsymbol{q}_1$ and $\boldsymbol{q}_2$ one obtains

$$
\frac{d\sigma}{\prod_{i=1}^{2} dx_i\, d\bar{x}_i\, d\Omega_i} \bigg|_{\mathrm{DDY}} = \frac{1}{C} \frac{d\hat{\sigma}_1}{d\Omega_1} \frac{d\hat{\sigma}_2}{d\Omega_2} \int d^2\boldsymbol{y}\, F(x_1, x_2, \boldsymbol{y})\, \bar{F}(\bar{x}_1, \bar{x}_2, \boldsymbol{y}) \,. \qquad (3.2)
$$

Equations (3.1) and (3.2) are schematic in that they omit labels for and summation over the quantum numbers of the partons (quarks vs. antiquarks, flavor, polarization and color). This information will be restored in section 3.3. We emphasize that these equations only give one contribution to the cross section for four-lepton production. Further contributions need to be added from the familiar single hard-scattering mechanism (where the four leptons are produced in a single parton-level process), the interference between single and double hard scattering, as well as double hard-scattering graphs with fermion number interference as discussed in section 2.3.2. The single hard-scattering contribution is straightforward to compute (see e.g. [92]), whereas the different interference contributions are not. The fermion number interference will be suppressed at larger Q_i by the Sudakov factor discussed in section 2.4.5, and as argued in [44] become relatively unimportant at small momentum fractions $x_i, \bar{x}_i$.
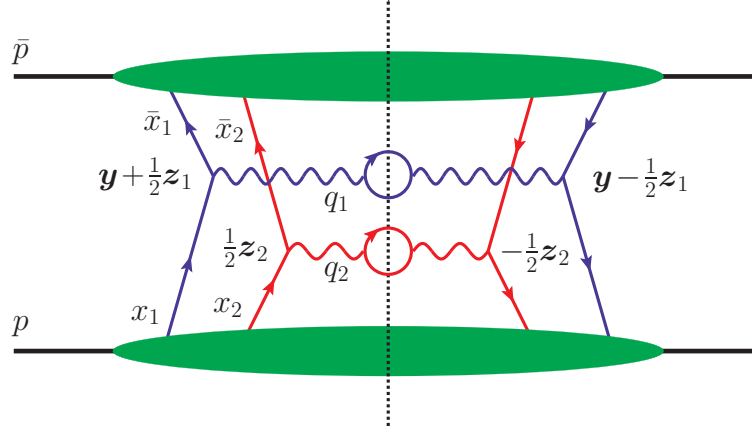
Figure 3.1: A graph for the double Drell-Yan process, where two quarks in the right-moving proton interact with two antiquarks in the left-moving proton. The figure shows the assignment of four-momenta (p, $\bar{p}$, q_1, q_2), of light-cone momentum fractions (x_i, $\bar{x}_i$) and of transverse position arguments as explained in the text. The dotted vertical line denotes the final-state cut.

3.2.1 Decomposition of double parton distributions

Let us now classify the different double parton distributions for the combinations of quark polarization of (2.48), taking into account the constraints of parity invariance [44]. For unpolarized and longitudinally polarized quarks we have

$$F_{qq} = f_{qq}(x_1, x_2, \boldsymbol{z}_1, \boldsymbol{z}_2, \boldsymbol{y}), \qquad\qquad F_{\Delta q \Delta q} = f_{\Delta q \Delta q}(x_1, x_2, \boldsymbol{z}_1, \boldsymbol{z}_2, \boldsymbol{y}),$$
$$F_{q \Delta q} = g_{q \Delta q}(x_1, x_2, \boldsymbol{z}_1, \boldsymbol{z}_2, \boldsymbol{y}), \qquad\qquad F_{\Delta qq} = g_{\Delta qq}(x_1, x_2, \boldsymbol{z}_1, \boldsymbol{z}_2, \boldsymbol{y}), \qquad (3.3)$$

where f denotes scalar and g pseudoscalar functions. $f_{\Delta q \Delta q}$ describes to which degree the helicities of the two quarks are aligned rather than anti-aligned, while $g_{\Delta qq}$ describes a correlation between the helicity of the quark and cross-products of the transverse position vectors of the partons, $\boldsymbol{z}_1$, $\boldsymbol{z}_2$ and $\boldsymbol{y}$. For transverse quark polarization the parton distributions carry a transverse index and can be decomposed as

$$F_{\Delta q \delta q}^{i} = M \left(\boldsymbol{y}^i f_{\Delta q \delta q} + \tilde{\boldsymbol{y}}^i g_{\Delta q \delta q} \right), \qquad\qquad F_{\delta q \Delta q}^{i} = M \left(\boldsymbol{y}^i f_{\delta q \Delta q} + \tilde{\boldsymbol{y}}^i g_{\delta q \Delta q} \right),$$
$$F_{q \delta q}^{i} = M \left(\tilde{\boldsymbol{y}}^i f_{q \delta q} + \boldsymbol{y}^i g_{q \delta q} \right), \qquad\qquad F_{\delta qq}^{i} = M \left(\tilde{\boldsymbol{y}}^i f_{\delta qq} + \boldsymbol{y}^i g_{\delta qq} \right), \qquad (3.4)$$

where the scalar and pseudoscalar functions depend on the same variables as in (3.3). Here $\tilde{\boldsymbol{y}}^i = \epsilon^{ij} \boldsymbol{y}^j$ is a transverse vector orthogonal to $\boldsymbol{y}^i$, defined in terms of the two-dimensional antisymmetric tensor ϵ^{ij} (with $\epsilon^{12} = 1$). Factors of the proton mass M have been introduced in order to have the same mass dimension for all distributions f and g. For two transversely polarized quarks we finally write

$$F_{\delta q \delta q}^{ij} = \delta^{ij} f_{\delta q \delta q} + M^2 \left(2 \boldsymbol{y}^i \boldsymbol{y}^j - \boldsymbol{y}^2 \delta^{ij} \right) f_{\delta q \delta q}^{t}$$
$$+ M^2 \left(\boldsymbol{y}^i \tilde{\boldsymbol{y}}^j + \tilde{\boldsymbol{y}}^i \boldsymbol{y}^j \right) g_{\delta q \delta q}^{s} + M^2 \left(\boldsymbol{y}^i \tilde{\boldsymbol{y}}^j - \tilde{\boldsymbol{y}}^i \boldsymbol{y}^j \right) g_{\delta q \delta q}^{a}. \qquad (3.5)$$

Decompositions analogous to (3.3) to (3.5) hold for antiquarks and for flavor interference distributions.

Corresponding definitions apply for two partons in a left-moving proton, with $+$ and $-$ components interchanged in (2.48) to (2.50). Note that the covariant expression of the two-dimensional antisymmetric tensor in terms of the four-dimensional one is $\epsilon^{ij} = \epsilon^{+-ij}$ (with $\epsilon_{0123} = 1$). In the analogs of (3.3) to (3.5) for left-moving partons one hence needs to change the sign of $\tilde{\boldsymbol{y}}$ and of the pseudoscalar functions g (which can be written as ϵ^{ij} contracted with a parity even tensor constructed from $\boldsymbol{z}_1$, $\boldsymbol{z}_2$ and $\boldsymbol{y}$).

All distributions discussed so far allow for the two color structures of section 2.3.2, one where the two fields in the operator $\mathcal{O}_{a_i}$ are coupled to a color singlet and one where they are coupled to a color octet. This requires a further index on all distributions, which we will not display in the present chapter for brevity.

For the distributions integrated over transverse momenta, the number of different distributions decrease:

$$\begin{aligned}
F_{qq}(x_1, x_2, \boldsymbol{y}) &= f_{qq}(x_1, x_2, y)\,, \\
F_{\Delta q \Delta q}(x_1, x_2, \boldsymbol{y}) &= f_{\Delta q \Delta q}(x_1, x_2, y)\,, \\
F^j_{\Delta q \delta q}(x_1, x_2, \boldsymbol{y}) &= \boldsymbol{y}^j M f_{\Delta q \delta q}(x_1, x_2, y)\,, \\
F^j_{\delta q \Delta q}(x_1, x_2, \boldsymbol{y}) &= \boldsymbol{y}^j M f_{\delta q \Delta q}(x_1, x_2, y)\,, \\
F^j_{q \delta q}(x_1, x_2, \boldsymbol{y}) &= \tilde{\boldsymbol{y}}^j M f_{q \delta q}(x_1, x_2, y)\,, \\
F^j_{\delta q q}(x_1, x_2, \boldsymbol{y}) &= \tilde{\boldsymbol{y}}^j M f_{\delta q q}(x_1, x_2, y)\,, \\
F^{jj'}_{\delta q \delta q}(x_1, x_2, \boldsymbol{y}) &= \delta^{jj'} f_{\delta q \delta q}(x_1, x_2, y) + M^2 \left(2\boldsymbol{y}^i \boldsymbol{y}^j - \boldsymbol{y}^2 \delta^{ij}\right) f^t_{\delta q \delta q}(x_1, x_2, y)\,.
\end{aligned} \qquad (3.6)$$

Note that all pseudoscalar distributions g in (3.3) to (3.5) have vanished since one cannot create a pseudoscalar with only one vector $\boldsymbol{y}$, and in addition the color singlet distribution with $\Delta q \delta q$ ($\delta q \Delta q$) vanish due to time reversal. The transverse polarizations describe an interference between quarks of different helicities. As we shall see in chapter 4, $f^t_{\delta q \delta q}$ describes the case when the helicity interference results in a helicity difference of two units between the amplitude and the conjugate amplitude, while $f_{\delta q \delta q}$ describes the case when the helicity interferences in the two interactions compensate one another.

3.2.2   Reference frames

Let us now introduce the reference frames and coordinate axes needed to describe the angular dependence of the cross section. The angles describing the decay of the vector bosons will be defined in restframes of the respective boson. However, as we will demonstrate, the azimuthal angles can, to the accuracy of our calculation, be taken with respect to the X-axis in the pp center of mass frame - leading to substantial simplifications.

In the pp center-of-mass we have the z axis as in chapter 2 pointing along the momentum p. The four-vector defining this axis is hence

$$Z^\mu = (p - \bar{p})^\mu / \sqrt{2p\bar{p}}\,, \qquad (3.7)$$
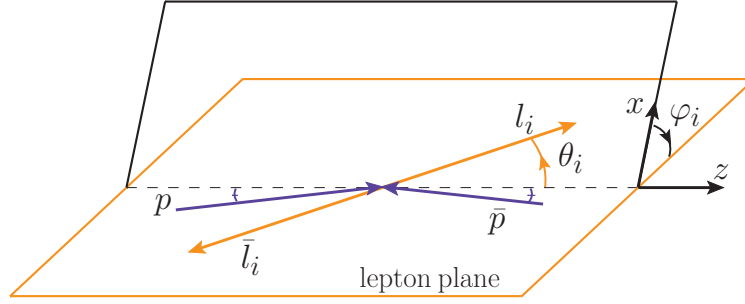
Figure 3.2: Coordinate system in the rest frame of vector boson V_i. The z axis bisects the angle between the spatial components of the momenta p and $-\bar{p}$, and the x axis corresponds to a fixed reference direction as explained in the text. (In general, the proton momenta are therefore not in the x-z plane.) l_i and $\bar{l}_i$ are the momenta of the lepton and the antilepton from the boson decay, respectively. θ_i denotes the polar and φ_i the azimuthal angle of the lepton. Note that φ_i is negative in this example.

where we neglect the proton mass here and in the following. We choose a fixed four-vector X^μ orthogonal to p and $\bar{p}$ to define the x axis. The precise choice does not matter for our purpose, but one may for instance adopt the convention to have the x direction point towards the center of the LHC ring. The y axis is then defined such that we obtain a right-handed coordinate system; the corresponding four-vector can be written as

$$Y^\mu = \epsilon^\mu{}_{\nu\rho\sigma} X^\nu \bar{p}^\rho p^\sigma / (p\bar{p}). \tag{3.8}$$

In order to describe the kinematics of the gauge boson decays into lepton pairs we define the z axis in the rest frame of the boson V_i by the four-vector

$$Z_i^\mu = \frac{1}{2}\sqrt{Q_i^2 + \boldsymbol{q}_i^2} \left[\frac{p^\mu}{pq_i} - \frac{\bar{p}^\mu}{\bar{p}q_i} \right], \tag{3.9}$$

where $\boldsymbol{q}_i$ is the transverse boson momentum in the pp center-of-mass as before. As illustrated for one boson in figure 3.2, the z axis bisects the angle between the spatial components of p and $-\bar{p}$ in the boson rest frame. The x axis is specified in terms of the pp center-of-mass axis X^μ by

$$X_i^\mu = \frac{1}{\sqrt{1 + (Xq_i)^2/Q_i^2}} \left[X^\mu - \frac{Xq_i}{Q_i^2} q_i^\mu \right] \tag{3.10}$$

and the y axis is again defined to obtain a right-handed coordinate system, i.e. by $Y_i^\mu = \epsilon^\mu{}_{\nu\rho\sigma} Z_i^\nu X_i^\rho q_i^\sigma / Q_i$. With these reference axes we define the polar and azimuthal angles θ_i and φ_i of the lepton (as opposed to the antilepton) in the decay of V_i, i.e. of ℓ^- in the decay of a γ^*, Z or W^- and of ν_ℓ in the decay of a W^+.

Noting that $X q_i$ is the x component of q_i in the pp center-of-mass, we see in (3.10) that X_1, X_2 and X differ from each other by terms of order $|\boldsymbol{q}_i|/Q_i$, which is a small parameter in our calculation of the cross section. Likewise, one finds differences of order $|\boldsymbol{q}_i|/Q_i$ between Y_1, Y_2 and Y. As we shall see shortly, this greatly simplifies the discussion of azimuthal angles in our calculation.

The physical cross section must of course not depend on the arbitrary fixed direction specified by X^μ. To understand how this happens, we anticipate that our results will depend only on the *difference* of azimuthal angles whose definition depends on X^μ, such as for instance $\varphi_1 - \varphi_2$. These angles are defined in different frames, but to the accuracy of our calculation we can replace them with the azimuthal angles of the leptons in the pp center-of-mass. This can be seen by writing trigonometric functions of φ_i in terms of invariant products $X_i l_i$ and $Y_i l_i$, where l_i is the four-momentum of the lepton from the decay of V_i. When calculating the cross section we neglect terms of order $|\boldsymbol{q}_i|/Q_i$ and can hence approximate $X_i l_i \approx X l_i$ and $Y_i l_i \approx Y l_i$, which gives azimuthal angles in the pp center-of-mass as announced.

Readers familiar with the analysis of single Drell-Yan production will recognize that our choice of z axes is the same as in the Collins-Soper frame [93]. Useful information about this frame can e.g. be found in [94, 95]. By contrast, we define x axes (and thus the azimuthal angles φ_i) starting from a fixed direction in space, whereas in the Collins-Soper frame the x axis is defined such that the proton momenta lie in the x-z plane. The latter choice becomes undefined when the transverse boson momentum in the pp center-of-mass goes to zero. For unpolarized single Drell-Yan production this is not a problem because in this limiting case all azimuthal dependence in the cross section must vanish due to rotation invariance. However, in the double Drell-Yan process there can be an azimuthal dependence even if $\boldsymbol{q}_1$ or $\boldsymbol{q}_2$ or both go to zero, as we shall see. Choosing one of these vectors (or any linear combination of them) to define x axes would therefore entail ill-defined azimuthal angles at some point in phase space where there can be a nontrivial azimuthal dependence.

3.3 Hard-scattering cross sections

If we restore the labels for quarks and antiquarks, their flavor and their polarization, the cross section formula (3.1) reads

$$
\frac{d\sigma}{\prod_{i=1}^{2} dx_i \, d\bar{x}_i \, d^2\boldsymbol{q}_i \, d\Omega_i} = \frac{1}{C} \sum_{a_1 a_2 a_3 a_4} \int \frac{d^2\boldsymbol{z}_1}{(2\pi)^2} \frac{d^2\boldsymbol{z}_2}{(2\pi)^2} \, e^{-i\boldsymbol{z}_1 \boldsymbol{q}_1 - i\boldsymbol{z}_2 \boldsymbol{q}_2} \int d^2\boldsymbol{y}
$$

$$
\times \left[\frac{d\hat{\sigma}_{a_1\bar{a}_3}}{d\Omega_1} \frac{d\hat{\sigma}_{a_2\bar{a}_4}}{d\Omega_2} F_{a_1 a_2} \bar{F}_{\bar{a}_3 \bar{a}_4} + \frac{d\hat{\sigma}_{a_1\bar{a}_3}}{d\Omega_1} \frac{d\hat{\sigma}_{\bar{a}_2 a_4}}{d\Omega_2} F_{a_1 \bar{a}_2} \bar{F}_{\bar{a}_3 a_4} \right.
$$

$$
\left. + \frac{d\hat{\sigma}_{\bar{a}_1 a_3}}{d\Omega_1} \frac{d\hat{\sigma}_{a_2\bar{a}_4}}{d\Omega_2} F_{\bar{a}_1 a_2} \bar{F}_{a_3 \bar{a}_4} + \frac{d\hat{\sigma}_{\bar{a}_1 a_3}}{d\Omega_1} \frac{d\hat{\sigma}_{\bar{a}_2 a_4}}{d\Omega_2} F_{\bar{a}_1 \bar{a}_2} \bar{F}_{a_3 a_4} \right]
$$

$$
+ \{\text{flavor interference}\} , \tag{3.11}
$$

where here and in the following we omit the label "DDY" for double Drell-Yan. In all terms the DPDs have arguments as in (3.1), which will be omitted henceforth for brevity. To distinguish the distributions for the left- and right-moving proton we use the notation F and $\bar{F}$, as in chapter 2, and a corresponding notation for the scalar and pseudoscalar functions $f, \bar{f}$ and $g, \bar{g}$ introduced in section 3.2.1. The first subscript in $d\sigma_{a_i \bar{a}_j}$ and $d\sigma_{\bar{a}_i a_j}$ denotes the right-moving parton and the second subscript the left-moving one. The sum over a_1 to a_4 runs over all quark flavors and polarizations $(q, \Delta q, \delta q)$.

The flavor interference terms involve the interference DPDs in (2.56) and corresponding interference terms for the hard scattering. These interference terms only appear if the produced bosons are both neutral or both charged, otherwise the quark and antiquark flavors in the annihilation processes do not match. We will return to this in the next section.

Labels for the color structure of the DPDs are not displayed in (3.11). With the conventions specified in 2.3.2, each factor $F \bar{F}$ is to be replaced with the sum ${}^1F \, {}^1\bar{F} + {}^8F \, {}^8\bar{F}$ of color singlet and color octet distributions, without change in the hard-scattering cross sections. This holds for the production of arbitrary color-neutral states in the hard-scattering processes.

It is straightforward to compute the tree-level cross section for quark-antiquark annihilation into a gauge boson followed by its leptonic decay. In accordance with the power counting scheme underlying the cross section formula (3.11), the transverse boson momenta $\boldsymbol{q}_i$ are set to zero in this calculation since by assumption they are small compared with the invariant mass Q_i. This also simplifies the kinematics of the gauge boson decays as we already noticed in section 3.2.2.

Consider first the case where both quark and antiquark are unpolarized or longitudinally polarized. The angular dependence of the cross section is then of the form

$$\frac{d\hat{\sigma}_{a_i \bar{a}_j}}{d\Omega_i} = \left(1 + \cos^2 \theta_i\right) K_{a_i \bar{a}_j}(Q_i) + 2 \cos \theta_i \, K'_{a_i \bar{a}_j}(Q_i), \tag{3.12}$$

with $a_i = q_i, \Delta q_i$ and $\bar{a}_j = \bar{q}_j, \Delta \bar{q}_j$. The integration element reads $d\Omega_i = d\varphi_i \, d\cos \theta_i$ as usual. The factors K and K' depend on coupling constants and on Q_i via the gauge boson propagators. One easily finds

$$K_{\Delta q_i \Delta \bar{q}_j} = -K_{q_i \bar{q}_j}, \qquad\qquad K_{q_i \Delta \bar{q}_j} = -K_{\Delta q_i \bar{q}_j} \tag{3.13}$$

and analogous relations for K', so that

$$\frac{d\hat{\sigma}_{q_i \bar{q}_j}}{d\Omega_i} = -\frac{d\hat{\sigma}_{\Delta q_i \Delta \bar{q}_j}}{d\Omega_i}, \qquad\qquad \frac{d\hat{\sigma}_{q_i \Delta \bar{q}_j}}{d\Omega_i} = -\frac{d\hat{\sigma}_{\Delta q_i \bar{q}_j}}{d\Omega_i}. \tag{3.14}$$

Because of chirality conservation for massless quarks one has vanishing parton-level cross sections for the annihilation of a transversely polarized parton with an unpolarized or longitudinally polarized one, $d\hat{\sigma}_{\delta q_i \bar{q}_j} = d\hat{\sigma}_{\delta q_i \Delta \bar{q}_j} = d\hat{\sigma}_{q_i \delta \bar{q}_j} = d\hat{\sigma}_{\Delta q_i \delta \bar{q}_j} = 0$. If both quark

and antiquark are transversely polarized, one finds

$$
\frac{d\hat{\sigma}_{\delta q_i \delta \bar{q}_j}^{kl}}{d\Omega_i} = \sin^2 \theta_i \left\{ \left[\cos(2\varphi_i)\, K_{\delta q_i \delta \bar{q}_j}(Q_i) - \sin(2\varphi_i)\, K'_{\delta q_i \delta \bar{q}_j}(Q_i) \right] \left(\boldsymbol{X}^k \boldsymbol{X}^l - \boldsymbol{Y}^k \boldsymbol{Y}^l \right) \right.
$$
$$
\left. + \left[\sin(2\varphi_i)\, K_{\delta q_i \delta \bar{q}_j}(Q_i) + \cos(2\varphi_i)\, K'_{\delta q_i \delta \bar{q}_j}(Q_i) \right] \left(\boldsymbol{X}^k \boldsymbol{Y}^l + \boldsymbol{Y}^k \boldsymbol{X}^l \right) \right\}
$$
$$(3.15)$$

with X and Y as defined in section 3.2.2. The transverse indices k, l in (3.15) refer to the pp center-of-mass, where they are to be contracted with the corresponding indices of the DPDs. We note that contraction of (3.15) with the transverse spin vectors $\boldsymbol{s}^k$, $\bar{\boldsymbol{s}}^l$ of the quark and the antiquark gives the simple expression

$$
\frac{d\hat{\sigma}_{\delta q_i \delta \bar{q}_j}^{kl}}{d\Omega_i}\, \boldsymbol{s}^k \bar{\boldsymbol{s}}^l = \sin^2 \theta_i \left[\cos(\varphi_s + \varphi_{\bar{s}} - 2\varphi_i)\, K_{\delta q_i \delta \bar{q}_j} + \sin(\varphi_s + \varphi_{\bar{s}} - 2\varphi_i)\, K'_{\delta q_i \delta \bar{q}_j} \right], \quad (3.16)
$$

where φ_s and $\varphi_{\bar{s}}$ are the azimuthal angles of the spin vectors in the pp center-of-mass and our normalization convention is $\boldsymbol{s}^2 = \bar{\boldsymbol{s}}^2 = 1$.

The preceding expressions hold for both neutral and charged vector bosons, and the coupling factors $K_{a_i \bar{a}_j}$ and $K'_{a_i \bar{a}_j}$ appearing in (3.12) and (3.15) are given in appendix A. For neutral boson production the annihilating quark and antiquark have the same flavor. In this case we will use $d\hat{\sigma}_{q_i \bar{q}_j}$, $d\hat{\sigma}_{q_i \Delta \bar{q}_j}$, ... with $i \neq j$ to denote the interference terms for flavor q_i in the amplitude and flavor q_j in the conjugate amplitude. The relations (3.12) to (3.16) remain valid for these interference terms. As can be seen in appendix A, the corresponding coupling factors are complex, and their imaginary parts change sign when the flavor (but not the spin) labels are interchanged, e.g.

$$
K_{q_1 \bar{q}_2} = \left(K_{q_2 \bar{q}_1} \right)^*, \qquad\qquad\qquad K'_{q_1 \Delta \bar{q}_2} = \left(K'_{q_2 \Delta \bar{q}_1} \right)^*. \qquad (3.17)
$$

We note that for invariant masses Q_i far below the Z mass, the neutral boson channel is well approximated by γ^* production alone. The only nonzero coupling factors in this case are $K_{q_i \bar{q}_j} = -K_{\Delta q_i \Delta \bar{q}_j} = K_{\delta q_i \delta \bar{q}_j}$.

For W boson production we use $d\hat{\sigma}_{q_i \bar{q}_j}$, $d\hat{\sigma}_{q_i \Delta \bar{q}_j}$ etc. to denote cross sections with different flavors q_i, q_j in the initial state. We do not need a separate notation for flavor interference terms in this case, because the product $d\hat{\sigma}_{a_1 \bar{a}_3}\, d\hat{\sigma}_{a_2 \bar{a}_4}$ of cross sections for WW production is equal to the product of the corresponding interference terms, except for CKM factors that can easily be identified. Using that W bosons only couple to left-handed fermions, we find further simplifications for the coupling factors:

$$
K_{q_i \bar{q}_j} = K_{q_i \Delta \bar{q}_j}, \qquad\qquad K_{\delta q_i \delta \bar{q}_j} = 0, \qquad\qquad K'_{a_1 \bar{a}_2} = K_{a_1 \bar{a}_2}, \qquad (3.18)
$$

where the second relation reflects that the operator $\mathcal{O}_{\delta q}$ for transverse quark polarization corresponds to the interference between left- and right-handed quarks. Together with the relations (3.13) we are thus left with only one independent coupling factor for W^- and only one for W^+ production.

So far we have discussed cross sections and interference terms $d\hat{\sigma}_{a_i\bar{a}_j}$ for the annihilation of a right-moving quark with a left-moving antiquark. The cross sections and interference terms $d\hat{\sigma}_{\bar{a}_j a_i}$ for right-moving antiquarks and left-moving quarks have the same form as in (3.12) and (3.15). The associated coupling factors are given by

$$K_{\bar{q}_j q_i} = \left(K_{q_i \bar{q}_j}\right)^*, \qquad\qquad\qquad K'_{\bar{q}_j q_i} = -\left(K'_{q_i \bar{q}_j}\right)^* \qquad (3.19)$$

and analogous relations for the spin combinations $\Delta q \Delta q$ and $\delta q \delta q$, and by

$$K_{\bar{q}_j \Delta q_i} = -\left(K_{q_i \Delta \bar{q}_j}\right)^*, \qquad\qquad\qquad K'_{\bar{q}_j \Delta q_i} = \left(K'_{q_i \Delta \bar{q}_j}\right)^* \qquad (3.20)$$

and an analogous relation for the spin combination $\Delta q q$.

3.3.1 Single polarized Drell-Yan

Before moving on to the cross section results for double Drell-Yan in unpolarized protons, let us briefly discuss single Drell-Yan production with polarized protons. The formalism for a single parton in a polarized proton resembles that of two partons in an unpolarized proton. Just as the polarization of two partons can be correlated, the polarization of one parton can be correlated with the polarization of the parent proton. As a double check of our calculation, we computed the cross section for single Drell-Yan in a collision between two unpolarized protons and between one unpolarized and one transversely polarized proton. The results for the photon confirm those in [95]. We also compared our results to the single Drell-Yan calculation in [96]. Agreement was found except for the sign of the γ^*/Z interference, for which we could verify our result by comparing to the calculation of the time reversed hard process in [64].

3.4 The double Drell-Yan cross section

Inserting the hard-scattering cross sections (3.12), (3.15) and the DPD decompositions (3.3) to (3.5) into the factorization formula (3.11), we obtain our final results for the double parton scattering contribution to four-lepton production.

For the production and decay of two W bosons, the result has a simple structure thanks to the relations (3.18),

$$\frac{d\sigma^{WW}}{\prod_{i=1}^{2} dx_i \, d\bar{x}_i \, d^2\boldsymbol{q}_i \, d\Omega_i} = \frac{1}{C} \sum_{q_1 q_2 q_3 q_4} K_{q_1 \bar{q}_3}(Q_1) \, K_{q_2 \bar{q}_4}(Q_2) \int \frac{d^2\boldsymbol{z}_1}{(2\pi)^2} \frac{d^2\boldsymbol{z}_2}{(2\pi)^2} \, e^{-i\boldsymbol{z}_1 \boldsymbol{q}_1 - i\boldsymbol{z}_2 \boldsymbol{q}_2} \int d^2\boldsymbol{y}$$

$$\times \left[(1 + \cos\theta_1)^2 (1 + \cos\theta_2)^2 \right.$$

$$\times (f_{q_1 q_2} + f_{\Delta q_1 \Delta q_2} - g_{\Delta q_1 q_2} - g_{q_1 \Delta q_2})(\bar{f}_{\bar{q}_3 \bar{q}_4} + \bar{f}_{\Delta \bar{q}_3 \Delta \bar{q}_4} - \bar{g}_{\Delta \bar{q}_3 \bar{q}_4} - \bar{g}_{\bar{q}_3 \Delta \bar{q}_4})$$

$$+ (1 + \cos\theta_1)^2 (1 - \cos\theta_2)^2$$

$$\left. \times (f_{q_1 \bar{q}_4} - f_{\Delta q_1 \Delta \bar{q}_4} + g_{\Delta q_1 \bar{q}_4} - g_{q_1 \Delta \bar{q}_4})(\bar{f}_{\bar{q}_3 q_2} - \bar{f}_{\Delta \bar{q}_3 \Delta q_2} + \bar{g}_{\bar{q}_3 \Delta q_2} - \bar{g}_{\Delta \bar{q}_3 q_2}) \right.$$
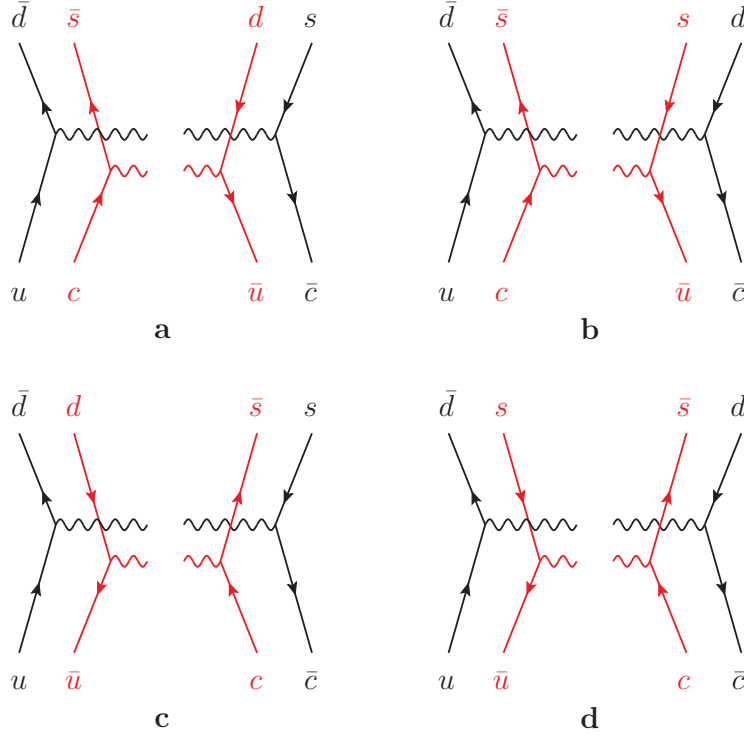
Figure 3.3: Hard-scattering graphs for the production of W^+W^+ (a, b) or of W^+W^- (c, d). The labels q and $\bar{q}$ indicate whether a parton corresponds to a quark field or a conjugate quark field in the relevant DPD. Graphs (b) and (d) are multiplied with interference distributions for one of the protons, whereas graphs (a) and (c) go along with interference distributions for both protons.

$$
\begin{aligned}
&+ (1 - \cos\theta_1)^2 \, (1 + \cos\theta_2)^2 \\
&\quad \times (f_{\bar{q}_3 q_2} - f_{\Delta\bar{q}_3 \Delta q_2} - g_{\bar{q}_3 \Delta q_2} + g_{\Delta\bar{q}_3 q_2})(\bar{f}_{q_1 \bar{q}_4} - \bar{f}_{\Delta q_1 \Delta \bar{q}_4} - \bar{g}_{q_1 \Delta \bar{q}_4} + \bar{g}_{\Delta q_1 \bar{q}_4}) \\
&+ (1 - \cos\theta_1)^2 \, (1 - \cos\theta_2)^2 \\
&\quad \times (f_{\bar{q}_3 \bar{q}_4} + f_{\Delta\bar{q}_3 \Delta \bar{q}_4} + g_{\bar{q}_3 \Delta \bar{q}_4} + g_{\Delta\bar{q}_3 \bar{q}_4})(\bar{f}_{q_1 q_2} + \bar{f}_{\Delta q_1 \Delta q_2} + \bar{g}_{q_1 \Delta q_2} + \bar{g}_{\Delta q_1 q_2}) \\
&+ \{\text{flavor interference}\} \bigg] ,
\end{aligned} \tag{3.21}
$$

where the sum over q_1 to q_4 runs over quark flavors. The flavor interference terms are obtained by replacing the DPDs in one or in both protons with their interference analogs and by appropriately changing the CKM factors in the product $K_{q_1 \bar{q}_3} K_{q_2 \bar{q}_4}$. Different types of flavor interference terms are shown in figure 3.3. Taking into account the minus sign in the definition of pseudoscalar distributions for left-moving partons, e.g. in $\bar{F}_{q_i \Delta \bar{q}_j} = -\bar{g}_{q_i \Delta \bar{q}_j}$, we recognize that the DPD combinations in (3.21) correspond to negative-helicity quarks and positive-helicity antiquarks, as required by the left-handed nature of the charged weak current.

We see that for W pair production the presence of longitudinal parton spin correlations in the proton changes the overall rate of the cross section as well as the distribution in the polar angles of the decay leptons.

For one or two neutral bosons (γ^*, Z) the structure of the cross section is more complicated. We split the cross section (3.11) into three parts, $\sigma^{(0)}$ for the case without transverse quark polarization and $\sigma^{(1)}$, $\sigma^{(2)}$ for the cases where one or two hard interactions are initiated by transversely polarized quarks. The contribution with only unpolarized and longitudinally polarized partons reads

$$
\frac{d\sigma^{(0)}}{\prod_{i=1}^{2} dx_i\, d\bar{x}_i\, d^2\boldsymbol{q}_i\, d\Omega_i} = \frac{1}{C} \sum_{q_1 q_2 q_3 q_4} \int \frac{d^2\boldsymbol{z}_1}{(2\pi)^2} \frac{d^2\boldsymbol{z}_2}{(2\pi)^2}\, e^{-i\boldsymbol{z}_1\boldsymbol{q}_1 - i\boldsymbol{z}_2\boldsymbol{q}_2} \int d^2\boldsymbol{y}
$$

$$
\times \Big\{ \big[(1+\cos^2\theta_1)K_{q_1\bar{q}_3} + 2\cos\theta_1\, K'_{q_1\bar{q}_3}\big]\big[(1+\cos^2\theta_2)K_{q_2\bar{q}_4} + 2\cos\theta_2\, K'_{q_2\bar{q}_4}\big]
$$

$$
\times \big(f_{q_1 q_2}\bar{f}_{\bar{q}_3\bar{q}_4} + f_{\Delta q_1\Delta q_2}\bar{f}_{\Delta\bar{q}_3\Delta\bar{q}_4} + g_{q_1 q_2}\bar{g}_{\bar{q}_3\bar{q}_4} + g_{\Delta q_1 q_2}\bar{g}_{\Delta\bar{q}_3\bar{q}_4}\big)
$$

$$
+ \big[(1+\cos^2\theta_1)K_{q_1\Delta\bar{q}_3} + 2\cos\theta_1\, K'_{q_1\Delta\bar{q}_3}\big]\big[(1+\cos^2\theta_2)K_{q_2\Delta\bar{q}_4} + 2\cos\theta_2\, K'_{q_2\Delta\bar{q}_4}\big]
$$

$$
\times \big(f_{q_1 q_2}\bar{f}_{\Delta\bar{q}_3\Delta\bar{q}_4} + f_{\Delta q_1\Delta q_2}\bar{f}_{\bar{q}_3\bar{q}_4} + g_{q_1 q_2}\bar{g}_{\Delta\bar{q}_3\bar{q}_4} + g_{\Delta q_1 q_2}\bar{g}_{\bar{q}_3\bar{q}_4}\big)
$$

$$
- \big[(1+\cos^2\theta_1)K_{q_1\bar{q}_3} + 2\cos\theta_1\, K'_{q_1\bar{q}_3}\big]\big[(1+\cos^2\theta_2)K_{q_2\Delta\bar{q}_4} + 2\cos\theta_2\, K'_{q_2\Delta\bar{q}_4}\big]
$$

$$
\times \big(g_{q_1\Delta q_2}\bar{f}_{\bar{q}_3\bar{q}_4} + g_{\Delta q_1 q_2}\bar{f}_{\Delta\bar{q}_3\Delta\bar{q}_4} + f_{q_1 q_2}\bar{g}_{\bar{q}_3\Delta\bar{q}_4} + f_{\Delta q_1\Delta q_2}\bar{g}_{\Delta\bar{q}_3\bar{q}_4}\big)
$$

$$
- \big[(1+\cos^2\theta_1)K_{q_1\Delta\bar{q}_3} + 2\cos\theta_1\, K'_{q_1\Delta\bar{q}_3}\big]\big[(1+\cos^2\theta_2)K_{q_2\bar{q}_4} + 2\cos\theta_2\, K'_{q_2\bar{q}_4}\big]
$$

$$
\times \big(g_{q_1\Delta q_2}\bar{f}_{\Delta\bar{q}_3\Delta\bar{q}_4} + g_{\Delta q_1 q_2}\bar{f}_{\bar{q}_3\bar{q}_4} + f_{q_1 q_2}\bar{g}_{\Delta\bar{q}_3\bar{q}_4} + f_{\Delta q_1\Delta q_2}\bar{g}_{\bar{q}_3\Delta\bar{q}_4}\big)\Big\}
$$

$$
+ \{\text{flavor interference}\} + \{q\bar{q}\ \text{permutations}\}. \tag{3.22}
$$

The $q\bar{q}$ permutation terms are obtained by permutation of the quark-antiquark assignments in the DPDs and in the coupling factors K, K' as specified in (3.11). For neutral bosons the annihilating quark and antiquark have the same flavor, i.e. one has $q_1 = q_3$ ($q_2 = q_4$) if V_1 (V_2) is neutral. The flavor interference term for neutral boson pairs is then obtained by replacing all distributions f, g, $\bar{f}$, $\bar{g}$ with their interference analogs f^I, g^I, $\bar{f}^I$, $\bar{g}^I$ and by interchanging $1 \leftrightarrow 2$ in the second subscript of the coupling factors, e.g. $K_{q_1\bar{q}_1}K'_{q_2\Delta\bar{q}_2} \to K_{q_1\bar{q}_2}K'_{q_2\Delta\bar{q}_1}$. The relations (2.58), (3.17) and their analogs for other polarizations ensure that the sum over all flavor assignments in (3.22) gives a real-valued cross section. Example graphs for flavor interference are shown in figure 3.4.

We see in (3.22) that longitudinal parton spin correlations change the overall rate of double parton scattering and the dependence on the polar angles of the leptons, due to the differences between the coupling factors $K_{q_i\bar{q}_j}$, $K'_{q_i\bar{q}_j}$ and $K_{q_i\Delta\bar{q}_j}$, $K'_{q_i\Delta\bar{q}_j}$. Only in the neutral boson channel at Q_i values small enough to neglect Z production does one have a fixed angular dependence $d\sigma^{(0)}/d\cos\theta_i \propto 1 + \cos^2\theta_i$.

We now turn towards the part of the cross section where one of the two annihilation processes involves transverse quark polarization (and thus produces a neutral gauge
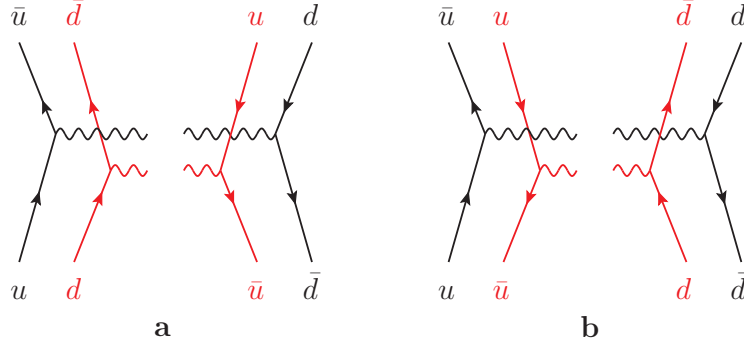
Figure 3.4: Hard-scattering graphs for the production of two neutral gauge bosons. The labels q and $\bar{q}$ have the same meaning as in figure 3.3.

boson). It reads

$$
\frac{d\sigma^{(1)}}{\prod_{i=1}^{2} dx_i\, d\bar{x}_i\, d^2\boldsymbol{q}_i\, d\Omega_i} = \frac{1}{C}\, \sin^2\theta_2 \sum_{q_1 q_2 q_3} \int \frac{d^2\boldsymbol{z}_1}{(2\pi)^2} \frac{d^2\boldsymbol{z}_2}{(2\pi)^2}\, e^{-i\boldsymbol{z}_1\boldsymbol{q}_1 - i\boldsymbol{z}_2\boldsymbol{q}_2} \int d^2\boldsymbol{y}\, \boldsymbol{y}^2 M^2
$$

$$
\times \Bigg(\Big[(1+\cos^2\theta_1) K_{q_1\bar{q}_3} + 2\cos\theta_1\, K'_{q_1\bar{q}_3} \Big]
$$

$$
\times \Bigg\{ \Big[\cos 2(\varphi_2 - \varphi_y)\, K_{\delta q_2 \delta\bar{q}_2} - \sin 2(\varphi_2 - \varphi_y)\, K'_{\delta q_2 \delta\bar{q}_2} \Big]
$$

$$
\times (f_{q_1\delta q_2}\bar{f}_{\bar{q}_3\delta\bar{q}_2} - g_{q_1\delta q_2}\bar{g}_{\bar{q}_3\delta\bar{q}_2} - f_{\Delta q_1\delta q_2}\bar{f}_{\Delta\bar{q}_3\delta\bar{q}_2} + g_{\Delta q_1\delta q_2}\bar{g}_{\Delta\bar{q}_3\delta\bar{q}_2})
$$

$$
+ \Big[\sin 2(\varphi_2 - \varphi_y)\, K_{\delta q_2 \delta\bar{q}_2} + \cos 2(\varphi_2 - \varphi_y)\, K'_{\delta q_2 \delta\bar{q}_2} \Big]
$$

$$
\times (f_{q_1\delta q_2}\bar{g}_{\bar{q}_3\delta\bar{q}_2} + g_{q_1\delta q_2}\bar{f}_{\bar{q}_3\delta\bar{q}_2} + f_{\Delta q_1\delta q_2}\bar{g}_{\Delta\bar{q}_3\delta\bar{q}_2} + g_{\Delta q_1\delta q_2}\bar{f}_{\Delta\bar{q}_3\delta\bar{q}_2}) \Bigg\}
$$

$$
- \Big[(1+\cos^2\theta_1) K_{q_1\Delta\bar{q}_3} + 2\cos\theta_1\, K'_{q_1\Delta\bar{q}_3} \Big]
$$

$$
\times \Bigg\{ \Big[\cos 2(\varphi_2 - \varphi_y)\, K_{\delta q_2 \delta\bar{q}_2} - \sin 2(\varphi_2 - \varphi_y)\, K'_{\delta q_2 \delta\bar{q}_2} \Big]
$$

$$
\times (f_{q_1\delta q_2}\bar{g}_{\Delta\bar{q}_3\delta\bar{q}_2} - g_{q_1\delta q_2}\bar{f}_{\Delta\bar{q}_3\delta\bar{q}_2} - f_{\Delta q_1\delta q_2}\bar{g}_{\bar{q}_3\delta\bar{q}_2} + g_{\Delta q_1\delta q_2}\bar{f}_{\bar{q}_3\delta\bar{q}_2})
$$

$$
+ \Big[\sin 2(\varphi_2 - \varphi_y)\, K_{\delta q_2 \delta\bar{q}_2} + \cos 2(\varphi_2 - \varphi_y)\, K'_{\delta q_2 \delta\bar{q}_2} \Big]
$$

$$
\times (f_{q_1\delta q_2}\bar{f}_{\Delta\bar{q}_3\delta\bar{q}_2} + g_{q_1\delta q_2}\bar{g}_{\Delta\bar{q}_3\delta\bar{q}_2} + f_{\Delta q_1\delta q_2}\bar{f}_{\bar{q}_3\delta\bar{q}_2} + g_{\Delta q_1\delta q_2}\bar{g}_{\bar{q}_3\delta\bar{q}_2}) \Bigg\} \Bigg)
$$

$$
+ \{\text{flavor interference}\} + \{q\bar{q}\text{ permutations}\} + \{\text{transv. pol. in interaction 1}\},
$$

$$
(3.23)
$$

where the flavor interference and $q\bar{q}$ permutation terms are obtained in the same way as in (3.22). The terms for transverse polarization in interaction 1 are obtained by replacing labels as $1 \to 2$, $2 \to 1$, $3 \to 4$ in the coupling factors and by making the same replacement in the DPD subscripts after interchanging their order, i.e. $f_{a_1\delta q_2} \to f_{\delta q_1 a_2}$, $\bar{g}_{\bar{a}_3\delta\bar{q}_2} \to \bar{g}_{\delta\bar{q}_1\bar{a}_4}$ etc.

The azimuthal angle φ_2 of the lepton produced in interaction 2 has already been defined, and φ_y is the azimuthal angle of $\boldsymbol{y}$ in the pp center-of-mass. As anticipated in section 3.2.2, the cross section depends only on the difference $\varphi_2 - \varphi_y$ of these angles, in agreement with rotation invariance. The φ_y dependence in (3.23) arises from the uncontracted vectors $\boldsymbol{y}$ and $\tilde{\boldsymbol{y}}$ in the DPDs (3.4) for transversely polarized partons: it is hence this polarization which enables a dependence of the cross section on the azimuthal angle of the produced lepton.

The transverse distance $\boldsymbol{y}$ is integrated over in (3.23) and hence not measurable. The $\boldsymbol{y}$ integration is nontrivial because the DPDs depend on the azimuthal angles between $\boldsymbol{y}$ and $\boldsymbol{z}_1$ and $\boldsymbol{z}_2$, whose directions are in turn correlated with those of $\boldsymbol{q}_1$ and $\boldsymbol{q}_2$ through the exponential $e^{-i\boldsymbol{z}_1 \boldsymbol{q}_1 - i\boldsymbol{z}_2 \boldsymbol{q}_2}$. The integral over $\boldsymbol{y}$, $\boldsymbol{z}_1$ and $\boldsymbol{z}_2$ in the cross section thus turns the φ_y dependence into a dependence on the azimuthal angles of the transverse momenta $\boldsymbol{q}_1$ and $\boldsymbol{q}_2$. All together we thus see that a correlation between $\boldsymbol{y}$ and the transverse polarization of parton 2 in the DPDs leads to an azimuthal correlation between the lepton from interaction 2 and both transverse vector boson momenta. This is similar (but not identical) to single Drell-Yan production, where a correlation between the transverse polarization of a parton and its transverse momentum induces an azimuthal correlation between the momenta of the vector boson and its decay lepton [96].

We finally turn to the case where both vector bosons are produced from transversely polarized quarks. The corresponding contribution to the cross section is

$$\frac{d\sigma^{(2)}}{\prod_{i=1}^{2} dx_i\, d\bar{x}_i\, d^2\boldsymbol{q}_i\, d\Omega_i} = \frac{1}{C}\, 2\sin^2\theta_1\, \sin^2\theta_2 \sum_{q_1 q_2} \int \frac{d^2\boldsymbol{z}_1}{(2\pi)^2} \frac{d^2\boldsymbol{z}_2}{(2\pi)^2}\, e^{-i\boldsymbol{z}_1 \boldsymbol{q}_1 - i\boldsymbol{z}_2 \boldsymbol{q}_2} \int d^2\boldsymbol{y}$$

$$\times \Big\{ \big[\cos 2(\varphi_1 - \varphi_2)\, (K_{\delta q_1 \delta \bar{q}_1} K_{\delta q_2 \delta \bar{q}_2} + K'_{\delta q_1 \delta \bar{q}_1} K'_{\delta q_2 \delta \bar{q}_2}) $$
$$- \sin 2(\varphi_1 - \varphi_2)\, (K'_{\delta q_1 \delta \bar{q}_1} K_{\delta q_2 \delta \bar{q}_2} - K_{\delta q_1 \delta \bar{q}_1} K'_{\delta q_2 \delta \bar{q}_2}) \big] $$
$$\times (f_{\delta q_1 \delta q_2} \bar{f}_{\delta \bar{q}_1 \delta \bar{q}_2} - \boldsymbol{y}^4 M^4 g^a_{\delta q_1 \delta q_2} \bar{g}^a_{\delta \bar{q}_1 \delta \bar{q}_2}) $$
$$+ \big[\sin 2(\varphi_1 - \varphi_2)\, (K_{\delta q_1 \delta \bar{q}_1} K_{\delta q_2 \delta \bar{q}_2} + K'_{\delta q_1 \delta \bar{q}_1} K'_{\delta q_2 \delta \bar{q}_2}) $$
$$+ \cos 2(\varphi_1 - \varphi_2)\, (K'_{\delta q_1 \delta \bar{q}_1} K_{\delta q_2 \delta \bar{q}_2} - K_{\delta q_1 \delta \bar{q}_1} K'_{\delta q_2 \delta \bar{q}_2}) \big] $$
$$\times \boldsymbol{y}^2 M^2\, (f_{\delta q_1 \delta q_2} \bar{g}^a_{\delta \bar{q}_1 \delta \bar{q}_2} + g^a_{\delta q_1 \delta q_2} \bar{f}_{\delta \bar{q}_1 \delta \bar{q}_2}) $$
$$+ \big[\cos 2(\varphi_1 + \varphi_2 - 2\varphi_y)\, (K_{\delta q_1 \delta \bar{q}_1} K_{\delta q_2 \delta \bar{q}_2} - K'_{\delta q_1 \delta \bar{q}_1} K'_{\delta q_2 \delta \bar{q}_2}) $$
$$- \sin 2(\varphi_1 + \varphi_2 - 2\varphi_y)\, (K'_{\delta q_1 \delta \bar{q}_1} K_{\delta q_2 \delta \bar{q}_2} + K_{\delta q_1 \delta \bar{q}_1} K'_{\delta q_2 \delta \bar{q}_2}) \big] $$
$$\times \boldsymbol{y}^4 M^4\, (f^t_{\delta q_1 \delta q_2} \bar{f}^t_{\delta \bar{q}_1 \delta \bar{q}_2} - g^s_{\delta q_1 \delta q_2} \bar{g}^s_{\delta \bar{q}_1 \delta \bar{q}_2}) $$
$$- \big[\sin 2(\varphi_1 + \varphi_2 - 2\varphi_y)\, (K_{\delta q_1 \delta \bar{q}_1} K_{\delta q_2 \delta \bar{q}_2} - K'_{\delta q_1 \delta \bar{q}_1} K'_{\delta q_2 \delta \bar{q}_2}) $$
$$+ \cos 2(\varphi_1 + \varphi_2 - 2\varphi_y)\, (K'_{\delta q_1 \delta \bar{q}_1} K_{\delta q_2 \delta \bar{q}_2} + K_{\delta q_1 \delta \bar{q}_1} K'_{\delta q_2 \delta \bar{q}_2}) \big] $$
$$\times \boldsymbol{y}^4 M^4\, (f^t_{\delta q_1 \delta q_2} \bar{g}^s_{\delta \bar{q}_1 \delta \bar{q}_2} + g^s_{\delta q_1 \delta q_2} \bar{f}^t_{\delta \bar{q}_1 \delta \bar{q}_2}) \Big\}$$

$$+ \{\text{flavor interference}\} + \{q\bar{q}\ \text{permutations}\} \tag{3.24}$$

and depends on the azimuthal angles φ_1, φ_2 and φ_y in addition to the polar angles θ_1 and θ_2. The flavor interference and $q\bar{q}$ permutation terms are again obtained as in (3.22).

The terms depending on $\varphi_1 - \varphi_2$ describe a transverse correlation between the leptonic decay planes of the vector bosons. By contrast, the terms with $\varphi_1 + \varphi_2 - 2\varphi_y$ describe an azimuthal correlation between the lepton momenta and the direction between the hard interactions, which after integration over $\boldsymbol{y}$, $\boldsymbol{z}_1$ and $\boldsymbol{z}_2$ turns into an azimuthal correlation between the lepton momenta and the momenta of the two bosons.

3.4.1   Cross section integrated over transverse boson momenta

Integration over the transverse momenta of the two vector bosons yields cross sections expressed in terms of the collinear double parton distributions $F(x_1, x_2, \boldsymbol{y})$, with spin structure is as in (3.6).

Upon integration over $\boldsymbol{q}_1$ and $\boldsymbol{q}_2$, the cross section (3.21) for W pair production becomes

$$
\frac{d\sigma^{WW}}{\prod_{i=1}^{2} dx_i \, d\bar{x}_i \, d\Omega_i} = \frac{1}{C} \sum_{q_1 q_2 q_3 q_4} K_{q_1 \bar{q}_3} K_{q_2 \bar{q}_4}
$$

$$
\times \left\{ (1 + \cos\theta_1)^2 \, (1 + \cos\theta_2)^2 \int d^2\boldsymbol{y} \, (f_{q_1 q_2} + f_{\Delta q_1 \Delta q_2})(\bar{f}_{\bar{q}_3 \bar{q}_4} + \bar{f}_{\Delta\bar{q}_3 \Delta\bar{q}_4}) \right.
$$

$$
+ (1 + \cos\theta_1)^2 \, (1 - \cos\theta_2)^2 \int d^2\boldsymbol{y} \, (f_{q_1 \bar{q}_4} - f_{\Delta q_1 \Delta\bar{q}_4})(\bar{f}_{\bar{q}_3 q_2} - \bar{f}_{\Delta\bar{q}_3 \Delta q_2})
$$

$$
+ (1 - \cos\theta_1)^2 \, (1 + \cos\theta_2)^2 \int d^2\boldsymbol{y} \, (f_{\bar{q}_3 q_2} - f_{\Delta\bar{q}_3 \Delta q_2})(\bar{f}_{q_1 \bar{q}_4} - \bar{f}_{\Delta q_1 \Delta\bar{q}_4})
$$

$$
\left. + (1 - \cos\theta_1)^2 \, (1 - \cos\theta_2)^2 \int d^2\boldsymbol{y} \, (f_{\bar{q}_3 \bar{q}_4} + f_{\Delta\bar{q}_3 \Delta\bar{q}_4})(\bar{f}_{q_1 q_2} + \bar{f}_{\Delta q_1 \Delta q_2}) \right\}
$$

$$
+ \{\text{flavor interference}\}\,, \tag{3.25}
$$

where the arguments of the distributions are $f(x_1, x_2, \boldsymbol{y})$ and $\bar{f}(\bar{x}_1, \bar{x}_2, \boldsymbol{y})$. In the general case we have a contribution

$$
\frac{d\sigma^{(0)}}{\prod_{i=1}^{2} dx_i \, d\bar{x}_i \, d\Omega_i} = \frac{1}{C} \sum_{q_1 q_2 q_3 q_4}
$$

$$
\times \left\{ \left[(1 + \cos^2\theta_1) K_{q_1 \bar{q}_3} + 2\cos\theta_1 \, K'_{q_1 \bar{q}_3} \right] \left[(1 + \cos^2\theta_2) K_{q_2 \bar{q}_4} + 2\cos\theta_2 \, K'_{q_2 \bar{q}_4} \right] \right.
$$

$$
\times \int d^2\boldsymbol{y} \, (f_{q_1 q_2} \bar{f}_{\bar{q}_3 \bar{q}_4} + f_{\Delta q_1 \Delta q_2} \bar{f}_{\Delta\bar{q}_3 \Delta\bar{q}_4})
$$

$$
+ \left[(1 + \cos^2\theta_1) K_{q_1 \Delta\bar{q}_3} + 2\cos\theta_1 \, K'_{q_1 \Delta\bar{q}_3} \right] \left[(1 + \cos^2\theta_2) K_{q_2 \Delta\bar{q}_4} + 2\cos\theta_2 \, K'_{q_2 \Delta\bar{q}_4} \right]
$$

$$
\left. \times \int d^2\boldsymbol{y} \, (f_{q_1 q_2} \bar{f}_{\Delta\bar{q}_3 \Delta\bar{q}_4} + f_{\Delta q_1 \Delta q_2} \bar{f}_{\bar{q}_3 \bar{q}_4}) \right\}
$$

$$
+ \{\text{flavor interference}\} + \{q\bar{q} \text{ permutations}\} \tag{3.26}
$$

from unpolarized and longitudinally polarized partons. The contribution with transverse quark polarization in one of the two hard interactions now vanishes,

$$\frac{d\sigma^{(1)}}{\prod_{i=1}^{2} dx_i\, d\bar{x}_i\, d\Omega_i} = 0\,. \tag{3.27}$$

This is because integration of (3.23) over $\boldsymbol{q}_1$ and $\boldsymbol{q}_2$ sets $\boldsymbol{z}_1 = \boldsymbol{z}_2 = \boldsymbol{0}$, after which the $\boldsymbol{y}$ integral gives zero due to the azimuthal dependence on φ_y. By contrast, the contribution with transverse quark polarization in both hard interactions remains nonzero,

$$\frac{d\sigma^{(2)}}{\prod_{i=1}^{2} dx_i\, d\bar{x}_i\, d\Omega_i} = \frac{1}{C}\, 2\sin^2\theta_1\,\sin^2\theta_2 \sum_{q_1 q_2}$$
$$\times \left\{ \left[\cos 2(\varphi_1 - \varphi_2)\, (K_{\delta q_1 \delta\bar{q}_1} K_{\delta q_2 \delta\bar{q}_2} + K'_{\delta q_1 \delta\bar{q}_1} K'_{\delta q_2 \delta\bar{q}_2}) \right. \right.$$
$$\left. \left. - \sin 2(\varphi_1 - \varphi_2)\, (K'_{\delta q_1 \delta\bar{q}_1} K_{\delta q_2 \delta\bar{q}_2} - K_{\delta q_1 \delta\bar{q}_1} K'_{\delta q_2 \delta\bar{q}_2}) \right] \int d^2\boldsymbol{y}\, f_{\delta q_1 \delta q_2} \bar{f}_{\delta\bar{q}_1 \delta\bar{q}_2} \right\}$$
$$+ \{\text{flavor interference}\} + \{q\bar{q}\text{ permutations}\}\,. \tag{3.28}$$

According to (3.6) the distribution $f_{\delta q_1 \delta q_2}$ describes the correlation between the directions of the transverse polarizations of two quarks in the proton. This correlation and its counterpart for antiquarks induce a correlation between the leptonic decay planes of the vector bosons, even if their transverse momenta are integrated over. Only if one integrates over the azimuthal angle of at least one of the leptons does the contribution from transverse quark polarization completely disappear from the cross section.

The cross section of the double Drell-Yan process with two photons was calculated in [50], integrated over the transverse boson momenta and over the angles of the decay leptons. The expression in equation (9) of [50] agrees with our result (3.26) (up to the combinatorial factor $1/C$, which was omitted in [50]).

3.5 Summary

Our detailed investigation of the double Drell-Yan process has shown how spin correlations between two partons in the proton affect the rate and the angular distribution of the final state in the production of four leptons via two electroweak gauge bosons. We considered both the case where the transverse momenta of the bosons are small (using transverse-momentum dependent factorization) and the case where they are integrated over (using collinear factorization).

We find that longitudinal spin correlations between the quarks or antiquarks in the proton affect the rate of double parton scattering, and in the presence of axial-vector currents also the polar distribution of the produced leptons. Correlations involving transversely polarized quarks or antiquarks induce azimuthal correlations between the final state leptons. A part of these correlations persists if the transverse momenta of the gauge bosons are integrated over. Having two "independent" hard interactions in

double parton scattering does hence not imply that the final states produced by the two interactions are independent of each other.

Double Drell-Yan production involves a particularly simple hard-scattering subprocess but nevertheless exhibits a rich pattern of angular effects induced by parton spin correlations. It is natural to expect that other processes, in particular those involving multijets, will share this feature. We note that the cross section dependence on angles between the final-state particles implies a dependence on the invariant mass of particle pairs, which is an important quantity in searches for new physics. An estimate of the possible size of such effects would therefore be of great value.

How large correlations between the polarization of two partons inside a proton actually are remains an open question, to which we now turn our attention for closer investigations in the next two chapters.

Chapter 4

Positivity bounds on double parton distributions

4.1 Introduction

Spin correlations between the two partons are quantified by polarized double parton distributions, which describe for instance the difference of the probability densities for finding two quarks with equal or with opposite helicities. In the last chapter we saw an example of how the polarized DPDs change the size and angular distribution of cross sections. It was argued in [44] that such correlations need not be small, and we discussed in chapter 2 that large spin correlations were found for the valence region in the MIT bag model. However, our knowledge of polarized DPDs is still poor at best and any information about them is valuable.

In this chapter, we derive model independent constraints on DPDs that follow from their interpretation as probability densities for finding two partons in a specified polarization state. Similar positivity bounds have been derived for single-parton distributions in the form of the Soffer bound [97] and of inequalities for transverse-momentum dependent distributions [98] and generalized parton distributions [99].

The structure of this chapter is as follows: In the next section we set the stage by introducing the DPDs for the different polarizations and parton species. In section 4.3 we derive the spin density matrices for two partons inside an unpolarized proton, and in section 4.4 we use these matrices to derive bounds on polarized DPDs. In section 4.5 we show that the leading-order evolution to higher scales preserves these bounds. We summarize in section 4.6 and some technical details are given in appendix B and C.

4.2 Polarized double parton distributions

Since we will need a probability interpretation, we restrict ourselves to distributions that are integrated over the transverse parton momenta and that have a trivial color structure. In the parlance of [44] these are collinear color-singlet distributions.

They were defined for quarks and antiquarks in (2.48), but for our purposes here we cast them in a format valid also when one or both partons are gluons. For two partons a_1 and a_2 in an unpolarized right-moving proton we write

$$F_{a_1 a_2}(x_1, x_2, \boldsymbol{y}) = 2p^+ (x_1 p^+)^{-n_1} (x_2 p^+)^{-n_2} \int \frac{dz_1^-}{2\pi} \frac{dz_2^-}{2\pi} \, dy^- \, e^{i(x_1 z_1^- + x_2 z_2^-)p^+}$$
$$\times \langle p| \, \mathcal{O}_{a_2}(0, z_2) \, \mathcal{O}_{a_1}(y, z_1) \, |p\rangle \,, \tag{4.1}$$

where $n_i = 1$ if parton number i is a gluon and $n_i = 0$ otherwise. The operators, which are collinear versions of the operators in (2.49), for quarks are

$$\mathcal{O}_{a_i}(y, z_i) = \bar{q}_i\big(y - \tfrac{1}{2}z_i\big) \, \Gamma_{a_i} \, q_i\big(y + \tfrac{1}{2}z_i\big)\Big|_{z_i^+ = y^+ = 0, \, \boldsymbol{z}_i = \boldsymbol{0}} \tag{4.2}$$

with the projections of (2.50) onto unpolarized quarks (q), longitudinally polarized quarks (Δq) and transversely polarized quarks (δq). The field with argument $y + \tfrac{1}{2}z_i$ in (4.2) is associated with a quark in the amplitude of a double scattering process, and the field with argument $y - \tfrac{1}{2}z_i$ is associated with a quark in the complex conjugate amplitude, as in figure 2.4. The operators for gluons are

$$\mathcal{O}_{a_i}(y, z_i) = \Pi_{a_i}^{jj'} \, G^{+j'}\big(y - \tfrac{1}{2}z_i\big) \, G^{+j}\big(y + \tfrac{1}{2}z_i\big)\Big|_{z_i^+ = y^+ = 0, \, \boldsymbol{z}_i = \boldsymbol{0}} \tag{4.3}$$

with projections

$$\Pi_g^{jj'} = \delta^{jj'}\,, \qquad\qquad \Pi_{\Delta g}^{jj'} = i\epsilon^{jj'}\,, \qquad\qquad [\Pi_{\delta g}^{kk'}]^{jj'} = \tau^{jj',kk'} \tag{4.4}$$

onto unpolarized gluons (g), longitudinally polarized gluons (Δg) and linearly polarized gluons (δg). The tensor

$$\tau^{jj',kk'} = \tfrac{1}{2}\big(\delta^{jk}\delta^{j'k'} + \delta^{jk'}\delta^{j'k} - \delta^{jj'}\delta^{kk'}\big) \tag{4.5}$$

satisfies $\tau^{jj',kk'}\tau^{kk',ll'} = \tau^{jj',ll'}$ and is symmetric and traceless in each of the index pairs (jj') and (kk'). Note that for gluons δg denotes linear polarization, i.e. the interference between gluons whose helicities differ by two units in the scattering amplitude and its conjugate, while for quarks δq symbolizes transverse polarization, where the interference is between quarks with a helicity difference of one unit. Since we limit ourselves to color-singlet distributions, a sum over the color indices of the quark fields in (4.2) and the gluon fields in (4.3) is implied. We do not write out the Wilson lines that make the operators gauge invariant, as discussed in section 2.4.4.

The different spin projections lead to a large number of DPDs. For collinear color-singlet distributions, several polarization combinations are zero due to time reversal and parity invariance. This concerns the DPDs with one longitudinally polarized and one unpolarized parton, as well as those with one longitudinally polarized parton and one transversely polarized (anti)quark or linearly polarized gluon. A decomposition of the nonzero distributions for two quarks in terms of real-valued scalar functions was given

in (3.6). Analogous decompositions hold for quark-antiquark distributions and for the distributions of two antiquarks.

Since quarks and gluons mix under evolution, we also need to consider DPDs involving gluons. We define

$$
\begin{aligned}
F_{qg}(x_1, x_2, \boldsymbol{y}) &= f_{qg}(x_1, x_2, y)\,, \\
F_{\Delta q \Delta g}(x_1, x_2, \boldsymbol{y}) &= f_{\Delta q \Delta g}(x_1, x_2, y)\,, \\
F_{q\delta g}^{jj'}(x_1, x_2, \boldsymbol{y}) &= \tau^{jj',\boldsymbol{yy}} M^2 f_{q\delta g}(x_1, x_2, y)\,, \\
F_{\delta q g}^{j}(x_1, x_2, \boldsymbol{y}) &= \tilde{\boldsymbol{y}}^j M f_{\delta q g}(x_1, x_2, y)\,, \\
F_{\delta q \delta g}^{j,kk'}(x_1, x_2, \boldsymbol{y}) &= -\, \tau^{\tilde{\boldsymbol{y}}j,kk'} M f_{\delta q \delta g}(x_1, x_2, y) \\
&\quad - \left(\tilde{\boldsymbol{y}}^j \tau^{kk',\boldsymbol{yy}} + \boldsymbol{y}^j \tau^{kk',\boldsymbol{y}\tilde{\boldsymbol{y}}} \right) M^3 f_{\delta q \delta g}^{t}(x_1, x_2, y)
\end{aligned}
\tag{4.6}
$$

for quark-gluon distributions, with analogous expressions for gluon-quark distributions and distributions where the quark is replaced by an antiquark. We use a shorthand notation where vectors $\boldsymbol{y}$ or $\tilde{\boldsymbol{y}}$ appearing as an index of τ denote contraction, i.e. $\tau^{jj',\boldsymbol{yy}} = \tau^{jj',kk'} \boldsymbol{y}^k \boldsymbol{y}^{k'}$ etc. For two-gluon distributions we write

$$
\begin{aligned}
F_{gg}(x_1, x_2, \boldsymbol{y}) &= f_{gg}(x_1, x_2, y)\,, \\
F_{\Delta g \Delta g}(x_1, x_2, \boldsymbol{y}) &= f_{\Delta g \Delta g}(x_1, x_2, y)\,, \\
F_{g\delta g}^{jj'}(x_1, x_2, \boldsymbol{y}) &= \tau^{jj',\boldsymbol{yy}} M^2 f_{g\delta g}(x_1, x_2, y)\,, \\
F_{\delta g g}^{jj'}(x_1, x_2, \boldsymbol{y}) &= \tau^{jj',\boldsymbol{yy}} M^2 f_{\delta g g}(x_1, x_2, y)\,, \\
F_{\delta g \delta g}^{jj',kk'}(x_1, x_2, \boldsymbol{y}) &= \tfrac{1}{2} \tau^{jj',kk'} f_{\delta g \delta g}(x_1, x_2, y)\,, \\
&\quad + \left(\tau^{jj',\boldsymbol{y}\tilde{\boldsymbol{y}}} \tau^{kk',\boldsymbol{y}\tilde{\boldsymbol{y}}} - \tau^{jj',\boldsymbol{yy}} \tau^{kk',\boldsymbol{yy}} \right) M^4 f_{\delta g \delta g}^{t}(x_1, x_2, y)\,.
\end{aligned}
\tag{4.7}
$$

We remark that, although linear gluon polarization is described by a tensor with two indices, the restriction that this tensor is symmetric and traceless gives rise to the same number of distributions as for transverse quark polarization, which is described by a vector. The prefactors in (4.6) and (4.7) have been chosen such that we will obtain a simple correspondence between quark and gluon distributions in the spin density matrices to be derived in the next section.

Note that DPDs involving gluons are not only relevant in the context of evolution but also enter directly in important double scattering processes such as the production of jets. Their properties are hence of considerable practical interest.

In complete analogy to the case of collinear single-parton distributions, the DPDs we have introduced can be interpreted as probability densities for finding two partons inside an unpolarized proton, with a relative transverse distance $\boldsymbol{y}$ and with longitudinal momentum fractions x_1 and x_2. This becomes for instance evident from their appearance in the cross section formula for double parton scattering in chapter 2. It can also be seen from a representation in terms of parton creation and annihilation operators or from a representation in terms of the light-cone wave functions of the proton, which are straightforward extensions of the corresponding representations for single-parton distributions (given for instance in sections 3.4 and 3.11 of [100]).

As in the case of single parton densities, this interpretation does however not strictly hold in QCD, because the distributions are defined with subtractions from the ultraviolet region of parton momenta. The subtraction terms can in principle invalidate the positivity of the distributions. Nevertheless, it is useful to explore the consequences of the probability interpretation as a guide for developing physically intuitive models of the distributions. This holds in particular if one works in leading order of α_s, where the connection between parton distributions and physical cross sections (which must of course be positive semi-definite) is most direct.

4.3   Two-parton spin density matrices

The polarization state of two partons in an unpolarized proton is described by a spin density matrix that can be written in terms of the DPDs we introduced in the previous section. We start by trading the projection operators (2.50) and (4.4) for operators that project onto quarks or gluons of definite helicity. We can then easily write down the spin density matrix for two partons in the helicity basis.

The projection operators $\Gamma_{\lambda'\lambda}$ for quarks, where λ (λ') refers to the quark helicity in the amplitude (conjugate amplitude), are given by [101]

$$\Gamma_{++} = \frac{\gamma^+}{4}\left(1+\gamma_5\right) = \frac{\Gamma_q + \Gamma_{\Delta q}}{2}\,, \qquad \Gamma_{+-} = \frac{i\sigma^{+1}}{4}\left(1-\gamma_5\right) = \frac{\Gamma_{\delta q}^1 + i\Gamma_{\delta q}^2}{2}\,,$$

$$\Gamma_{--} = \frac{\gamma^+}{4}\left(1-\gamma_5\right) = \frac{\Gamma_q - \Gamma_{\Delta q}}{2}\,, \qquad \Gamma_{-+} = -\frac{i\sigma^{+1}}{4}\left(1+\gamma_5\right) = \frac{\Gamma_{\delta q}^1 - i\Gamma_{\delta q}^2}{2}\,. \qquad (4.8)$$

The projection operators $\Pi^{jj'}_{\lambda'\lambda}$ for gluons, where λ and j (λ' and j') refer to the amplitude (conjugate amplitude), can be constructed from the polarization vectors

$$\boldsymbol{\epsilon}_+ = -\frac{1}{\sqrt{2}}\left(1, i\right), \qquad\qquad \boldsymbol{\epsilon}_- = \frac{1}{\sqrt{2}}\left(1, -i\right) \qquad (4.9)$$

and read

$$\Pi^{jj'}_{++} = \left(\epsilon^j_+\right)^* \epsilon^{j'}_+ = \frac{1}{2}\left(\Pi^{jj'}_g + \Pi^{jj'}_{\Delta g}\right),$$

$$\Pi^{jj'}_{--} = \left(\epsilon^j_-\right)^* \epsilon^{j'}_- = \frac{1}{2}\left(\Pi^{jj'}_g - \Pi^{jj'}_{\Delta g}\right),$$

$$\Pi^{jj'}_{+-} = \left(\epsilon^j_-\right)^* \epsilon^{j'}_+ = -\left[\Pi^{11}_{\delta g}\right]^{jj'} - i\left[\Pi^{12}_{\delta g}\right]^{jj'},$$

$$\Pi^{jj'}_{-+} = \left(\epsilon^j_+\right)^* \epsilon^{j'}_- = -\left[\Pi^{11}_{\delta g}\right]^{jj'} + i\left[\Pi^{12}_{\delta g}\right]^{jj'}. \qquad (4.10)$$

With the projection operators we can now relate the helicity distributions to the distributions for unpolarized partons, longitudinally polarized partons and transversely (linearly) polarized quarks (gluons). Taking the example of two quarks with positive helicity in the amplitude and negative helicity in the conjugate amplitude

$$\Gamma_{-+}\Gamma_{-+} = \frac{1}{4}\left(\Gamma_{\delta q_1}^1 - i\Gamma_{\delta q_1}^2\right)\left(\Gamma_{\delta q_2}^1 - i\Gamma_{\delta q_2}^2\right), \qquad (4.11)$$

gives in terms of the parton distributions

$$\frac{1}{4}\left[F^{11}_{\delta q_1 \delta q_2} - F^{22}_{\delta q_1 \delta q_2} - i\left(F^{11}_{\delta q_1 \delta q_2} + F^{11}_{\delta q_1 \delta q_2}\right)\right]. \tag{4.12}$$

Taking the parameterization of the DPD for two transversely polarized quarks in (3.6) results in

$$\frac{1}{2}y^2 M^2 e^{2i\varphi_y} f^t_{\delta q_1 \delta q_2}. \tag{4.13}$$

We can now organize the distributions in matrices where the columns (rows) correspond to helicity states $++, -+, +-, --$ of the two partons in the amplitude (conjugate amplitude). The spin density matrix for two quarks reads

$$\rho = \frac{1}{4}\begin{pmatrix} f_{qq} + f_{\Delta q \Delta q} & -ie^{i\varphi_y}yMf_{\delta qq} & -ie^{i\varphi_y}yMf_{q\delta q} & 2e^{2i\varphi_y}y^2M^2 f^t_{\delta q\delta q} \\ ie^{-i\varphi_y}yMf_{\delta qq} & f_{qq} - f_{\Delta q\Delta q} & 2f_{\delta q\delta q} & -ie^{i\varphi_y}yMf_{q\delta q} \\ ie^{-i\varphi_y}yMf_{q\delta q} & 2f_{\delta q\delta q} & f_{qq} - f_{\Delta q\Delta q} & -ie^{i\varphi_y}yMf_{\delta qq} \\ 2e^{-2i\varphi_y}y^2M^2 f^t_{\delta q\delta q} & ie^{-i\varphi_y}yMf_{q\delta q} & ie^{-i\varphi_y}yMf_{\delta qq} & f_{qq} + f_{\Delta q\Delta q} \end{pmatrix}, \tag{4.14}$$

where the angle φ_y describes the orientation of the vector $\boldsymbol{y} = y\left(\cos\varphi_y, \sin\varphi_y\right)$ in the transverse plane. With the caveat spelled out at the end of the previous section, the diagonal matrix elements can be interpreted as the probability densities for finding two partons in definite helicity states inside an unpolarized proton. Specifically, $f_{qq} + f_{\Delta q\Delta q}$ is the probability density for finding two quarks with positive helicities, which in an unpolarized proton is equal to the probability density for finding two quarks with negative helicities. The probability density for finding two quarks with opposite helicities is $f_{qq} - f_{\Delta q\Delta q}$. The off-diagonal elements of ρ describe helicity interference, with $f^t_{\delta q\delta q}$ in the right upper corner corresponding for instance to the case where both quarks have negative helicity in the amplitude and positive helicity in the conjugate amplitude. This leads to a helicity difference between the amplitude and its conjugate, which is balanced by two units of orbital angular momentum indicated by an exponential $e^{2i\varphi_y}$ and an associated factor y^2. By contrast, $f_{\delta q\delta q}$ describes the case when the helicity difference is $+1$ for one quark and -1 for the other, so that the overall helicity is balanced.

Turning now to gluons, we have a spin density matrix

$$\frac{1}{4}\begin{pmatrix} f_{qg} + f_{\Delta q\Delta g} & -ie^{i\varphi_y}yMf_{\delta qg} & -e^{2i\varphi_y}y^2M^2 f_{q\delta g} & -2ie^{3i\varphi_y}y^3M^3 f^t_{\delta q\delta g} \\ ie^{-i\varphi_y}yMf_{\delta qg} & f_{qg} - f_{\Delta q\Delta g} & -2ie^{i\varphi_y}yMf_{\delta q\delta g} & -e^{2i\varphi_y}y^2M^2 f_{q\delta g} \\ -e^{-2i\varphi_y}y^2M^2 f_{q\delta g} & 2ie^{-i\varphi_y}yMf_{\delta q\delta g} & f_{qg} - f_{\Delta q\Delta g} & -ie^{i\varphi_y}yMf_{\delta qg} \\ 2ie^{-3i\varphi_y}y^3M^3 f^t_{\delta q\delta g} & -e^{-2i\varphi_y}y^2M^2 f_{q\delta g} & ie^{-i\varphi_y}yMf_{\delta qg} & f_{qg} + f_{\Delta q\Delta g} \end{pmatrix} \tag{4.15}$$

for quark-gluon distributions and an analogous matrix for gluon-quark distributions. For

two-gluon distributions we find

$$
\frac{1}{4}
\begin{pmatrix}
f_{gg} + f_{\Delta g \Delta g} & -e^{2i\varphi_y} y^2 M^2 f_{\delta gg} & -e^{2i\varphi_y} y^2 M^2 f_{g \delta g} & -2e^{4i\varphi_y} y^4 M^4 f_{\delta g \delta g}^t \\
-e^{-2i\varphi_y} y^2 M^2 f_{\delta gg} & f_{gg} - f_{\Delta g \Delta g} & 2 f_{\delta g \delta g} & -e^{2i\varphi_y} y^2 M^2 f_{g \delta g} \\
-e^{-2i\varphi_y} y^2 M^2 f_{g \delta g} & 2 f_{\delta g \delta g} & f_{gg} - f_{\Delta g \Delta g} & -e^{2i\varphi_y} y^2 M^2 f_{\delta gg} \\
-2e^{-4i\varphi_y} y^4 M^4 f_{\delta g \delta g}^t & -e^{-2i\varphi_y} y^2 M^2 f_{g \delta g} & -e^{-2i\varphi_y} y^2 M^2 f_{\delta gg} & f_{gg} + f_{\Delta g \Delta g}
\end{pmatrix} .
$$

$$(4.16)$$

The matrices for distributions where quarks are replaced by antiquarks are analogous to (4.14) and (4.15). We see that the parameterization of DPDs in the previous section gives simple expressions for the spin density matrices and similar structures for all types of partons.

The difference in spin between quarks and gluons causes the different dependence on the azimuthal angle φ_y in (4.14), (4.15) and (4.16). A mismatch of n units between the sum of parton helicities in the amplitude and its conjugate goes along with an exponential $e^{\pm n i \varphi_y}$ and an associated factor y^n. The gluon matrix does not include any factors of i. These originate from odd powers of $\tilde{\boldsymbol{y}}$ present for the parity odd functions F_{ab} involving transversely polarized quarks for two quark distributions and for mixed quark gluon distributions

4.4 Positivity bounds

We now show how the probability interpretation of DPDs constrains the size of the polarized distributions. Since the probability density for finding two partons in a general polarization state is positive semi-definite, we have

$$
\sum_{\lambda_1' \lambda_2' \lambda_1 \lambda_2} v_{\lambda_1' \lambda_2'}^* \, \rho_{(\lambda_1' \lambda_2')(\lambda_1 \lambda_2)} \, v_{\lambda_1 \lambda_2} \geq 0 \tag{4.17}
$$

with arbitrary complex coefficients $v_{\lambda_1 \lambda_2}$ normalized as $\sum_{\lambda_1 \lambda_2} |v_{\lambda_1 \lambda_2}|^2 = 1$. The helicity matrices are therefore positive semi-definite. The same property has been derived for the spin density matrices associated with transverse-momentum dependent distributions [98] or generalized parton distributions [99].

To simplify the algebra, we first cast all helicity matrices into a common form that is independent of the angle φ_y. This is achieved by unitary transformations, multiplying by a matrix U from the right and by $U^\dagger$ from the left. The transformation matrices for the parton combinations in (4.14) to (4.16) are

$$
\begin{aligned}
U_{qq} &= \operatorname{diag}\left(-e^{2i\varphi_y}, -i e^{i\varphi_y}, -i e^{i\varphi_y}, 1 \right), \\
U_{qg} &= \operatorname{diag}\left(i e^{3i\varphi_y}, -e^{2i\varphi_y}, -i e^{i\varphi_y}, 1 \right), \\
U_{gg} &= \operatorname{diag}\left(e^{4i\varphi_y}, -e^{2i\varphi_y}, -e^{2i\varphi_y}, 1 \right).
\end{aligned}
\tag{4.18}
$$

After these transformations and their analog for gluon-quark distributions, the spin density matrices can be written as

$$\rho = \frac{1}{4}\begin{pmatrix} f_{ab} + f_{\Delta a\Delta b} & h_{\delta ab} & h_{a\delta b} & -2h^t_{\delta a\delta b} \\ h_{\delta ab} & f_{ab} - f_{\Delta a\Delta b} & 2h_{\delta a\delta b} & h_{a\delta b} \\ h_{a\delta b} & 2h_{\delta a\delta b} & f_{ab} - f_{\Delta a\Delta b} & h_{\delta ab} \\ -2h^t_{\delta a\delta b} & h_{a\delta b} & h_{\delta ab} & f_{ab} + f_{\Delta a\Delta b} \end{pmatrix} \tag{4.19}$$

with the following identification of distributions for different parton combinations:

$$f_{ab} = f_{qq}, \ f_{qg}, \ f_{gq}, \ f_{gg},$$
$$f_{\Delta a\Delta b} = f_{\Delta q\Delta q}, \ f_{\Delta q\Delta g}, \ f_{\Delta g\Delta q}, \ f_{\Delta g\Delta g},$$
$$h_{\delta ab} = yMf_{\delta qq}, \ yMf_{\delta qg}, \ y^2M^2f_{\delta gq}, \ y^2M^2f_{\delta gg},$$
$$h_{a\delta b} = yMf_{q\delta q}, \ y^2M^2f_{q\delta g}, \ yMf_{g\delta q}, \ y^2M^2f_{g\delta g},$$
$$h_{\delta a\delta b} = f_{\delta q\delta q}, \ yMf_{\delta q\delta g}, \ yMf_{\delta g\delta q}, \ f_{\delta g\delta g},$$
$$h^t_{\delta a\delta b} = y^2M^2f^t_{\delta q\delta q}, \ y^3M^3f^t_{\delta q\delta g}, \ y^3M^3f^t_{\delta g\delta q}, \ y^4M^4f^t_{\delta g\delta g}. \tag{4.20}$$

Analogous expressions hold if quarks are replaced by antiquarks. Positivity[1] of the diagonal elements of ρ yields the trivial bounds

$$f_{ab} \geq \left| f_{\Delta a\Delta b} \right|. \tag{4.21}$$

The principal minors of the two-dimensional sub-spaces must be positive semi-definite as well, which gives upper bounds on the distributions for one or two transversely or linearly polarized partons:

$$f_{ab} + f_{\Delta a\Delta b} \geq 2\left| h^t_{\delta a\delta b} \right|,$$
$$f_{ab} - f_{\Delta a\Delta b} \geq 2\left| h_{\delta a\delta b} \right|,$$
$$f^2_{ab} \geq (f_{ab} + f_{\Delta a\Delta b})(f_{ab} - f_{\Delta a\Delta b}) \geq h^2_{\delta ab},$$
$$f^2_{ab} \geq (f_{ab} + f_{\Delta a\Delta b})(f_{ab} - f_{\Delta a\Delta b}) \geq h^2_{a\delta b}. \tag{4.22}$$

The principal minors of dimension three

$$(f_{ab} - f_{\Delta a\Delta b})(f^2_{ab} - f^2_{\Delta a\Delta b} - h^2_{\delta ab} - h^2_{a\delta b}) - 4(f_{ab} + f_{\Delta a\Delta b})h^2_{\delta a\delta b} + 4h_{\delta ab}h_{a\delta b}h_{\delta a\delta b} \geq 0, \tag{4.23}$$

$$(f_{ab} + f_{\Delta a\Delta b})(f^2_{ab} - f^2_{\Delta a\Delta b} - h^2_{\delta ab} - h^2_{a\delta b}) - 4(f_{ab} - f_{\Delta a\Delta b})h^{t2}_{\delta a\delta b} - 4h_{\delta ab}h_{a\delta b}h^t_{\delta a\delta b} \geq 0, \tag{4.24}$$

as well as $\det(\rho)$

$$\left[f^2_{ab} - (h_{\delta ab} + h_{a\delta b})^2 + 2f_{ab}(h_{\delta a\delta b} - h^t_{\delta a\delta b}) - (f_{\Delta a\Delta b} - 2h_{\delta a\delta b})(f_{\Delta a\Delta b} - 2h^t_{\delta a\delta b}) \right]$$
$$\times \left[f^2_{ab} - (h_{\delta ab} - h_{a\delta b})^2 - 2f_{ab}(h_{\delta a\delta b} - h^t_{\delta a\delta b}) - (f_{\Delta a\Delta b} + 2h_{\delta a\delta b})(f_{\Delta a\Delta b} + 2h^t_{\delta a\delta b}) \right] \geq 0 \tag{4.25}$$

---

[1]For ease of language we use "positivity" in the sense of "positive semi-definite" here and in the following.

provide further, rather cumbersome bounds. The strongest bounds can be obtained from the positivity of the eigenvalues of ρ, which is a sufficient and necessary condition for the positivity of ρ. Calculating the eigenvalues we obtain

$$f_{ab} + h_{\delta a \delta b} - h_{\delta a \delta b}^t \pm \sqrt{(h_{\delta ab} + h_{a \delta b})^2 + (f_{\Delta a \Delta b} - h_{\delta a \delta b} - h_{\delta a \delta b}^t)^2} \geq 0\,,$$

$$f_{ab} - h_{\delta a \delta b} + h_{\delta a \delta b}^t \pm \sqrt{(h_{\delta ab} - h_{a \delta b})^2 + (f_{\Delta a \Delta b} + h_{\delta a \delta b} + h_{\delta a \delta b}^t)^2} \geq 0\,. \qquad (4.26)$$

These inequalities set upper limits on the size of spin correlations between two partons in an unpolarized proton. They can be used either to construct double parton distributions or to put limits on polarization effects in double hard scattering processes.

We note that positive semidefinite combinations of DPDs were discussed already in the pioneering studies [72, 89]. Distributions that involve a helicity mismatch between the amplitude and its conjugate (see section 4.3) were however not considered in that work. The derivation in [72, 89] thus corresponds to our results (4.21) and (4.22) if all distributions multiplied with a power of y in (4.20) are set to zero.

4.5 Stability under evolution

The ultraviolet subtractions mentioned at the end of section 4.2 induce a scale dependence, which for collinear parton distributions is described by the DGLAP evolution equations. While the subtractions themselves may invalidate positivity of the distributions and thus their density interpretation, the evolution equations can be interpreted in a probabilistic manner provided that one takes the leading-order approximation of the evolution kernels [102, 103]. Specifically, one finds that if parton distributions are positive semi-definite at a certain scale, this property is preserved by leading-order evolution to higher scales. This also holds for the Soffer inequality, which expresses positivity in the sector of transverse quark polarization [104, 105]. For evolution at next-to-leading order in α_s the situation is less clear-cut and a discussion of positivity depends in particular on the scheme in which the distributions are defined. We refer to [106] and [107, 108] for a discussion of the situation for longitudinal and transverse parton polarization, respectively.

Returning to double parton distributions, we now show that the bounds derived in the previous section are stable under leading-order evolution to higher scales. The strategy for the derivation is as follows: we first introduce linear combinations of double parton distributions whose positivity is necessary and sufficient for the positivity of the spin density matrices and then show that these linear combinations remain positive semi-definite under evolution. The positivity of the spin density matrices then guarantees the stability of the positivity bounds.

4.5.1 Evolution of double parton distributions

To begin with, let us specify the evolution of collinear DPDs in the color-singlet sector. We consider the homogeneous evolution equations in the transverse position represen-
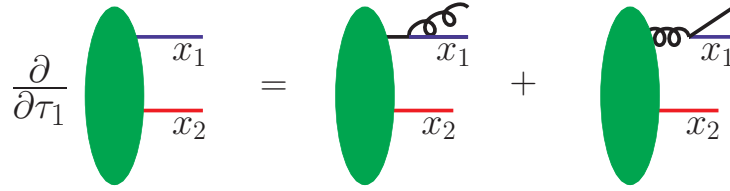
Figure 4.1: Illustration of the double parton evolution for one of the parton legs (4.27)

tation (2.64). For the reasons given in section 2.4.1, this equation does not include the inhomogeneous term for the splitting of one parton into two that has been previously discussed in the literature [74–78].

For our purpose, it is useful to take different renormalization scales μ_1 and μ_2 for the two partons, corresponding to separate ultraviolet renormalization of the operators $\mathcal{O}_{a_1}$ and $\mathcal{O}_{a_2}$ in (4.1). The evolution equation , illustrated in figure 4.1, for the unpolarized double quark distributions in the first scale then reads

$$\frac{\partial f_{qq}(x_1, x_2, y; \mu_1, \mu_2)}{\partial \tau_1} = P_{qq} \otimes_1 f_{qq} + P_{qg} \otimes_1 f_{gq} , \tag{4.27}$$

where $\otimes_1$ is a convolution in the first argument of the DPDs with the leading-order splitting functions P_{ab}, defined in (2.65). The kernels appearing in (4.27) for quark-quark and gluon-quark transitions are [66]

$$P_{qq}(z) = C_F \left[\frac{1 + z^2}{(1 - z)_+} + \frac{3}{2} \delta(1 - z) \right],$$
$$P_{qg}(z) = \frac{z^2 + (1 - z)^2}{2}. \tag{4.28}$$

As in chapter 2, we note that the leading-order splitting functions are the same for quarks and antiquarks, i.e. one has $P_{qq} = P_{\bar{q}\bar{q}}$, $P_{qg} = P_{\bar{q}g}$, $P_{gq} = P_{g\bar{q}}$ and analogous relations for polarized partons. In appendix B we give the explicit evolution equations for all polarized DPDs and list the associated splitting functions.

The evolution variable in (4.27) is taken as

$$\tau_1 = \int^{\mu_1^2} \frac{d\mu^2}{\mu^2} \frac{\alpha_s(\mu)}{2\pi} , \tag{4.29}$$

where the lower limit of integration is irrelevant in the derivative $\partial f/\partial \tau_1$. The use of τ_1 is just a matter of convenience as it removes the running coupling from the leading-order splitting functions.

The analog of (4.27) for the scale associated with the second parton is

$$\frac{\partial f_{qq}(x_1, x_2, y; \mu_1, \mu_2)}{\partial \tau_2} = P_{qq} \otimes_2 f_{qq} + P_{qg} \otimes_2 f_{qg} . \tag{4.30}$$

The evolution equation for equal scales, i.e. for $f_{qq}(x_1, x_2, y; \mu, \mu)$, is obtained by adding the right-hand sides of (4.27) and (4.30) which combine to reproduce (2.64). We will show that positivity is preserved for separate evolution in μ_1. The same then obviously holds for evolution in μ_2 and hence for the evolution in a single common scale $\mu_1 = \mu_2$.

4.5.2 Linear quark bounds

Before turning to the general case we warm up by demonstrating the stability of a simpler bound for the two quark distributions. From the eigenvalues (4.26) we can build the linear bound

$$f_{q_1 q_2} \geq |f_{\delta q_1 \delta q_2} - y^2 M^2 f^t_{\delta q_1 \delta q_1}|, \tag{4.31}$$

similar to the Soffer inequality. Defining two distributions

$$Q^+ = f_{q_1 q_2} + (f_{\delta q_1 \delta q_2} - y^2 M^2 f^t_{\delta q_1 \delta q_1}),$$
$$Q^+ = f_{q_1 q_2} + (f_{\delta q_1 \delta q_2} - y^2 M^2 f^t_{\delta q_1 \delta q_1}) \tag{4.32}$$

the bound takes the form $Q^{\pm}_{q_1 q_2} \geq 0$. With the evolution equations for unpolarized and transversely polarized quarks in appendix B the evolution of these two linear combinations is

$$\frac{\partial}{\partial \tau_1} \begin{pmatrix} Q^+ \\ Q^- \end{pmatrix} = \begin{pmatrix} P^+ & P^- \\ P^- & P^+ \end{pmatrix} \otimes_1 \begin{pmatrix} Q^+ \\ Q^- \end{pmatrix} + \begin{pmatrix} P_{qg} & P_{qg} \\ P_{qg} & P_{qg} \end{pmatrix} \otimes_1 \begin{pmatrix} f_{gq_2} \\ f_{gq_2} \end{pmatrix}, \tag{4.33}$$

where the plus and minus kernels are defined as

$$P^+ = \frac{1}{2C_F} \left[\frac{(1+z)^2}{(1-z)_+} + 3\delta(1-z) \right]$$
$$P^- = \frac{C_F}{2}(1-z). \tag{4.34}$$

The key property is that P^-_{qq} and P_{qg} are positive for all z values and that the only negative part of P^+_{qq} is the virtual (plus prescription) part. In the evolution the virtual term is proportional to the function itself and does not change the sign of the function. Since all other parts are positive, the positivity of the two distributions at the starting scale (together with $f_{gq_2} \geq 0$) guarantees the positivity at higher scales. A more detailed discussion will be given in the next section, when we generalized this technique such that it incorporates all of the positivity bounds.

4.5.3 Linear combinations of DPDs

A key ingredient in our argument is to form suitable linear combinations of double parton distributions, which we now introduce. Positivity of the spin density matrix ρ means

that $v^\dagger \rho\, v \geq 0$ for any complex vector v, as we spelled out in (4.17). Parameterizing the vector as

$$v^T = (a_1 + ib_1, a_2 + ib_2, a_3 + ib_3, a_4 + ib_4) \tag{4.35}$$

with real numbers a_i, b_i and performing the multiplication with the matrix in (4.19) gives

$$Q^+_{ab} = c_1 f_{ab} + c_2 h_{a\delta b} + c_3 f_{\Delta a \Delta b} + c_4 h_{\delta a b} + c_5 h_{\delta a \delta b} + c_6 h^t_{\delta a \delta b} \geq 0\,, \tag{4.36}$$

where $Q^+_{ab} = 4 v^\dagger \rho\, v$ and the coefficients c_i are given by

$$
\begin{aligned}
c_1 &= a_1^2 + b_1^2 + a_2^2 + b_2^2 + a_3^2 + b_3^2 + a_4^2 + b_4^2\,, & c_2 &= 2(a_1 a_3 + b_1 b_3 + a_2 a_4 + b_2 b_4)\,, \\
c_3 &= a_1^2 + b_1^2 - a_2^2 - b_2^2 - a_3^2 - b_3^2 + a_4^2 + b_4^2\,, & c_4 &= 2(a_1 a_2 + b_1 b_2 + a_3 a_4 + b_3 b_4)\,, \\
c_5 &= 4(a_2 a_3 + b_2 b_3)\,, & c_6 &= -4(a_1 a_4 + b_1 b_4)\,.
\end{aligned}
\tag{4.37}
$$

We will prove the stability of the positivity bounds by showing that for arbitrary values of a_i and b_i the inequality (4.36) is stable under evolution to higher scales. It will be convenient to consider further linear combinations of double parton distributions. Changing signs of the parameters $a_1 \to -a_1$, $b_1 \to -b_1$, $a_3 \to -a_3$, $b_3 \to -b_3$ we get

$$Q^-_{ab} = c_1 f_{ab} + c_2 h_{a\delta b} + c_3 f_{\Delta a \Delta b} - c_4 h_{\delta a b} - c_5 h_{\delta a \delta b} - c_6 h^t_{\delta a \delta b} \geq 0\,. \tag{4.38}$$

Adding (4.36) and (4.38) gives the simpler inequality

$$B^+_{ab} = c_1 f_{ab} + c_2 h_{a\delta b} + c_3 f_{\Delta a \Delta b} \geq 0\,, \tag{4.39}$$

and interchanging indices ($1 \leftrightarrow 2$ and $3 \leftrightarrow 4$) in the elements of v gives

$$B^-_{ab} = c_1 f_{ab} + c_2 h_{a\delta b} - c_3 f_{\Delta a \Delta b} \geq 0\,. \tag{4.40}$$

If (4.36) holds at a given scale for arbitrary values of a_i and b_i, then (4.38) to (4.40) hold at that scale as well.

We will see that the evolution equations in the scale μ_1 can be formulated in terms of Q^+_{ab}, Q^-_{ab} and B^-_{ab} alone.[2] This becomes plausible if we note that these three functions are linear combinations of $(c_1 f_{ab} + c_2 h_{a\delta b})$, $f_{\Delta a \Delta b}$ and $(c_4 h_{\delta a b} + c_5 h_{\delta a \delta b} + c_6 h^t_{\delta a \delta b})$ and that for evolution in μ_1 only the polarization of the first parton is relevant but not the polarization of the second parton. The linear combinations $Q^\pm_{ab}$ may be regarded as generalizations of the distributions $Q_\pm = \frac{1}{2}(q + \bar{q}) \pm \delta q$ introduced in [105], where it was shown that the Soffer bound for the quark transversity distribution δq is stable under leading-order evolution to higher scales.

---

[2]The combination $B^+_{ab} = (Q^+_{ab} + Q^-_{ab})/2$ is not independent and just used as an abbreviation.

4.5.4   Evolution of the linear combinations

We now show that the distributions $Q_{ab}^{\pm}$ and $B_{ab}^{\pm}$ remain positive semi-definite under leading-order evolution to higher scales. This implies the positivity of the spin density matrices and thereby the validity of the bounds derived in section 4.4.

The evolution equations for the distributions $Q_{ab}^{\pm}$ are

$$
\frac{\partial}{\partial \tau_1} \begin{pmatrix} Q_{qb}^+ \\ Q_{qb}^- \end{pmatrix} = \begin{pmatrix} \delta P_{qq}^+ & \delta P_{qq}^- \\ \delta P_{qq}^- & \delta P_{qq}^+ \end{pmatrix} \otimes_1 \begin{pmatrix} Q_{qb}^+ \\ Q_{qb}^- \end{pmatrix} + \begin{pmatrix} P_{qg}^+ & P_{qg}^- \\ P_{qg}^+ & P_{qg}^- \end{pmatrix} \otimes_1 \begin{pmatrix} B_{gb}^+ \\ B_{gb}^- \end{pmatrix}
$$
$$
+ \begin{pmatrix} P_{qq}^- & P_{qq}^- \\ P_{qq}^- & P_{qq}^- \end{pmatrix} \otimes_1 \begin{pmatrix} B_{qb}^+ \\ B_{qb}^- \end{pmatrix} \tag{4.41}
$$

if the first parton is a quarks and

$$
\frac{\partial}{\partial \tau_1} \begin{pmatrix} Q_{gb}^+ \\ Q_{gb}^- \end{pmatrix} = \begin{pmatrix} \delta P_{gg}^+ & \delta P_{gg}^- \\ \delta P_{gg}^- & \delta P_{gg}^+ \end{pmatrix} \otimes_1 \begin{pmatrix} Q_{gb}^+ \\ Q_{gb}^- \end{pmatrix} + \sum_{a=q,\bar{q}} \begin{pmatrix} P_{ga}^+ & P_{ga}^- \\ P_{ga}^+ & P_{ga}^- \end{pmatrix} \otimes_1 \begin{pmatrix} B_{ab}^+ \\ B_{ab}^- \end{pmatrix}
$$
$$
+ \begin{pmatrix} P_{gg}^- & P_{gg}^- \\ P_{gg}^- & P_{gg}^- \end{pmatrix} \otimes_1 \begin{pmatrix} B_{gb}^+ \\ B_{gb}^- \end{pmatrix} \tag{4.42}
$$

if the first parton is a gluon. The evolution equations for $B_{ab}^{\pm}$ read

$$
\frac{\partial}{\partial \tau_1} \begin{pmatrix} B_{qb}^+ \\ B_{qb}^- \end{pmatrix} = \begin{pmatrix} P_{qq}^+ & P_{qq}^- \\ P_{qq}^- & P_{qq}^+ \end{pmatrix} \otimes_1 \begin{pmatrix} B_{qb}^+ \\ B_{qb}^- \end{pmatrix} + \begin{pmatrix} P_{qg}^+ & P_{qg}^- \\ P_{qg}^- & P_{qg}^+ \end{pmatrix} \otimes_1 \begin{pmatrix} B_{gb}^+ \\ B_{gb}^- \end{pmatrix} \tag{4.43}
$$

for a quark and

$$
\frac{\partial}{\partial \tau_1} \begin{pmatrix} B_{gb}^+ \\ B_{gb}^- \end{pmatrix} = \begin{pmatrix} P_{gg}^+ & P_{gg}^- \\ P_{gg}^- & P_{gg}^+ \end{pmatrix} \otimes_1 \begin{pmatrix} B_{gb}^+ \\ B_{gb}^- \end{pmatrix} + \sum_{a=q,\bar{q}} \begin{pmatrix} P_{ga}^+ & P_{ga}^- \\ P_{ga}^- & P_{ga}^+ \end{pmatrix} \otimes_1 \begin{pmatrix} B_{ab}^+ \\ B_{ab}^- \end{pmatrix} \tag{4.44}
$$

for a gluon. The evolution equations have the same form for antiquarks, i.e. (4.41) and (4.43) remain valid if we replace $q \to \bar{q}$ everywhere (except in the label b for the second parton, which always remains fixed when we consider evolution in μ_1).

The splitting functions appearing in the above equations are defined as

$$
P_{ab}^{\pm} = \frac{1}{2} \left(P_{ab} \pm P_{\Delta a \Delta b} \right), \qquad\qquad \delta P_{ab}^{\pm} = \frac{1}{2} \left(P_{\Delta a \Delta b} \pm P_{\delta a \delta b} \right) \tag{4.45}
$$

for all parton indices a and b. We remark that the kernels P_{ab}^+ (P_{ab}^-) correspond to the case where the parton helicity is conserved (flipped). The only splitting functions that receive contributions from virtual graphs and hence contain a plus-prescription or an

explicit δ-function are

$$P_{qq}^+ = \frac{C_F}{2}\left[\frac{2(1+z^2)}{(1-z)_+} + 3\delta(1-z)\right],$$

$$\delta P_{qq}^+ = \frac{C_F}{2}\left[\frac{(1+z)^2}{(1-z)_+} + 3\delta(1-z)\right],$$

$$P_{gg}^+ = 2N_c\left[\frac{z}{(1-z)_+} + \frac{(1-z)(1+z)^2}{2z}\right] + \frac{\beta_0}{2}\delta(1-z),$$

$$\delta P_{gg}^+ = 2N_c\left[\frac{z}{(1-z)_+} + 1 - z\right] + \frac{\beta_0}{2}\delta(1-z) \tag{4.46}$$

with $N_c = 3$, $C_F = 4/3$ and

$$\beta_0 = \frac{11}{3}N_c - \frac{2}{3}n_f, \tag{4.47}$$

where n_f is the number of active quark flavors. They are all positive for $0 < z < 1$ but have negative contributions at $z = 1$ that arise from the plus-prescription, whose form is recalled in (C.3). In appendix C we show explicitly that the virtual contribution to the evolution cannot change the sign of the distributions, which has previously been argued to be the case based on the probabilistic interpretation of leading-order evolution and its relation to the Boltzmann equation [102, 103, 105]. The reason for this property is that the virtual contribution to the evolution of a function is proportional to the function itself. We can then conclude that the diagonal terms in the evolution equations (4.41) to (4.44) preserve positivity. The off-diagonal kernels

$$P_{qq}^- = 0, \qquad\qquad P_{gg}^- = N_c(1-z)^3/z,$$

$$\delta P_{qq}^- = C_F(1-z)/2, \qquad\qquad \delta P_{gg}^- = 2N_c(1-z) \tag{4.48}$$

and

$$P_{qg}^+ = z^2/2, \qquad\qquad P_{gq}^+ = C_F/z,$$

$$P_{qg}^- = (1-z)^2/2, \qquad\qquad P_{gq}^- = C_F(1-z)^2/z. \tag{4.49}$$

are all positive or zero for $0 < z < 1$ and regular at $z = 1$. Therefore they only reinforce positivity. In summary, if we have positive semi-definite initial conditions for all functions $Q_{ab}^\pm$ and $B_{ab}^\pm$ at some scale, then evolution to higher scales preserves this property. Thus the spin-density matrices stay positive semidefinite and the positivity bounds remain stable under leading-order evolution. A more explicit derivation is given in appendix C.

4.6 Summary

We have derived spin density matrices for double parton distributions of quarks, anti-quarks and gluons. These matrices reveal the full polarization structure of two partons

in an unpolarized proton and show the correspondence between the different polarized double parton distributions and parton helicities. The probabilistic interpretation of the double parton distribution for an arbitrary polarization state of the two partons sets upper limits on the size of the spin correlations. The positivity bounds can be useful for modeling the otherwise poorly constrained double parton distributions. They can further be used to derive upper limits on polarization effects in double hard scattering processes, such as the ones found in chapter 3 for the double Drell-Yan process. We have shown that the bounds are stable under leading order evolution to higher scales.

In the next chapter, we make use of these bounds in order to build starting distributions for numerical studies on the evolution of the linearly polarized gluons and transversely polarized quarks.

Chapter 5

Modeling and evolution

5.1 Introduction

In this chapter we turn our attention towards the numerical effects of the double DGLAP evolution. Due to the lack of information on the double parton distributions, our starting conditions for the evolution builds on products of single-parton distributions - with specific modifications to suit the investigation at hand. Since the evolution we consider consists of individual evolution of the two partons, the effect will in general be to wash out correlations between them. Our investigations aim at quantifying this statement in a couple of selected situations.

To this end, we make use of a double parton evolution code written by J. Gaunt and J. Stirling [77], modified for our purposes. After a discussion of the code, the modifications made and the tests performed, we make use of the setup in three different numerical studies. In section 5.3 we explore the evolution of a Gaussian ansatz for the transverse dependence of the DPDs, inspired by data on generalized parton distributions [109–112]. Thereafter, in section 5.4 we study the distribution of two linearly polarized gluons and investigate how evolution affects the relative importance of gluons with linear polarization compared to unpolarized gluons. We contrast our findings with results on the evolution of transversely polarized quarks. The evolution of transversely polarized quarks in single-parton distributions has been studied in context of the Soffer bound in [113]. Finally, we study the difference in integration limits between the evolution equations for single and double parton distributions in section 5.5, with a focus on the extent to which evolution propagates the effects of this difference down towards lower x_i values.

After these numerical investigations we study, in section 5.6, the correlations between longitudinal momentum fractions and transverse structure of the double parton distributions in a simple model of the proton and discuss their consequence for the transverse-momentum spectrum of double Drell-Yan production. We end the chapter with a summary of our findings.

5.2 Evolution code

Originally the evolution code was constructed to solve the evolution equations of [74, 75] in order to produce a set of unpolarized double parton distributions [77, 114]. We have modified the code such that the single feed term, discussed in section 2.4.1, has been removed and such that it handles the evolution of polarized distributions.

The double DGLAP equations are solved directly in x-space, on a grid in x_1, x_2 and $t = \ln \mu^2$. The x_i grid points are evenly spaced in $\log \frac{x_i}{1-x_i}$, with an equal number of points in both directions. The grids are bound from above by conservation of momentum $x_1 + x_2 \leq 1$ and from below by the choice of $x_{\min} = 10^{-6}$. The grid points are evenly spaced in t, ranging from t_0 to t_{max} for which we make different choices depending on the investigation. The number of grid points chosen in each of the x_i directions was for our studies between 120 and 240, and 60 grid points in t.

For the solution of the evolution equations a double parton version of the single parton "evolution basis" is used. The "evolution basis" for single-parton distributions is defined by:

$$\Sigma = \sum_i q_i^+ , \qquad\qquad V_i = q_i^- ,$$
$$T_3 = u^+ - d^+ , \qquad\qquad T_{15} = u^+ + d^+ + s^+ - 3c^+ ,$$
$$T_8 = u^+ + d^+ - 2s^+ , \qquad\qquad T_{24} = u^+ + d^+ + s^+ + c^+ - 4b^+ ,$$
$$T_{35} = u^+ + d^+ + s^+ + c^+ + b^+ - 5t^+ , \qquad\qquad (5.1)$$

where $q_i^\pm = q_i \pm \bar{q}_i$. This basis makes the single parton evolution particularly simple, since the only mixing is between the singlet (Σ) and the gluon, while the different vector (V) and tensor (T) combinations evolve separately. For the up and down quarks, V_i corresponds to the valence contributions u_v and d_v, while the sea contribution u_s (d_s) equals $u - u_v$ ($d - d_v$). The evolution code makes use of the double evolution basis where the basis (5.1) is made for both partons. As an example, the DPD of two valence up quarks can be written in terms of up quark and anti-up quark distributions as

$$F_{u_v u_v} = F_{(u-\bar{u})(u-\bar{u})} = F_{uu} - F_{u\bar{u}} - F_{\bar{u}u} + F_{\bar{u}\bar{u}}. \qquad (5.2)$$

The evolution is performed step wise in t by a fourth-order Runge-Kutta method in a variable flavor number scheme. The default settings have n_f between 3 and 5 with quark masses $m_c = 1.40$ GeV and $m_b = 4.75$ GeV and leading order running of the strong coupling,

$$\alpha_s(t) = \frac{\alpha_s(t')}{1 + \alpha_s(t')b(t - t')} , \qquad\qquad b = \frac{33 - 2n_f}{12\pi} \qquad (5.3)$$

with matching at the mass thresholds to ensure continuity. The accuracy of the program was investigated in [77] with error estimations of less than 1% for $x_i \leq 0.3$ for an evolution from $Q = 1$ GeV to $Q = 100$ GeV. The program was supplemented with an interpolation

	MSTW	GJR	BB
m_c [GeV]	1.40	1.3	1.4
m_b [GeV]	4.75	4.2	4.5
$\alpha_s(Q = 1$ GeV$)$	0.6818	0.4482	0.4810

Table 5.1: Strong coupling constant and quark masses in the evolution program for the three different choices of leading order single-parton distributions.

routine, reading in values from the grid files as well as interpolating between the grid points. For further details see [77].

The evolution code was modified as to remove the single feed terms from the evolution equations, for reasons given in section 2.4.1. In addition, since the original code was only concerned with unpolarized evolution, we implemented the leading-order polarized splitting kernels, of appendix B, for the different polarizations of quarks, antiquarks and gluons. In addition, we made some smaller changes to the distribution of grid points stored in the output grid files and changed the interpolation routines such that they could handle polarized distributions - in particular the presence of zero crossings and negative distributions.

Due to the lack of knowledge even of unpolarized double parton distributions, our investigations will start from a base of a product of two leading order single-parton distributions. For most studies we use the leading order MSTW2008 distributions [115], but we make use also of the leading order GJR distributions [116] and of the leading order BB distributions [117], the latter describing polarized partons in a polarized proton. The set of mass parameters and coupling constants was generically changed for the different runs to match the values of the parton distributions used, as summarized in table 5.1. The default settings for the code are those of the MSTW distributions.

5.2.1   Controls and checks

In order to control that our changes were implemented correctly and to get to know the limitations of the code we performed extensive tests. This was done by evolving products of single-parton distributions and comparing them to the product of the original distributions at different scales. For example, starting from a product of MSTW distributions at $\mu_0 = 1$ GeV, evolving the product to a larger scale μ_1, we compared the result to a product of MSTW distribution at the higher scale μ_1. This can be done since the solution to the evolution of the product of two single-parton distributions is a product of the two distributions, up to effects due to the integration limits which we discuss in section 5.5. When estimating the accuracy of the code we therefore exclude the region where these effects are large. The unpolarized DPD evolution was checked by comparing to a product of MSTW distributions, while the polarized evolution was tested by comparing to a product of BB parton distributions for polarized single-parton distributions. For comparison, the BB distributions were evolved with QCDNUM [118], since the BB default uses a fixed flavor number scheme. In order to test the evolution for

transversely polarized quarks and linearly polarized gluons we implemented the corresponding splitting kernels into QCDNUM, and used this to evolve the BB distributions.

In general good agreement was reached in the comparison, except for extreme corners of parameter space, such as large x_i values, and in very extreme situations. The latter is specifically referring to the evolution of the polarized BB gluon distribution at $x \sim 10^{-5}$ and $Q \sim 2$ where a rapid decrease is followed by a rapid increase. The comparison of the BB distributions, evolved with the double parton evolution, to the product of single-parton distributions evolved with QCDNUM, seemed to give larger differences at first sight. These were however limited to areas around zero crossings where small numerical differences caused large relative errors. Even when these areas are excluded, the more complicated structure of the polarized distributions lead to slightly larger errors than for the unpolarized evolution with MSTW input.

Generically the evolution of quark and antiquark distributions have an accuracy at the level of one percent for the unpolarized evolution, and in some cases decreasing to a few percent for the polarized evolution of the BB distributions. For the gluonic distributions, we find an accuracy of comparable size, i.e. of down to a few percent.

5.3   Transverse structure

We investigate the evolution of the transverse dependence of the unpolarized double parton distributions. In our study, we will start from a product of MSTW distributions, multiplied by a factor retaining the dependence of the DPDs on the transverse vector $\boldsymbol{y}$, including an interplay between longitudinal and transverse degrees of freedom. Insights into the transverse structure of the proton can be obtained from generalized parton distributions. As ansatz for the transverse dependence we take the transverse momentum dependence suggested for generalized parton distributions [109]

$$\exp\{-\boldsymbol{r}^2(\alpha'_{f_i} \ln \frac{1}{x_i} + B_{f_i})\}. \tag{5.4}$$

The parameters α_{f_i} and B_{f_i} take the values

$$\alpha'_{q_v} = 0.9 \text{ GeV}^{-2}\,, \qquad\qquad B_{q_v} = 0.59 \text{ GeV}^{-2} \tag{5.5}$$
$$\alpha'_{q_s} = \alpha'_{\bar{q}} = 0.164 \text{ GeV}^{-2}\,, \qquad\qquad B_{q_s} = B_{\bar{q}} = 2.4 \text{ GeV}^{-2} \tag{5.6}$$
$$\alpha'_{g} = 0.164 \text{ GeV}^{-2}\,, \qquad\qquad B_{g} = 1.2 \text{ GeV}^{-2}, \tag{5.7}$$

at the starting scale of our evolution, $\mu = \sqrt{2}$ GeV. The parameter α'_{f_i} of the term containing the interplay between longitudinal and transverse variables (x_i and $\boldsymbol{r}$) is the same for gluons and sea quarks/antiquarks but has a larger value for the valence contribution. The parameter of the pure transverse piece is taken to have different values for valence quarks, sea quarks and gluons. The values for gluons were chosen to agree with the H1 data on J/ψ production [110], while the valence quark values were obtain by a fit to data in [112]. In contrast to the analysis of generalized parton distributions in [109], we have chosen different values for the sea quarks. These values have been chosen to
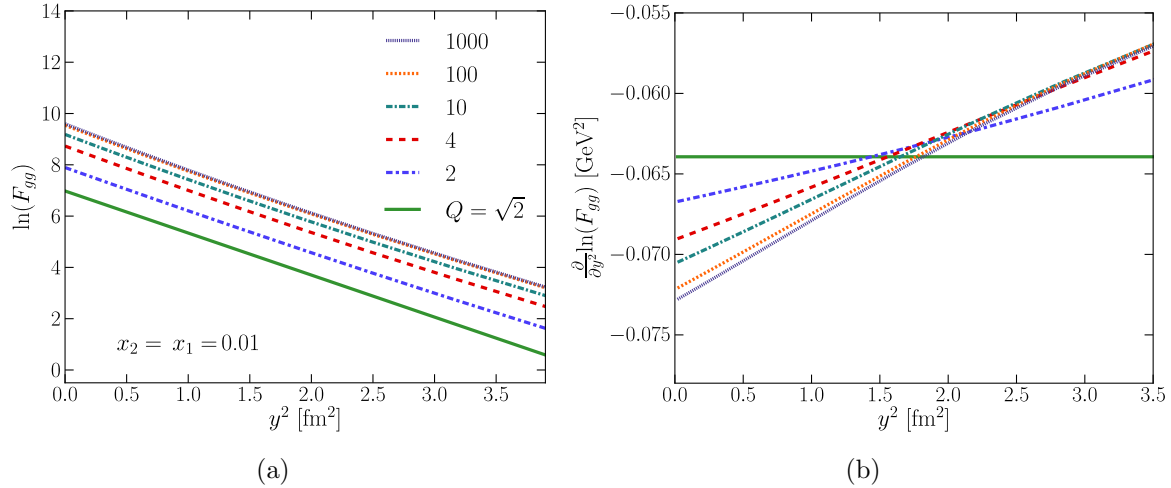
Figure 5.1: Dependence on the magnitude of the transverse vector $\boldsymbol{y}^2$ of the logarithm of the double parton distribution for two unpolarized gluons (a), and the slope of the curves (b). The longitudinal momentum fractions are fixed at $x_1 = x_2 = 0.01$.

agree with another H1 measurement, namely of deeply virtual Compton scattering [111]. The larger value of α' for the valence quarks causes a stronger interplay between the transverse and longitudinal variables. Inspired by (2.63), we used the ansatz (5.4) for each parton in the double parton distribution. After a Fourier transform to configuration space the ansatz for the dependence of the unpolarized DPDs on $\boldsymbol{y}$ equals

$$F(x_1, x_2, \boldsymbol{y}) \sim \frac{1}{4\pi h_{f_1 f_2}} \exp\{\frac{-\boldsymbol{y}^2}{4h_{f_1 f_2}}\}, \tag{5.8}$$

with

$$h_{f_1 f_2} = \alpha'_{f_1} \log \frac{1}{x_1} + \alpha'_{f_2} \log \frac{1}{x_2} + B_{f_1} + B_{f_2}. \tag{5.9}$$

Note that the transverse dependence is no longer separable into contributions from each of the partons.

Apart from causing an overall decrease, an increasing y has two qualitatively different effects. Firstly, changing y causes a change of the relative importance of valence quarks, sea quarks and gluons. The B terms favor larger width for the gluons, while the α' terms lead to a larger width for the valence quark in the small x region. Secondly, increasing y increases the relative importance of regions of small x_i values. In some respects, these two effects are compensatory. For example, in the small x_i region the first effect leads to a relative increase of the valence quarks. On the other hand, the valence quarks are generically more important at large x_i values, and thus the second effect decreases the relative importance of the valence quarks.

With starting point of the Gaussian ansatz (5.8) it is interesting to examine to what extent the evolution preserves Gaussianity. To this end, figure 5.1 (a) shows how evolution changes the natural logarithm of the double parton distribution for two gluons
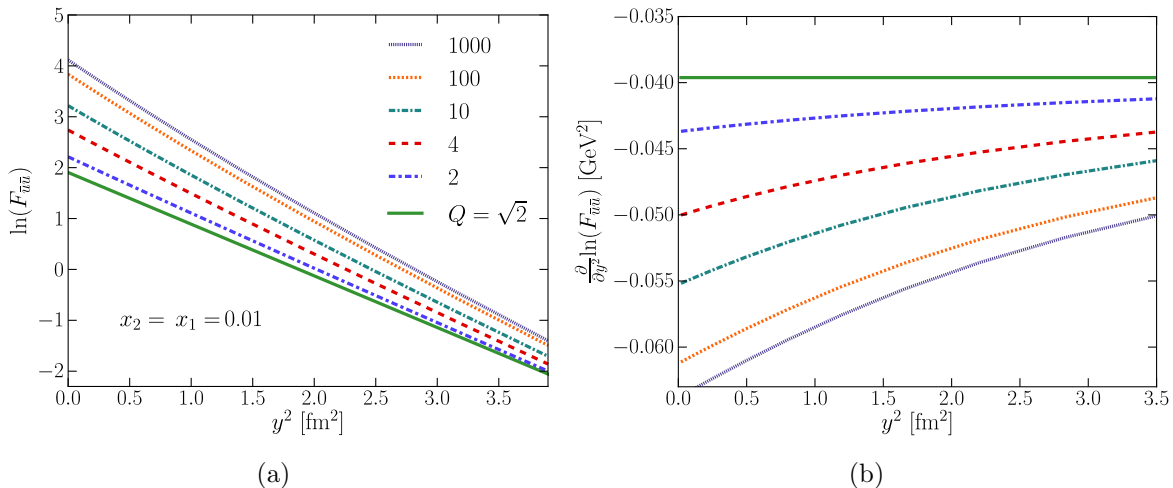
Figure 5.2: Dependence on the magnitude of the transverse vector $\boldsymbol{y}^2$ of the logarithm of the double parton distribution for two unpolarized anti-up quarks (a), and the slope of the curves (b). The longitudinal momentum fractions are fixed at $x_1 = x_2 = 0.01$.

at $x_1 = x_2 = 0.01$. As the scale Q increases, the overall size of the gluonic distribution increases, as does the relative portion of gluons at small y values. Figure 5.1 (b) shows the slope of the curves in figure (a). Note that due to the negative sign of the slopes, a decreasing slope lead to a steeper curve and thus a more narrow width. For the exact Gaussian at the initial scale ($Q = \sqrt{2}$) we get a straight line, and thus a constant slope. The slope decreases somewhat with evolution scale at small y values, while it at first experiences an increase at large y values, but the average slope always remains rather similar.

Turning towards the anti-quark distributions, the corresponding figures 5.2 for the distribution of two anti-up quarks show a qualitative difference. The curves all approach each other for large y values, which is due to the steady decrease of the slope with evolution scale. The gluons, which dominate the evolution, push the slope down towards larger negative values. The decrease of the slope is faster at low y. The gluons are more concentrated at low y and hence have a larger impact on in this area, and in addition the gluons themselves have a steeper slope at low y. For large Q the slope of the double anti-up distribution changes by up to 30% in the probed y range and the distribution of the anti-up quarks is hence steeper at small y values and with a longer tail than a Gaussian fit would allow.

For the distribution with two up quarks in figure 5.3 the situation is similar to that of the antiquarks, but the curves are less steep. Due to the mix of valence and sea quark contributions, not even the initial distribution is an exact Gaussian. Note also that the difference in slope between up quarks and their anti-partners remain approximately constant. The decrease of the slope for the quark and antiquark distributions with Q lead to a decrease in the relative width, the Gaussian falls off steeper - although the increase in the peak value dominates extending the radius of partons inside the proton. Further
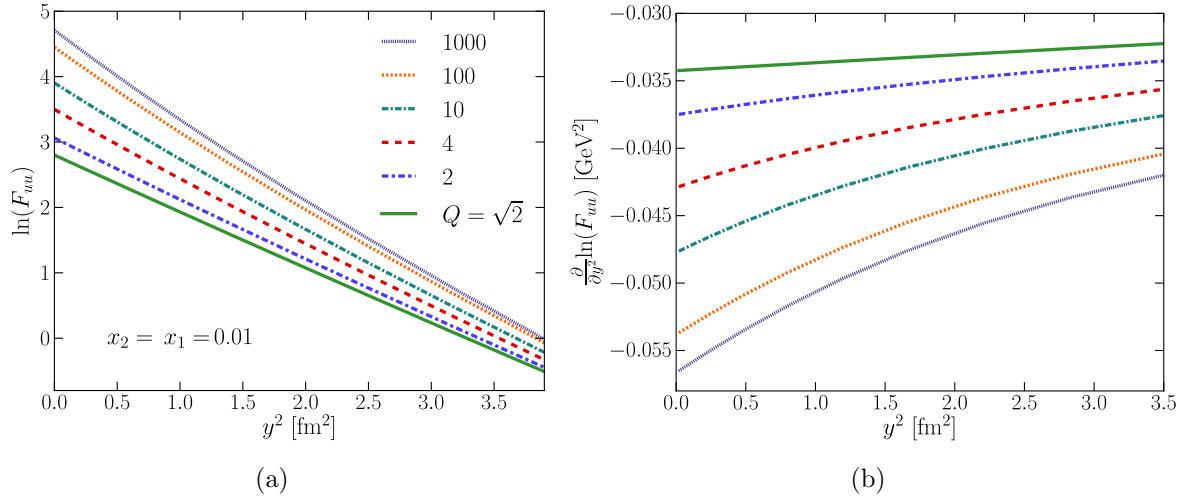
Figure 5.3: Dependence on the magnitude of the transverse vector $\boldsymbol{y}^2$ of the logarithm of the double parton distribution for two unpolarized up quarks (a), and the slope of the curves (b). The longitudinal momentum fractions are fixed at $x_1 = x_2 = 0.01$.

it can be said that the exponent for the gluons experiences a more rapid change at low Q while those for quarks and antiquarks experience a change over a wider Q range.

5.4 Linearly polarized gluons

A question of particular interest for physics at the LHC is how quickly the linear gluon polarization is washed out by evolution. We saw in Chapter 3 that the transversely polarized quarks gave rise to azimuthal asymmetries between the two hard interactions and similar structures are expected for linearly polarized gluons. These effects can at least potentially produce azimuthal asymmetries between the directions of jets and hadrons, which has been a hot topic at the LHC since the observation of the CMS ridge in proton-proton collisions [119].

With this in mind, we investigate the evolution at relatively low Q, comparing linearly polarized to unpolarized gluons. The leading order splitting kernel (appendix B) for unpolarized gluons has a $1/z$ dependence, leading to a very rapid increase of the unpolarized gluon distributions at small x values. For the linearly polarized gluons the kernel is instead proportional to z, leading to a slower evolution of the distribution at small x values. Therefore a large suppression of the linear polarization compared to the unpolarized is to be expected at small x_i. In order to quantify this statements, we again turn to an ansatz for the DPDs of unpolarized gluons in terms of two single-parton distributions. To obtain an ansatz for the linearly polarized distribution we make use of the positivity bounds (4.26) derived in the previous chapter. Saturating the bound we choose the ansatz where the linearly polarized distribution is half of the unpolarized at the starting scale, $Q = 1$ GeV.
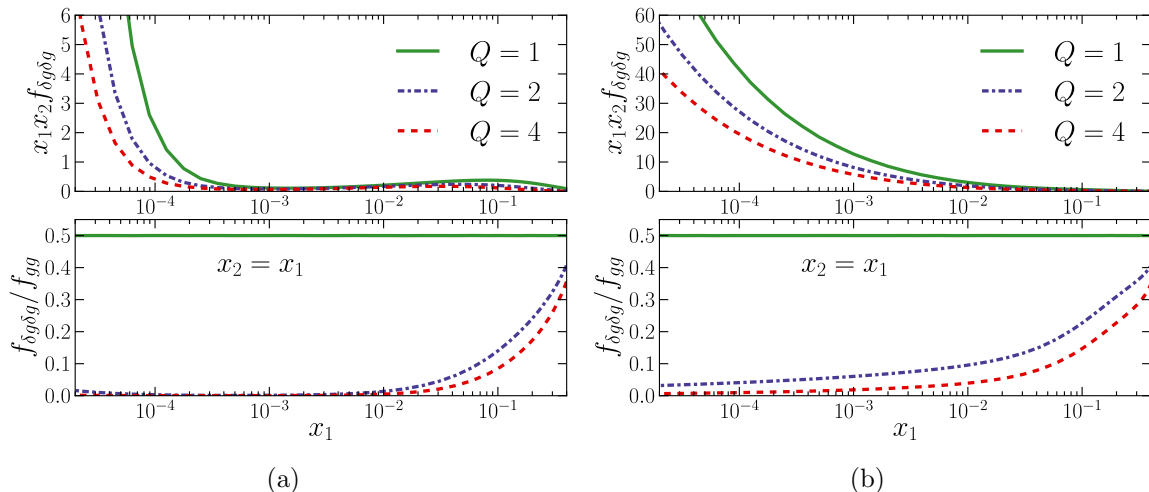
Figure 5.4: Double parton distributions for two linearly polarized gluons (first row) and their ratio to the unpolarized gluons (second row) - starting with a product of single-parton distributions from (a) MSTW (b) GJR. At the initial scale the polarized distribution is taken to be half of the unpolarized.

Starting from a product of the leading order MSTW distributions the effects of the evolution for two linearly polarized gluons, as well as their ratio to the distribution of two unpolarized gluons is shown in the left of figure 5.4. As evident from the ratio plot, the density of linearly polarized gluons quickly becomes negligible compared to the unpolarized density at small x values. Already at $Q = 2$ GeV the ratio is close to zero. If we however, choose a different set of single-parton distributions, namely the GJR distributions, as can be seen in the right hand figure of 5.4 the situation changes. In this case, the linearly polarized gluons stay sizable down to significantly smaller x_i. The GJR distributions here were chosen because of their qualitatively different shape at the input scale. While MSTW has a gluon distribution decreasing with $1/x$ in the range below $x = 0.1$ the GJR distribution shows a steady increase with $1/x$. Part, but not all, of this difference can be traced back to the value of the strong coupling used for the two sets of distributions, table 5.1. We note here that the $\delta g \delta g$ distribution at the input scale is much larger for the GJR input than for the MSTW input, due to the large size difference of the single-parton distributions. A closer look at the single-parton distributions reveal that these differences get smaller as Q increases, and are comparably small already at $Q = 4$. When dividing by the unpolarized contribution in the two cases, we thereby divide by approximately the same function and the linearly polarized gluons play a larger role for the GJR case. Noting that the major effect of the suppression comes from the evolution of the unpolarized distributions, one can estimate the effect of using other single-parton distribution sets by comparing their relative increase with the increase of GJR and MSTW. A comparison of different leading order sets of parton distributions can for instance be found in [120]. Taking for example the CTEQ6l distribution [121], which for intermediate x has a gluon distribution more similar to GJR than to MSTW,

one should expect the linear gluons to be of similar importance as for GJR and thus larger than for MSTW, with the ansatz for the polarized distribution used here.
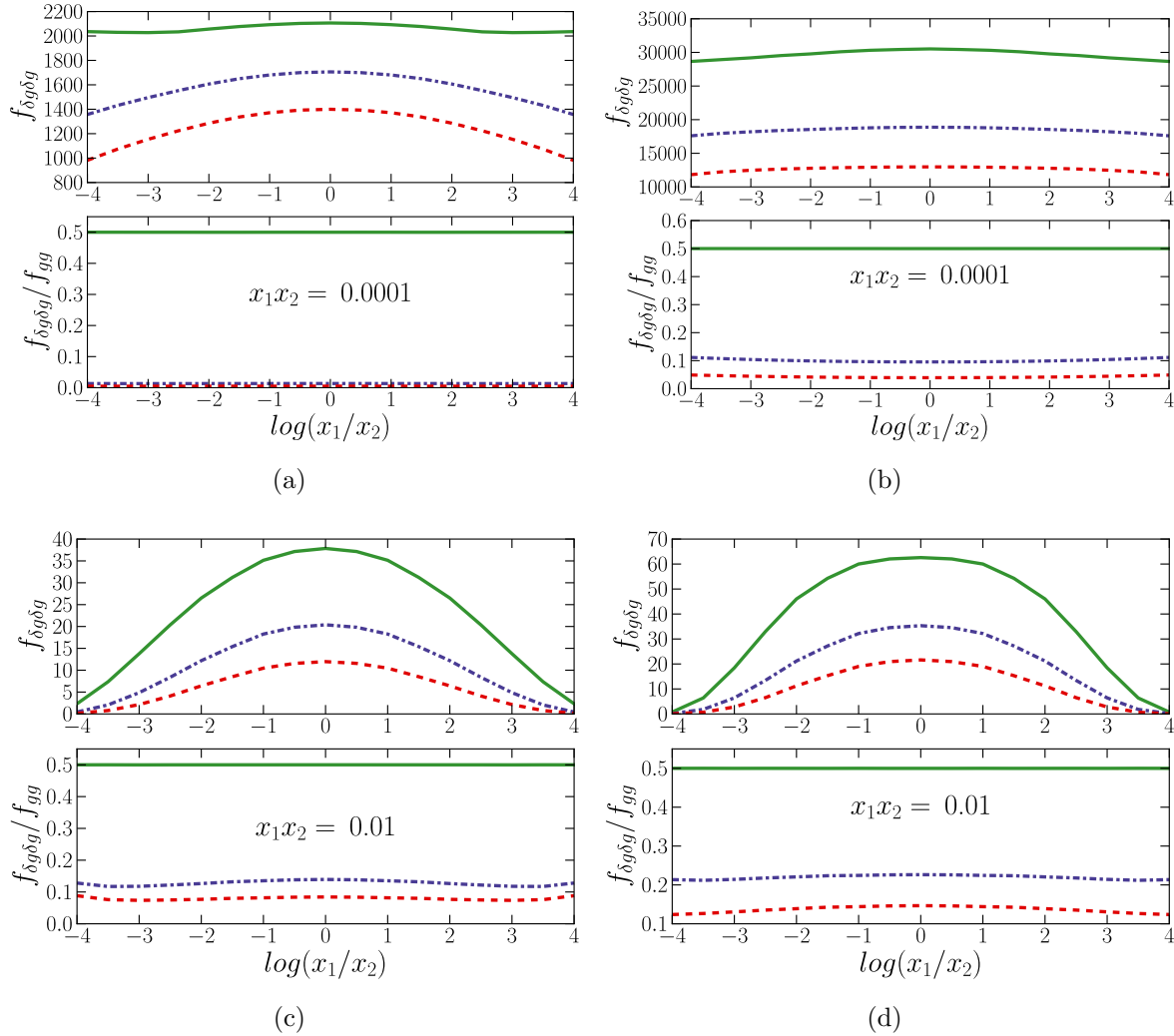
Figure 5.5: Double linearly polarized gluons at different $x_1 x_2$ values starting from a product of MSTW distributions in (a) and (c) and starting from a product of GJR distributions in (b) and (d).

Taking a closer look at the relative size of the linearly polarized distributions, we plot the distributions for both cases, as well as the ratio to the unpolarized distributions against $\log(x_1/x_2)$ at two fixed values of $x_1 x_2 = 0.01, 0.0001$ in figure 5.5. $\log(x_1/x_2)$ is related to the rapidity (2.9),

$$Y_1 - Y_2 = \tfrac{1}{2}\log\frac{q_1^+}{q_1^-} - \tfrac{1}{2}\log\frac{q_2^+}{q_2^-} = \log\frac{x_1}{x_2} + \tfrac{1}{2}\log\frac{q_2^2}{q_1^2} \qquad (5.10)$$

such that it equals the rapidity difference between the two processes when their scales are equal. Fixed $x_1 x_2$ leads to symmetric distributions around zero and a ratio which is
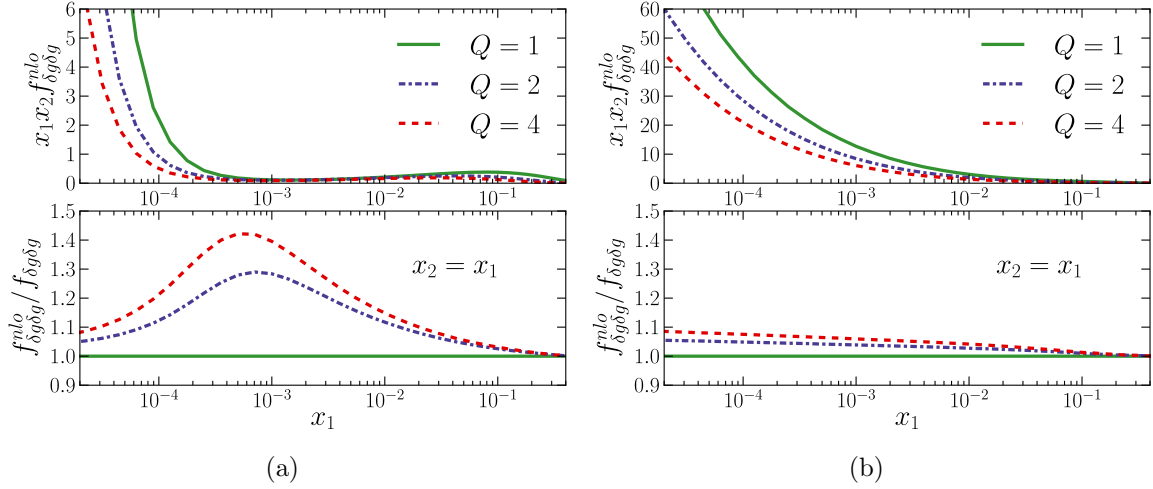
Figure 5.6: Effects of the NLO correction included for the splitting kernels of linearly polarized gluons, starting from MSTW (a) and starting from GJR (b).

independent of $\log x_1/x_2$. In order to get a significant contribution in the MSTW case we need to go to x values of around 0.1, but for the GJR the ratio to unpolarized gluons remains around 10% at $Q = 2$ GeV and 5% at $Q = 4$ GeV.

At next-to-leading order, the splitting kernel for the linearly polarized gluons has a qualitatively different behavior than at leading order. The NLO kernel contains a piece behaving as $1/z$ for small z. In order to investigate the effect of this qualitatively different term we included this part of the NLO splitting kernel in the evolution of the linearly polarized gluons. The $1/z$ part of the NLO correction to the $P_{\delta g \delta g}$ kernel in appendix B is [113]

$$P_{\delta g \delta g}^{nlo}(z) = \left[N_c^2 + (N_c - 2C_F) \, n_f \right] \frac{1 - z^3}{6z}. \tag{5.11}$$

The results for both MSTW and GJR can be found in figure 5.6. Notice that the ratio in this case is taken with respect to the linearly polarized gluons without the NLO part of the evolution kernel. Although there is a clear impact, especially for the MSTW case around $x_1 = x_2 = 10^{-3}$ it does not to any large extent change the overall picture. The relatively large effect for the MSTW in this specific x_i range is due to the small distribution at these x_i values where the migration of partons towards smaller x_i leads to a larger relative effect.

We now take the analogous initial conditions for quarks, i.e. with the distribution of unpolarized quarks as a product of single parton distributions and with the distribution of transversely polarized quarks saturating the positivity bounds, i.e. $f_{\delta q \delta q} = \frac{1}{2} f_{qq}$. Contrasting the evolution of the linearly polarized gluons with the evolution of transversely polarized up-quarks in figure 5.7, we see that the transverse polarization stays a significant contribution down to very small x_i values. Furthermore, in this case the MSTW starting point leads to a larger ratio at very small momentum fractions than starting with the GJR distributions, but the differences between the two starting sets
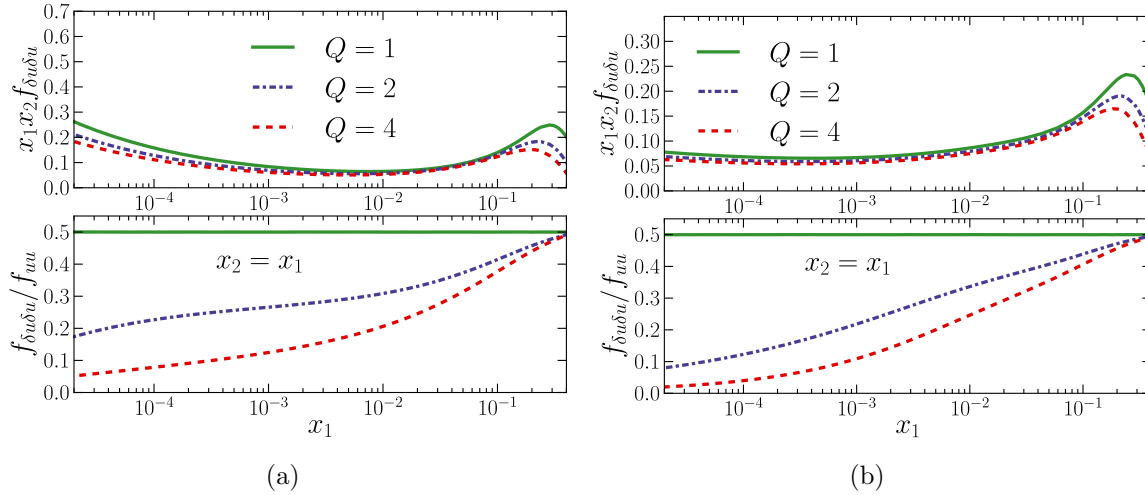
Figure 5.7: Double transversely polarized up quarks at different $x_1 x_2$ values starting from a product of MSTW distributions in (a) and GJR distributions in (b).

are smaller than for the gluons. It would be interesting to extend the current analysis in order to examine to how high Q values the transversely polarized quarks can still play a significant role.

5.5 Integration limits

Perhaps the most immediate difference between single and double parton DGLAP evolution is the difference in integration limits. While the single parton evolution integrates the momentum fractions all the way up to 1, the integration of double parton evolution

$$\int_{x_1}^{1-x_2} \frac{du_1}{u_1},$$

(5.12)

is by momentum conservation bound to $1 - x_2$, for evolution of the parton with momentum fraction x_1. That the integration limit difference has an impact for very large x_i values is obvious, but through evolution the effect can propagate down towards smaller x_i. We investigate this effect by evolving a product of MSTW distributions, either with the correct DPD evolution limits f_{DPI} or extending the integration all the way up to 1, f_{SPI}. We study the ratio of the distributions obtained in the two cases in order to see how far down in x_i values there are still differences. Figure 5.8 shows the minimal $x_1 = x_2$ values for which the ratio between the two cases differs from unity by more than 10%, i.e. where

$$\left| 1 - \frac{f_{\mathrm{DPI}}}{f_{\mathrm{SPI}}} \right| \geq 10\%,$$

(5.13)

as a function of the evaluation scale. For quarks, such as the f_{uu} distribution the differences remain at large x_i values. For gluons, which have a stronger evolution, the
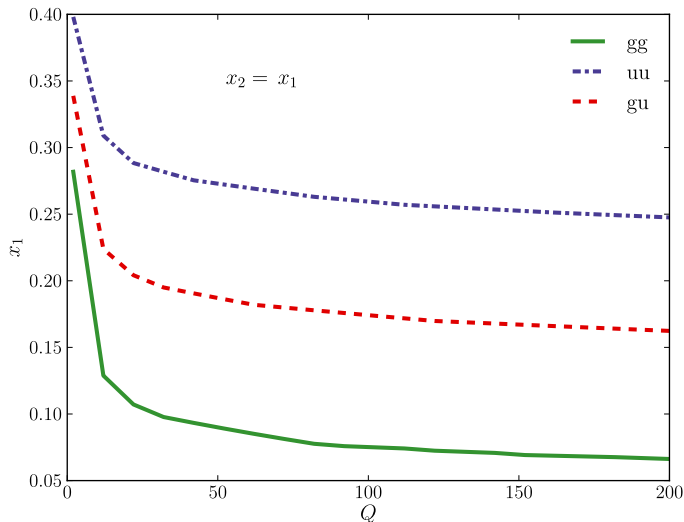
Figure 5.8: The minimum x_1 for which the of the DPDs evolved with single parton evolution limit to DPDs evolved with proper double parton integration limit differing from 1 by more than 10%, as in (5.13).

difference propagates down in x_i and already at moderately large Q we have 10% differences for momentum fractions below 0.1. The distribution with one up-quark and one gluon is, as expected, half way between the *uu* and *gg* curves. It must be pointed out that a 10% effect is not too large, but it shows that even in the case that one starts with the DPD factorized into a product of single parton distributions at a low scale, the factorization does not strictly hold at larger scales.

5.6   Three-quark model

So far in this chapter our investigations have dealt with the collinear double parton distributions. We now turn towards the transverse momentum dependent DPDs, where unpolarized partons can have correlations affecting the dependence of DPDs on the transverse variables $\boldsymbol{y}$, $\boldsymbol{z}_1$ and $\boldsymbol{z}_2$, the interplay between these variables and the longitudinal momentum fractions. There are indeed reasons to expect such correlations, see e.g. [27] and section 2.6 of [44], but not much is currently known about them.

In the present section we take a brief look at this issue by using a simple model in which the proton is described by a three-quark wave function. This is clearly too simple to describe the physics of small momentum fractions most relevant at the LHC, although it may actually be used for modeling quark DPDs at momentum fractions in the valence region. We proceed with this model in the spirit of an exploratory study.

Our model ansatz for the three-quark light-cone wave function of the proton is

$$\Psi(x_i, \boldsymbol{b}_i - \boldsymbol{b}) = \Phi(x_i) \exp\left[-\frac{1}{4a^2} \sum_{i=1}^{3} x_i(\boldsymbol{b}_i - \boldsymbol{b})^2\right], \tag{5.14}$$

where a is parameter of dimension length, $\boldsymbol{b} = x_1\boldsymbol{b}_1 + x_2\boldsymbol{b}_2 + x_3\boldsymbol{b}_3$ is the transverse position of the proton, and $x_1 + x_2 + x_3 = 1$. The corresponding wave function depending on transverse momenta is a Gaussian with exponent $-a^2 \sum_i \boldsymbol{k}_i^2/x_i$, which was long ago proposed in [122] and is often used for the phenomenology of valence dominated quantities, see e.g. [123]. The relation between the light-cone wave functions in transverse momentum and transverse position representation can be found in [100]. We do not specify the longitudinal part $\Phi(x_i)$ of the wave function nor its spin-flavor dependence here, since the focus of our study is on the transverse variables.

From the light-cone wave function (5.14) one can compute the contribution of the three-quark Fock state to the DPD of two quarks in the proton, in full analogy to the well-known case of single parton distributions (discussed e.g. in [100]). Up to a factor depending only on the longitudinal momentum fractions x_i, the double parton distribution is given by

$$F(x_i, \boldsymbol{z}_i, \boldsymbol{y}) \propto \exp\left[-\frac{1}{8a^2}\left\{x_1(1-x_1)\boldsymbol{z}_1^2 - 2x_1x_2\boldsymbol{z}_1\boldsymbol{z}_2 + x_2(1-x_2)\boldsymbol{z}_2^2 + \frac{4x_1x_2}{x_1+x_2}\boldsymbol{y}^2\right\}\right]$$
$$\times \int d^2\boldsymbol{b} \exp\left[-\frac{1}{2a^2}\frac{x_1+x_2}{1-x_1-x_2}\left(\boldsymbol{b}+\frac{x_1}{x_1+x_2}\boldsymbol{y}\right)^2\right], \tag{5.15}$$

where $\boldsymbol{b}$ is the transverse position of the proton, averaged over the scattering amplitude and its conjugate as specified in [44]. The second line in (5.15) just gives an x_i dependent factor after integration over $\boldsymbol{b}$.

5.6.1 Cross section effects

Inserting (5.15) into the cross section formula (2.33) for the double Drell-Yan process and performing the integrals over all transverse positions, one obtains a cross section for double hard scattering that depends on the transverse boson momenta as

$$\exp\left\{-a^2\left[\boldsymbol{q}_1^2\, C_{11}(x_i, \bar{x}_i) + 2\boldsymbol{q}_1\boldsymbol{q}_2\, C_{12}(x_i, \bar{x}_i) + \boldsymbol{q}_2^2\, C_{22}(x_i, \bar{x}_i)\right]\right\} \tag{5.16}$$

with dimensionless functions C_{ij} of the momentum fractions x_1, x_2 and $\bar{x}_1, \bar{x}_2$, which are somewhat lengthy and will not be given here. The expression in square brackets is positive definite, so that the transverse momentum dependence has a Gaussian falloff at large transverse momenta. The coefficient C_{12} describing the correlation between $\boldsymbol{q}_1$ and $\boldsymbol{q}_2$ is positive as well, so that one finds a preference for the two vector bosons to have opposite transverse momenta. We see that even with the simple wave function ansatz (5.14) the dependence of the cross section on the transverse momenta of the gauge bosons is not independent of their longitudinal momenta.

Taking the ansatz in (2.61) with the DPD expressed as a convolution of two single parton distributions and evaluating the single parton distributions for the light-cone wave function (5.14) one obtains

$$
\begin{aligned}
F(x_i, \boldsymbol{z}_i, \boldsymbol{y}) \propto \int d^2\boldsymbol{b} \, \exp&\left[-\frac{1}{8a^2}\frac{x_2}{1-x_2}\left\{(1-x_2)^2\boldsymbol{z}_2^2 + (2\boldsymbol{b}+x_1\boldsymbol{z}_1)^2\right\}\right] \\
\times \exp&\left[-\frac{1}{8a^2}\frac{x_1}{1-x_1}\left\{(1-x_1)^2\boldsymbol{z}_1^2 + (2\boldsymbol{b}+2\boldsymbol{y}-x_2\boldsymbol{z}_2)^2\right\}\right] \\
\propto \exp&\left[-\frac{1}{8a^2}\left\{x_1(1-x_1)\boldsymbol{z}_1^2 + x_2(1-x_2)\boldsymbol{z}_2^2 \right.\right. \\
&\left.\left. + \frac{x_1 x_2}{x_1(1-x_2)+(1-x_1)x_2}\Big(2\boldsymbol{y}-x_1\boldsymbol{z}_1-x_2\boldsymbol{z}_2\Big)^2\right\}\right] \quad (5.17)
\end{aligned}
$$

for the transverse dependence of the double parton distribution. This is visibly different from the result (5.15) of the direct calculation. Although the ansatz (2.61) involves the convolution of two single parton distributions, thus suggesting that the two partons are distributed independently, it induces correlations between transverse and longitudinal variables in $F(x_i, \boldsymbol{z}_i, \boldsymbol{y})$.

Inserting the form (5.17) into the cross section formula one obtains again a Gaussian behavior as in (5.16), but with different coefficients C_{ij}. In particular, the sign of C_{12} is then equal to the sign of $(x_1 - \bar{x}_1)(x_2 - \bar{x}_2)$, so that depending on the longitudinal momentum fractions the transverse boson momenta tend to be in the same hemisphere or in opposite ones. This difference in qualitative behavior shows that the ansatz (2.61) must be used with great care when one is interested in correlation effects.

Setting $\boldsymbol{z}_1 = \boldsymbol{z}_2 = \boldsymbol{0}$ in (5.15) and (5.17) gives collinear DPDs with a Gaussian dependence on $\boldsymbol{y}$. The Gaussian width depends on x_1 and x_2 and differs in the two cases,

$$
\begin{aligned}
F(x_i, \boldsymbol{y})\Big|_{(5.15)} &\propto \exp\left[-\frac{1}{2a^2}\frac{x_1 x_2}{x_1+x_2}\boldsymbol{y}^2\right], \\
F(x_i, \boldsymbol{y})\Big|_{(5.17)} &\propto \exp\left[-\frac{1}{2a^2}\frac{x_1 x_2}{x_1+x_2-2x_1 x_2}\boldsymbol{y}^2\right]. \quad (5.18)
\end{aligned}
$$

We see that, within our model, the ansatz (2.61) does not reproduce the interplay between $\boldsymbol{y}$ and the momentum fractions. It does, however, provide a valid approximation unless x_1 and x_2 are both rather large.

5.7   Summary

With a Gaussian ansatz for the transverse distance dependence of the input double parton distributions, including an interplay with the longitudinal momentum fractions, we find that evolution induces a departure from the Gaussian shape. The most sizable deviations are for the distributions of sea quarks/antiquarks but the effect is visible also for gluons.

The difference between the Gaussian dependence of the different distributions decreases with evolution, but sizable differences remain even at high scales. The slow convergence indicates a violation of universality of the transverse dependence of the double parton distributions, often used in phenomenological studies.

Our study of the linearly polarized gluons shows that they are heavily suppressed in processes at large or medium Q, but that they can still be significant at low scales. Their relative size in our investigation depends strongly on the set of input single parton distributions. With a MSTW input the large coupling and small size of the gluon distribution at the starting scale leads to a quick suppression at all but the largest x values, while a GJR input gives a significantly larger density of linearly polarized gluons. We find that the ratios between distributions of transversely polarized quarks/antiquarks and their unpolarized counterparts only slowly decrease with evolution scale. These distributions can have a significant size compared to their unpolarized counterparts up to high scales, and it would be interesting to extend this study with evolution up to larger Q values.

We demonstrate that the difference in integration limits between the single and double parton evolution equations has an impact on the evolved distributions. The impact propagates down to lower x_i values when increasing the evolution scale, in particular for double parton distributions involving gluons. Although the effects are rather small, they demonstrate that even starting from factorized ansatz, as a product of single parton distribution, evolution will strictly speaking break the factorization at larger scales.

In addition to the numerical results we find correlations between the transverse distribution and longitudinal momentum fractions of the partons in a simple model with a three-quark wave function. Within this model we also find that the often used ansatz to represent double parton distributions as convolutions of single parton distributions is inadequate to describe details of the kinematic dependence in double parton scattering.

Chapter 6

Conclusions and outlook

Double parton scattering in high energy proton-proton collisions can give sizable contributions to the production of high multiplicity final states in parts of phase space. A systematic treatment of double parton scattering within perturbative QCD is under development, but many aspects are still missing. The complications arising when treating two separate hard interactions lead to a substantial gap between theory and experiment. The present thesis aims at filling parts of this gap and bring the theory closer to definite experimental predictions.

The double Drell-Yan process is one of the simplest double parton scattering processes. We have calculated the leading-order cross section in the case where the transverse momenta of the bosons are small (using transverse-momentum dependent factorization) and the case where these momenta are integrated over (using collinear factorization). Our calculation can serve as a prototype for the calculation of more complicated cross sections. The result demonstrates the impact of the correlations between the polarizations of quarks and antiquarks inside an unpolarized proton on the rate and distribution of the produced leptons. In the cross section differential in transverse boson momenta, transversely polarized quarks lead to azimuthal asymmetries in the decay products. Part of the asymmetries remain when the cross section is integrated over the transverse boson momenta. Having two separate hard interactions in double parton scattering does therefore not imply that the final state particles produced in the two interactions are independent of each other.

Given that the correlations occur between the directions of decay products in the two hard interactions of the Double Drell-Yan process, one would expect similar features in other processes with larger cross sections, such as double dijet production and the production of two jets in association with a vector boson. The dependence of the cross section on the angles between produced particles implies a dependence on their invariant mass, which is an important variable in searches for new physics. Estimations of the size of these effects would therefore be of importance. The size of the spin correlations, and thereby the degree to which the decay products are correlated, depends on unknown double parton distributions.

In order to obtain some information on the possible size of the polarization effects, we derived positivity bounds on the double parton distributions following from their

probability interpretation. In order to acquire the bounds, we constructed spin density matrices, revealing the full polarization structure of two partons in an unpolarized proton. We showed that the positivity bounds are stable under leading order double DGLAP evolution. The bounds constrain the size of the double parton distributions of polarized partons and therefore the size of spin induced correlations between the hard interactions in double parton scattering. They can further be used to aid in the construction of double parton distributions.

We made direct use of the positivity bounds in a numerical study on the evolution of the double parton distribution for two linearly polarized gluons inside an unpolarized proton. With an ansatz building on single parton distributions which saturates the positivity bounds, we showed that the double DGLAP evolution rapidly suppresses the linearly polarized gluons, such that they are negligible in processes at medium and large scales. At low scales, the relative importance of the linear polarization depends strongly on the ansatz for the double parton distribution of unpolarized gluons. The lack of knowledge of even the single-parton distributions for gluons at low scales prevents us from drawing reliable conclusions. The ratio of the distribution for transversely polarized quarks to the unpolarized counterpart is much less affected by evolution. The transversely polarized quarks can thus stay significant up to larger scales, but a dedicated study would be necessary to determine up to what scale they can have an impact.

The leading topic through most of this thesis has been correlations between the polarization of two partons in an unpolarized proton. We did however also investigate other types of correlations. Our Drell-Yan cross section calculation included color and flavor interference. The color interference is suppressed at high scales by a Sudakov factor, and is therefore likely to be small in the production of Z and W bosons. Flavor interference can in principle be sizable, affecting the magnitude of the double Drell-Yan cross section but does not lead to the changes in distributions induced by the correlations between polarizations. In a simple model of the proton with a three-quark wave function we found correlations between longitudinal momentum fractions and the transverse distribution. Within this model, the approximation of the double parton distributions as a convolution of single-parton distributions was inadequate to describe the details of the kinematic dependence of the double Drell-Yan process.

Using a Gaussian ansatz for the transverse distance dependence of the double parton distributions, we showed that the homogeneous double DGLAP evolution cause deviations from the Gaussian shape. In particular the sea-quarks/antiquarks at larger scales showed a steeper central slope and a longer tail than a Gaussian fit would allow. The convergence with evolution of the transverse dependence for the different parton species was found to be slow, and sizable differences remained at large scales. This indicates a breakdown of the assumption of a universal $\boldsymbol{y}$ dependence necessary for splitting the double parton cross section into single parton cross sections, frequently used in phenomenological studies. We demonstrated that even when starting from double parton distributions as a product of single parton distributions at a low scale, homogeneous evolution leads to a slight breaking of the factorization at larger scales.

Several of these studies indicate that the approximations necessary for a simple de-

scription of double parton scattering in terms of cross sections for single parton scattering and σ_{eff} does not hold true. Even so, this simple description still provides the most practical connection between theory and experiment.

There are many interesting open questions in double parton scattering. We have addressed some of these in the thesis, and identified places where further studies would be useful. Other open questions we briefly mentioned in the overview of double parton scattering, whilst still others we did not touch upon. It would be interesting to further develop the study of the linearly polarized gluons at low Q and investigate if they can lead to features similar to the CMS ridge. The numerical study of the double DGLAP evolution should and will be further pursued, by studying distributions with other polarization types and extending the investigation of transversely polarized quarks up to higher scales. The interesting issues of factorization in double parton scattering and the separation from single parton scattering need to be further investigated. In addition, further studies of models for the double parton distributions would be of interest, as would further investigations of double and multiparton scattering in Monte Carlo generators. Making closer connections between the Monte-Carlo generators and the theory of multiparton scattering could both help in modeling multiparton interactions and provide a method by with which the theoretical description could be brought closer to experimental results.

The content of this thesis takes steps within the systematic QCD treatment of double parton scattering towards making experimental predictions, but there remains more to be done. There are still important steps to take, issues to resolve and measurements to make in order to bridge the gap and create a close connection between theory and experiment.

Appendix A

Coupling factors

In this appendix we list the coupling factors K and K' appearing in the double Drell-Yan cross section. Further relations between these factors are given in section 3.3.

A.1 Charged vector bosons

For W^+ production one has

$$K_{q_i \bar{q}_j} = \frac{\alpha^2}{4N_c} \frac{|V_{q_i q_j}|^2}{(2\sin\theta_w)^4} \frac{Q_i^2}{(Q_i^2 - m_W^2)^2 + m_W^2 \Gamma_W^2}, \qquad (e_{q_i} - e_{q_j} = 1), \qquad (\text{A.1})$$

and for W^- production

$$K_{q_i \bar{q}_j} = \frac{\alpha^2}{4N_c} \frac{|V_{q_j q_i}|^2}{(2\sin\theta_w)^4} \frac{Q_i^2}{(Q_i^2 - m_W^2)^2 + m_W^2 \Gamma_W^2}, \qquad (e_{q_i} - e_{q_j} = -1). \qquad (\text{A.2})$$

Here $N_c = 3$ is the number of colors, $V_{q_i q_j}$ a CKM matrix element, θ_w the weak mixing angle, α the electromagnetic fine structure constant, and e_{q_i} the charge of quark q_i in units of the positron charge.

A.2 Neutral vector bosons

For a lepton pair $\ell^+ \ell^-$ produced via a γ^*, Z or their interference, one has coupling factors

$$K_{q_i \bar{q}_j} = \frac{\alpha^2}{4N_c} \left\{ \frac{e_{q_i} e_{q_j}}{Q_i^2} - A(Q_i) \, g_\ell^V (e_{q_i} g_{q_j}^V + e_{q_j} g_{q_i}^V) - i B(Q_i) \, g_\ell^V (e_{q_i} g_{q_j}^V - e_{q_j} g_{q_i}^V) \right.$$
$$\left. + C(Q_i) \left[(g_\ell^V)^2 + (g_\ell^A)^2 \right] (g_{q_i}^V g_{q_j}^V + g_{q_j}^A g_{q_i}^A) \right\},$$

$$K'_{q_i \bar{q}_j} = \frac{\alpha^2}{4N_c} \left\{ -A(Q_i) \, g_\ell^A (e_{q_i} g_{q_j}^A + e_{q_j} g_{q_i}^A) - i B(Q_i) \, g_\ell^A (e_{q_i} g_{q_j}^A - e_{q_j} g_{q_i}^A) \right.$$

$$+ C(Q_i)\, 2g_\ell^V g_\ell^A (g_{q_i}^V g_{q_j}^A + g_{q_j}^V g_{q_i}^A) \Big\} ,$$

$$K_{q_i \Delta \bar{q}_j} = \frac{\alpha^2}{4N_c} \Big\{ -A(Q_i)\, g_\ell^V (e_{q_i} g_{q_j}^A + e_{q_j} g_{q_i}^A) - iB(Q_i)\, g_\ell^V (e_{q_i} g_{q_j}^A - e_{q_j} g_{q_i}^A)$$

$$+ C(Q_i) \left[(g_\ell^V)^2 + (g_\ell^A)^2 \right] (g_{q_i}^V g_{q_j}^A + g_{q_j}^V g_{q_i}^A) \Big\} ,$$

$$K'_{q_i \Delta \bar{q}_j} = \frac{\alpha^2}{4N_c} \Big\{ -A(Q_i)\, g_\ell^A (e_{q_i} g_{q_j}^V + e_{q_j} g_{q_i}^V) - iB(Q_i)\, g_\ell^A (e_{q_i} g_{q_j}^V - e_{q_j} g_{q_i}^V)$$

$$+ C(Q_i)\, 2g_\ell^V g_\ell^A (g_{q_i}^V g_{q_j}^V + g_{q_j}^A g_{q_i}^A) \Big\} \tag{A.3}$$

and

$$K_{\delta q_i \delta \bar{q}_j} = \frac{\alpha^2}{4N_c} \Big\{ \frac{e_{q_i} e_{q_j}}{Q_i^2} - A(Q_i)\, g_\ell^V (e_{q_i} g_{q_j}^V + e_{q_j} g_{q_i}^V) - iB(Q_i)\, g_\ell^V (e_{q_i} g_{q_j}^V - e_{q_j} g_{q_i}^V)$$

$$+ C(Q_i) \left[(g_\ell^V)^2 + (g_\ell^A)^2 \right] (g_{q_i}^V g_{q_j}^V - g_{q_j}^A g_{q_i}^A) \Big\} ,$$

$$K'_{\delta q_i \delta \bar{q}_j} = \frac{\alpha^2}{4N_c} \Big\{ -B(Q_i)\, g_\ell^V (e_{q_i} g_{q_j}^A + e_{q_j} g_{q_i}^A) + iA(Q_i)\, g_\ell^V (e_{q_i} g_{q_j}^A - e_{q_j} g_{q_i}^A)$$

$$- iC(Q_i) \left[(g_\ell^V)^2 + (g_\ell^A)^2 \right] (g_{q_i}^V g_{q_j}^A - g_{q_j}^V g_{q_i}^A) \Big\} . \tag{A.4}$$

Here we have used the conventional vector and axial fermion couplings to the Z boson,

$$g_f^V = I_f^3 - 2e_f \sin^2 \theta_w , \qquad\qquad g_f^A = I_f^3 , \tag{A.5}$$

where I_f^3 is the third component of the weak isospin of the left handed fermion f and e_f its charge in units of positron charge. Since we do not consider Z decays to neutrinos, ℓ is always a negatively charged lepton. We have furthermore used the abbreviations

$$A(Q_i) = \frac{1}{\sin^2 2\theta_w} \frac{Q_i^2 - m_Z^2}{(Q_i^2 - m_Z^2)^2 + m_Z^2 \Gamma_Z^2} , \quad B(Q_i) = \frac{1}{\sin^2 2\theta_w} \frac{m_Z \Gamma_Z}{(Q_i^2 - m_Z^2)^2 + m_Z^2 \Gamma_Z^2} ,$$

$$C(Q_i) = \frac{1}{\sin^4 2\theta_w} \frac{Q_i^2}{(Q_i^2 - m_Z^2)^2 + m_Z^2 \Gamma_Z^2} . \tag{A.6}$$

For the usual hard-scattering cross sections one has equal flavors $q_i = q_j$ in the above coupling factors and finds that their imaginary parts are zero. This is not the case for the coupling factors describing flavor interference, where $q_i \neq q_j$.

Appendix B

Evolution equations and splitting functions

For completeness we give here the leading-order evolution equations for the first parton in the double parton distributions. When the first parton is a quark, we have

$$
\frac{\partial f_{qb}}{\partial \tau_1} = P_{qq} \otimes_1 f_{qb} + P_{qg} \otimes_1 f_{gb} ,
$$

$$
\frac{\partial f_{q\delta b}}{\partial \tau_1} = P_{qq} \otimes_1 f_{q\delta b} + P_{qg} \otimes_1 f_{g\delta b} ,
$$

$$
\frac{\partial f_{\Delta q \Delta b}}{\partial \tau_1} = P_{\Delta q \Delta q} \otimes_1 f_{\Delta q \Delta b} + P_{\Delta q \Delta g} \otimes_1 f_{\Delta g \Delta b} ,
$$

$$
\frac{\partial f_{\delta q b}}{\partial \tau_1} = P_{\delta q \delta q} \otimes_1 f_{\delta q b} , \qquad \frac{\partial f_{\delta q \delta b}}{\partial \tau_1} = P_{\delta q \delta q} \otimes_1 f_{\delta q \delta b} , \qquad \frac{\partial f^t_{\delta q \delta b}}{\partial \tau_1} = P_{\delta q \delta q} \otimes_1 f^t_{\delta q \delta b} \qquad \text{(B.1)}
$$

for $b = q, \bar{q}, g$. The arguments of the distributions are as in (4.27) and (2.65). Analogous equations hold if the first parton is an antiquark. For gluons we have

$$
\frac{\partial f_{gb}}{\partial \tau_1} = P_{gg} \otimes_1 f_{gb} + \sum_{a=q,\bar{q}} P_{ga} \otimes_1 f_{ab} ,
$$

$$
\frac{\partial f_{g\delta b}}{\partial \tau_1} = P_{gg} \otimes_1 f_{g\delta b} + \sum_{a=q,\bar{q}} P_{ga} \otimes_1 f_{a\delta b} ,
$$

$$
\frac{\partial f_{\Delta g \Delta b}}{\partial \tau_1} = P_{\Delta g \Delta g} \otimes_1 f_{\Delta g \Delta b} + \sum_{a=q,\bar{q}} P_{\Delta g \Delta a} \otimes_1 f_{\Delta a \Delta b} ,
$$

$$
\frac{\partial f_{\delta g b}}{\partial \tau_1} = P_{\delta g \delta g} \otimes_1 f_{\delta g b} , \qquad \frac{\partial f_{\delta g \delta b}}{\partial \tau_1} = P_{\delta g \delta g} \otimes_1 f_{\delta g \delta b} , \qquad \frac{\partial f^t_{\delta g \delta b}}{\partial \tau_1} = P_{\delta g \delta g} \otimes_1 f^t_{\delta g \delta b} . \qquad \text{(B.2)}
$$

The leading-order splitting functions have been derived in [66, 124]. They are given by

$$
P_{qq}(z) = C_F \left[\frac{1 + z^2}{(1 - z)_+} + \frac{3}{2} \delta(1 - z) \right] ,
$$

$$P_{\Delta q \Delta q}(z) = P_{qq}(z) \,,$$

$$P_{\delta q \delta q}(z) = P_{qq}(z) - C_F(1 - z) \tag{B.3}$$

for quark-quark transitions and by

$$P_{gg}(z) = 2N_c \left[\frac{z}{(1 - z)_+} + \frac{(1 - z)(1 + z^2)}{z} \right] + \frac{\beta_0}{2} \delta(1 - z) \,,$$

$$P_{\Delta g \Delta g}(z) = P_{gg}(z) - 2N_c \frac{(1 - z)^3}{z} \,,$$

$$P_{\delta g \delta g}(z) = P_{gg}(z) - 2N_c \frac{(1 - z)(1 + z^2)}{z} \tag{B.4}$$

for gluons. The splitting functions that mix quarks and gluons read

$$P_{qg} = \frac{z^2 + (1 - z)^2}{2} \,, \qquad\qquad P_{gq} = C_F \frac{1 + (1 - z)^2}{z} \,,$$

$$P_{\Delta q \Delta g} = \frac{z^2 - (1 - z)^2}{2} \,, \qquad\qquad P_{\Delta g \Delta q} = C_F \frac{1 - (1 - z)^2}{z} \,. \tag{B.5}$$

As already mentioned below (2.65), the splitting functions are identical for quarks and antiquarks, i.e. (B.3) and (B.5) remain valid if we replace $q \to \bar{q}$. At leading order in α_s there are no direct transitions between quarks and antiquarks.

Appendix C

Elements of a stability proof

In this appendix we show in more detail that the evolution equations in section 4.5.4 preserve positivity, taking particular care of the negative terms in the splitting functions that arise from virtual graphs and are implicit in the plus-prescription. We first consider the evolution of a single distribution and then extend the argument to the full coupled system of evolution equations.

We examine a function evolving as

$$\frac{\partial}{\partial \tau} f(x, \tau) = \int_x^v \frac{du}{u} P\left(\frac{x}{u}\right) f(u, \tau) \tag{C.1}$$

with $0 < x < v \leq 1$ and separate the splitting function as

$$P(z) = \frac{P_s(z)}{(1-z)_+} + P_r(z) + P_\delta \, \delta(1-z) \,, \tag{C.2}$$

where $P_s(z)$ and $P_r(z)$ are positive semi-definite for $0 < z < 1$ and regular at $z = 1$. The constant P_δ may be positive, negative or zero. The plus-prescription is defined as usual by

$$[s(z)]_+ = s(z) - \delta(1-z) \int_0^1 dz' \, s(z') \,, \tag{C.3}$$

where it is understood that the non-integrable singularity in the last term cancels when (C.3) is integrated over with a smooth test function. The plus-prescription part of the convolution in (C.1) can be written as

$$\int_x^v \frac{du}{u} \frac{P_s(x/u)}{(1-x/u)_+} f(u, \tau)$$
$$= \int_{x+\epsilon}^v du \, \frac{P_s(x/u)}{u-x} f(u, \tau) + \int_0^{x-\epsilon} du \, \frac{P_s(1)}{u-x} f(x, \tau) + \mathcal{O}(\epsilon) \,, \tag{C.4}$$

where for the error estimate we have assumed that $f(u, \tau)$ is differentiable at $u = x$. Defining

$$g_\epsilon(x, \tau; f) = \int_{x+\epsilon}^{v} du \left[\frac{P_s(x/u)}{u - x} + \frac{P_r(x/u)}{u} \right] f(u, \tau),$$

$$h_\epsilon(x) = -P_\delta + P_s(1) \int_0^{x-\epsilon} \frac{du}{x - u} \tag{C.5}$$

we can approximate the evolution of f by

$$\frac{\partial}{\partial \tau} f(x, \tau) = g_\epsilon(x, \tau; f) - h_\epsilon(x) f(x, \tau) \tag{C.6}$$

with an error that becomes arbitrarily small for $\epsilon \to 0$. In a more formal proof, one would replace f with f_ϵ in (C.6) and show that $\lim_{\epsilon \to 0} f_\epsilon$ is a solution of (C.1) . We now rewrite (C.6) as

$$\frac{\partial}{\partial \tau} \left[e^{\tau h_\epsilon(x)} f(x, \tau) \right] = e^{\tau h_\epsilon(x)} g_\epsilon(x, \tau; f) . \tag{C.7}$$

Since g_ϵ is the convolution of $f(x, \tau)$ with a positive semi-definite integral kernel, the r.h.s. of this equation is positive semi-definite as long as $f(x, \tau)$ is. With initial conditions $f(x, \tau_0) \geq 0$ for all x at a starting scale τ_0, the function $e^{\tau h_\epsilon(x)} f(x, \tau)$ can therefore not decrease as τ increases, so that $f(x, \tau)$ stays positive semi-definite for all $\tau > \tau_0$. We note that the sign of $h_\epsilon(x)$ and thus of the constant P_δ is irrelevant for this argument.

We now consider the coupled system of evolution equations given by (4.41) to (4.44). Using a vector notation $f^i(x, \tau)$ for the $8n_f + 4$ functions $Q_{ab}^+, Q_{ab}^-, B_{ab}^+, B_{ab}^-$ with $a = q, \bar{q}, g$ (and b fixed), we can cast their evolution into the form

$$\frac{\partial}{\partial \tau} f^i(x, \tau) = g_\epsilon^i(x, \tau; f^i) - h_\epsilon^i(x) f^i(x, \tau) + \sum_{i \neq j} \int_x^v \frac{du}{u} P^{ij}\left(\frac{x}{u}\right) f^j(u, \tau) \tag{C.8}$$

with $i = 1, \ldots, 8n_f + 4$. Here g_ϵ^i and h_ϵ^i are defined as in (C.5) with regular and positive semi-definite functions $P_s^i(z)$ and $P_r^i(z)$. The mixing kernels $P^{ij}(z)$ in (C.8) are regular and positive semi-definite as well. Rewriting the evolution as

$$\frac{\partial}{\partial \tau} \left[e^{\tau h_\epsilon(x)} f^i(x, \tau) \right] = e^{\tau h_\epsilon(x)} \left[g_\epsilon^i(x, \tau; f^i) + \sum_{i \neq j} \int_x^v \frac{du}{u} P^{ij}\left(\frac{x}{u}\right) f^j(u, \tau) \right] \tag{C.9}$$

we see that if one has initial conditions $f^j(x, \tau_0) \geq 0$ for all j then all functions $f^j(x, \tau)$ remain positive semi-definite for $\tau > \tau_0$.

Bibliography

[1] A. Del Fabbro and D. Treleani, *A Double parton scattering background to Higgs boson production at the LHC*, Phys.Rev. **D61** (2000) 077502, [`hep-ph/9911358`].

[2] R. Godbole, S. Gupta, and J. Lindfors, *Double parton scattering contribution to W + jets*, Z.Phys. **C47** (1990) 69–74.

[3] O. J. Eboli, F. Halzen, and J. Mizukoshi, *The associated production of weak bosons and jets by multiple parton interactions*, Phys.Rev. **D57** (1998) 1730–1734, [`hep-ph/9710443`].

[4] E. Cattaruzza, A. Del Fabbro, and D. Treleani, *Fractional momentum correlations in multiple production of W bosons and of $b\bar{b}$ pairs in high energy pp collisions*, Phys.Rev. **D72** (2005) 034022, [`hep-ph/0507052`].

[5] E. Maina, *Multiple parton interactions, top-antitop and W + 4j production at the LHC*, JHEP **0904** (2009) 098, [`arXiv:0904.2682`].

[6] E. Maina, *Multiple parton interactions in Z+4j, W+- W+- + 0/2j and W+ W- + 2j production at the LHC*, JHEP **0909** (2009) 081, [`arXiv:0909.1586`].

[7] E. Maina, *Multiple parton interactions in Z+ jets production at the LHC. A comparison of factorized and non-factorized double parton distribution functions*, JHEP **1101** (2011) 061, [`arXiv:1010.5674`].

[8] A. Kulesza and W. J. Stirling, *Like sign W boson production at the LHC as a probe of double parton scattering*, Phys.Lett. **B475** (2000) 168–175, [`hep-ph/9912232`].

[9] J. R. Gaunt, C.-H. Kom, A. Kulesza, and W. Stirling, *Same-sign W pair production as a probe of double parton scattering at the LHC*, Eur.Phys.J. **C69** (2010) 53–65, [`hep-ph/1003.3953`].

[10] E. L. Berger, C. Jackson, S. Quackenbush, and G. Shaughnessy, *Calculation of W b bbar production via double parton scattering at the LHC*, Phys.Rev. **D84** (2011) 074021, [`arXiv:1107.3150`].

[11] B. Humpert, *Are there multi - quark interactions?*, Phys.Lett. **B131** (1983) 461.

[12] B. Humpert and R. Odorico, *Multiparton scattering and QCD radiation as sources of four jet events*, Phys.Lett. **B154** (1985) 211.

[13] L. Ametller, N. Paver, and D. Treleani, *Possible signature of multiple parton interactions in collider four jet events*, Phys.Lett. **B169** (1986) 289.

[14] M. L. Mangano, *Four jet production at the Tevatron collider*, Z.Phys. **C42** (1989) 331.

[15] M. Drees and T. Han, *Signals for double parton scattering at the Fermilab Tevatron*, Phys.Rev.Lett. **77** (1996) 4142–4145, [`hep-ph/9605430`].

[16] A. Del Fabbro and D. Treleani, *Double parton scatterings in b quark pairs production at the CERN LHC*, Phys.Rev. **D66** (2002) 074012, [`hep-ph/0207311`].

[17] S. Domdey, H.-J. Pirner, and U. A. Wiedemann, *Testing the scale dependence of the scale factor delta(eff) in double dijet production at the LHC*, Eur.Phys.J. **C65** (2010) 153–162, [`arXiv:0906.4335`].

[18] E. L. Berger, C. Jackson, and G. Shaughnessy, *Characteristics and estimates of double parton scattering at the Large Hadron Collider*, Phys.Rev. **D81** (2010) 014014, [`arXiv:0911.5348`].

[19] H. Baer, V. Barger, P. Huang, D. Mickelson, A. Mustafayev, et al., *Same sign diboson signature from supersymmetry models with light higgsinos at the LHC*, `arXiv:1302.5816`.

[20] D. d'Enterria and A. M. Snigirev, *Same-sign WW production in proton-nucleus collisions at the LHC as a signal for double parton scattering*, Phys.Lett. **B718** (2013) 1395–1400, [`arXiv:1211.0197`].

[21] D. d'Enterria and A. M. Snigirev, *Enhanced J/Psi production from double parton scatterings in nucleus-nucleus collisions at the Large Hadron Collider*, `arXiv:1301.5845`.

[22] T. Sjöstrand and M. van Zijl, *Multiple parton-parton interactions in an impact parameter picture*, Phys.Lett. **B188** (1987) 149.

[23] T. Sjöstrand and M. van Zijl, *A multiple interaction model for the event structure in hadron collisions*, Phys.Rev. **D36** (1987) 2019.

[24] J. Butterworth, J. R. Forshaw, and M. Seymour, *Multiparton interactions in photoproduction at HERA*, Z.Phys. **C72** (1996) 637–646, [`hep-ph/9601371`].

[25] T. Sjöstrand and P. Z. Skands, *Multiple interactions and the structure of beam remnants*, JHEP **0403** (2004) 053, [`hep-ph/0402078`].

[26] R. Corke and T. Sjöstrand, *Multiparton interactions and rescattering, JHEP* **1001** (2010) 035, [arXiv:0911.1909].

[27] R. Corke and T. Sjöstrand, *Multiparton interactions with an x-dependent proton size, JHEP* **1105** (2011) 009, [arXiv:1101.5953].

[28] M. Bahr, S. Gieseke, and M. H. Seymour, *Simulation of multiple partonic interactions in Herwig++, JHEP* **0807** (2008) 076, [arXiv:0803.3633].

[29] e. Bartalini, P. and e. Fano, L., *Multiple partonic interactions at the LHC. Proceedings, 1st International Workshop, MPI'08, Perugia, Italy, October 27-31, 2008*, arXiv:1003.4220.

[30] P. Bartalini, E. Berger, B. Blok, G. Calucci, R. Corke, et al., *Multi-parton interactions at the LHC*, arXiv:1111.0469.

[31] **Axial Field Spectrometer Collaboration** Collaboration, T. Akesson et al., *Double parton scattering in p p collisions at S**(1/2) = 63-GeV, Z.Phys.* **C34** (1987) 163.

[32] **UA2 Collaboration** Collaboration, J. Alitti et al., *A Study of multi - jet events at the CERN anti-p p collider and a search for double parton scattering, Phys.Lett.* **B268** (1991) 145–154.

[33] **CDF Collaboration** Collaboration, F. Abe et al., *Study of four jet events and evidence for double parton interactions in $p\bar{p}$ collisions at $\sqrt{s} = 1.8$ TeV, Phys.Rev.* **D47** (1993) 4857–4871.

[34] **CDF Collaboration** Collaboration, F. Abe et al., *Measurement of double parton scattering in $\bar{p}p$ collisions at $\sqrt{s} = 1.8$ TeV, Phys.Rev.Lett.* **79** (1997) 584–589.

[35] **CDF Collaboration** Collaboration, F. Abe et al., *Double parton scattering in $\bar{p}p$ collisions at $\sqrt{s} = 1.8 TeV$, Phys.Rev.* **D56** (1997) 3811–3832.

[36] **D0 Collaboration** Collaboration, V. Abazov et al., *Double parton interactions in photon+3 jet events in p p-bar collisions sqrts=1.96 TeV, Phys.Rev.* **D81** (2010) 052012, [arXiv:0912.5104].

[37] **D0 Collaboration** Collaboration, V. M. Abazov et al., *Azimuthal decorrelations and multiple parton interactions in photon+2 jet and photon+3 jet events in $p\bar{p}$ collisions at $\sqrt{s} = 1.96$ TeV, Phys.Rev.* **D83** (2011) 052008, [arXiv:1101.1509]. Submitted to Phys. Rev. D.

[38] **ATLAS Collaboration** Collaboration, G. Aad et al., *Measurement of hard double-parton interactions in W->lν+ 2 jet events at sqrt(s)=7 TeV with the ATLAS detector, New J.Phys.* **15** (2013) 033038, [arXiv:1301.6872].

[39] **LHCb Collaboration** Collaboration, L. collaboration et al., *Observation of double charm production involving open charm in pp collisions at $\sqrt{s}=7$ TeV*, *JHEP* **1206** (2012) 141, [arXiv:1205.0975].

[40] **CMS collaboration** Collaboration, P. Bartalini and L. Fano, *Multiple parton interactions studies at CMS*, arXiv:1103.6201.

[41] B. Blok, Y. Dokshitzer, L. Frankfurt, and M. Strikman, *The Four jet production at LHC and Tevatron in QCD*, *Phys.Rev.* **D83** (2011) 071501, [arXiv:1009.2714].

[42] B. Blok, Y. Dokshitser, L. Frankfurt, and M. Strikman, *pQCD physics of multiparton interactions*, *Eur.Phys.J.* **C72** (2012) 1963, [arXiv:1106.5533].

[43] M. Diehl and A. Schäfer, *Theoretical considerations on multiparton interactions in QCD*, *Phys.Lett.* **B698** (2011) 389–402, [arXiv:1102.3081].

[44] M. Diehl, D. Ostermeier, and A. Schäfer, *Elements of a theory for multiparton interactions in QCD*, *JHEP* **1203** (2012) 089, [arXiv:1111.0910].

[45] J. Bartels and M. Ryskin, *Recombination within multi-chain contributions in pp scattering*, arXiv:1105.1638.

[46] M. Ryskin and A. Snigirev, *A fresh look at double parton scattering*, *Phys.Rev.* **D83** (2011) 114047, [arXiv:1103.3495].

[47] M. Ryskin and A. Snigirev, *Double parton scattering in double logarithm approximation of perturbative QCD*, *Phys.Rev.* **D86** (2012) 014018, [arXiv:1203.2330].

[48] J. R. Gaunt and W. Stirling, *Double parton scattering singularity in one-loop integrals*, *JHEP* **1106** (2011) 048, [arXiv:1103.1888].

[49] J. R. Gaunt, *Single perturbative splitting diagrams in double parton scattering*, *JHEP* **1301** (2013) 042, [arXiv:1207.0480].

[50] A. V. Manohar and W. J. Waalewijn, *A QCD analysis of double parton scattering: color correlations, interference effects and evolution*, *Phys.Rev.* **D85** (2012) 114009, [arXiv:1202.3794].

[51] A. V. Manohar and W. J. Waalewijn, *What is double parton scattering?*, *Phys.Lett.* **B713** (2012) 196–201, [arXiv:1202.5034].

[52] G. Calucci and D. Treleani, *Mini - jets and the two-body parton correlation*, *Phys.Rev.* **D57** (1998) 503–511, [hep-ph/9707389].

[53] G. Calucci and D. Treleani, *Proton structure in transverse space and the effective cross-section*, *Phys.Rev.* **D60** (1999) 054023, [hep-ph/9902479].

[54] A. Del Fabbro and D. Treleani, *Scale factor in double parton collisions and parton densities in transverse space*, Phys.Rev. **D63** (2001) 057901, [hep-ph/0005273].

[55] C. Flensburg, G. Gustafson, L. Lonnblad, and A. Ster, *Correlations in double parton distributions at small x*, JHEP **1106** (2011) 066, [arXiv:1103.4320].

[56] T. Rogers and M. Strikman, *Multiple hard partonic collisions with correlations in proton-proton scattering*, Phys.Rev. **D81** (2010) 016013, [arXiv:0908.0251].

[57] M. Rinaldi, S. Scopetta, and V. Vento, *Double parton correlations in constituent quark models*, arXiv:1302.6462.

[58] T. Kasemets and M. Diehl, *Angular correlations in the double Drell-Yan process*, JHEP **1301** (2013) 121, [arXiv:1210.5434].

[59] M. Diehl and T. Kasemets, *Positivity bounds on double parton distributions*, arXiv:1303.0842.

[60] D. Binosi and L. Theussl, *JaxoDraw: A Graphical user interface for drawing Feynman diagrams*, Comput.Phys.Commun. **161** (2004) 76–86, [hep-ph/0309015].

[61] J. D. Hunter, *Matplotlib: A 2d graphics environment*, Computing In Science & Engineering **9** (May-Jun, 2007) 90–95.

[62] J. Vermaseren, *New features of FORM*, math-ph/0010025.

[63] I. Wolfram Research, *Mathematica Edition: Version 8.0*. Wolfram Research, Inc., 2010.

[64] R. K. Ellis, W. J. Stirling, and B. Webber, *QCD and collider physics*, Camb.Monogr.Part.Phys.Nucl.Phys.Cosmol. **8** (1996) 1–435.

[65] J. Collins, *Foundations of perturbative QCD*. Cambridge University Press, 2011.

[66] G. Altarelli and G. Parisi, *Asymptotic freedom in parton language*, Nucl.Phys. **B126** (1977) 298.

[67] L. Lipatov, *The parton model and perturbation theory*, Sov.J.Nucl.Phys. **20** (1975) 94–102.

[68] V. Gribov and L. Lipatov, *Deep inelastic e p scattering in perturbation theory*, Sov.J.Nucl.Phys. **15** (1972) 438–450.

[69] Y. L. Dokshitzer, *Calculation of the Structure Functions for Deep Inelastic Scattering and e+ e- Annihilation by Perturbation Theory in Quantum Chromodynamics.*, Sov.Phys.JETP **46** (1977) 641–653.

[70] T. C. Rogers and P. J. Mulders, *No generalized TMD-factorization in hadro-production of high transverse momentum hadrons*, *Phys.Rev.* **D81** (2010) 094006, [`arXiv:1001.2977`].

[71] N. Paver and D. Treleani, *Multi - quark scattering and large p(t) jet production in hadronic collisions*, *Nuovo Cim.* **A70** (1982) 215.

[72] M. Mekhfi, *Multiparton processes: An application to double Drell-Yan*, *Phys.Rev.* **D32** (1985) 2371.

[73] C. Nishi, *Simple derivation of general Fierz-like identities*, *Am.J.Phys.* **73** (2005) 1160–1163, [`hep-ph/0412245`].

[74] R. Kirschner, *Generalized Lipatov-Altarelli-Parisi equations and jet calculus rules*, *Phys.Lett.* **B84** (1979) 266.

[75] V. Shelest, A. Snigirev, and G. Zinovev, *The multiparton distribution equations in QCD*, *Phys.Lett.* **B113** (1982) 325.

[76] A. Snigirev, *Double parton distributions in the leading logarithm approximation of perturbative QCD*, *Phys.Rev.* **D68** (2003) 114012, [`hep-ph/0304172`].

[77] J. R. Gaunt and W. J. Stirling, *Double parton distributions incorporating perturbative QCD evolution and momentum and quark number sum rules*, *JHEP* **1003** (2010) 005, [`arXiv:0910.4347`].

[78] F. A. Ceccopieri, *An update on the evolution of double parton distributions*, *Phys.Lett.* **B697** (2011) 482–487, [`arXiv:1011.6586`].

[79] J. C. Collins and D. E. Soper, *Back-to-back jets in QCD*, *Nucl.Phys.* **B193** (1981) 381.

[80] X.-d. Ji, J.-p. Ma, and F. Yuan, *QCD factorization for semi-inclusive deep-inelastic scattering at low transverse momentum*, *Phys.Rev.* **D71** (2005) 034005, [`hep-ph/0404183`].

[81] J. Collins, T. Rogers, and A. Stasto, *Fully unintegrated parton correlation functions and factorization in lowest-order hard scattering*, *Phys.Rev.* **D77** (2008) 085009, [`arXiv:0708.2833`].

[82] J.-y. Chiu, A. Jain, D. Neill, and I. Z. Rothstein, *The rapidity renormalization group*, *Phys.Rev.Lett.* **108** (2012) 151601, [`arXiv:1104.0881`].

[83] J.-Y. Chiu, A. Jain, D. Neill, and I. Z. Rothstein, *A formalism for the systematic treatment of rapidity logarithms in Quantum Field Theory*, *JHEP* **1205** (2012) 084, [`arXiv:1202.0814`].

[84] J. C. Collins, D. E. Soper, and G. F. Sterman, *Transverse momentum distribution in Drell-Yan pair and W and Z boson production, Nucl.Phys.* **B250** (1985) 199.

[85] M. Mekhfi and X. Artru, *Sudakov suppression of color correlations in multiparton scattering, Phys.Rev.* **D37** (1988) 2618–2622.

[86] H.-M. Chang, A. V. Manohar, and W. J. Waalewijn, *Double parton correlations in the bag model*, `arXiv:1211.3132`.

[87] D. Treleani, *Double parton scattering, diffraction and effective cross section, Phys.Rev.* **D76** (2007) 076006, [`arXiv:0708.2603`].

[88] M. Bähr, M. Myska, M. H. Seymour, and A. Siodmok, *Extracting sigma_effective from the CDF gamma+3jets measurement, JHEP* **1303** (2013) 129, [`arXiv:1302.4325`].

[89] M. Mekhfi, *Correlations in color and spin in multiparton processes, Phys.Rev.* **D32** (1985) 2380.

[90] C. Goebel, F. Halzen, and D. Scott, *Double Drell-Yan annihilations in hadron collisions: novel tests of the constituent picture, Phys.Rev.* **D22** (1980) 2789.

[91] F. Halzen, P. Hoyer, and W. J. Stirling, *Evidence for multiple parton interactions from the observation of multi - muon events in Drell-Yan experiments, Phys.Lett.* **B188** (1987) 375–378.

[92] C. Kom, A. Kulesza, and W. Stirling, *Prospects for observation of double parton scattering with four-muon final states at LHCb, Eur.Phys.J.* **C71** (2011) 1802, [`hep-ph/1109.0309`].

[93] J. C. Collins and D. E. Soper, *Angular distribution of dileptons in high-energy hadron collisions, Phys. Rev.* **D16** (1977) 2219.

[94] D. Boer and W. Vogelsang, *Drell-Yan lepton angular distribution at small transverse momentum, Phys. Rev.* **D74** (2006) 014004, [`hep-ph/0604177`].

[95] S. Arnold, A. Metz, and M. Schlegel, *Dilepton production from polarized hadron hadron collisions, Phys.Rev.* **D79** (2009) 034005, [`arXiv:0809.2262`].

[96] D. Boer, *Investigating the origins of transverse spin asymmetries at RHIC, Phys.Rev.* **D60** (1999) 014012, [`hep-ph/9902255`].

[97] J. Soffer, *Positivity constraints for spin dependent parton distributions, Phys.Rev.Lett.* **74** (1995) 1292–1294, [`hep-ph/9409254`].

[98] A. Bacchetta, M. Boglione, A. Henneman, and P. Mulders, *Bounds on transverse momentum dependent distribution and fragmentation functions, Phys.Rev.Lett.* **85** (2000) 712–715, [`hep-ph/9912490`].

[99] M. Diehl and P. Hägler, *Spin densities in the transverse plane and generalized transversity distributions*, Eur.Phys.J. **C44** (2005) 87–101, [`hep-ph/0504175`].

[100] M. Diehl, *Generalized parton distributions*, Phys.Rept. **388** (2003) 41–277, [`hep-ph/0307382`].

[101] M. Diehl, *Generalized parton distributions with helicity flip*, Eur.Phys.J. **C19** (2001) 485–492, [`hep-ph/0101335`].

[102] L. Durand and W. Putikka, *Probabilistic derivation of parton splitting functions*, Phys.Rev. **D36** (1987) 2840.

[103] J. C. Collins and J.-w. Qiu, *A new derivation of the Altarelli-Parisi equations*, Phys.Rev. **D39** (1989) 1398.

[104] V. Barone, *On the QCD evolution of the transversity distribution*, Phys.Lett. **B409** (1997) 499–502, [`hep-ph/9703343`].

[105] C. Bourrely, J. Soffer, and O. Teryaev, *The Q**2 evolution of Soffer inequality*, Phys.Lett. **B420** (1998) 375–381, [`hep-ph/9710224`].

[106] G. Altarelli, S. Forte, and G. Ridolfi, *On positivity of parton distributions*, Nucl.Phys. **B534** (1998) 277–296, [`hep-ph/9806345`].

[107] W. Vogelsang, *Next-to-leading order evolution of transversity distributions and Soffer's inequality*, Phys.Rev. **D57** (1998) 1886–1894, [`hep-ph/9706511`].

[108] O. Martin, A. Schäfer, M. Stratmann, and W. Vogelsang, *Soffer's inequality and the transversely polarized Drell-Yan process at next-to-leading order*, Phys.Rev. **D57** (1998) 3084–3090, [`hep-ph/9710300`].

[109] M. Diehl and W. Kugler, *Some numerical studies of the evolution of generalized parton distributions*, Phys.Lett. **B660** (2008) 202–211, [`arXiv:0711.2184`].

[110] **H1 Collaboration** Collaboration, A. Aktas et al., *Elastic J/psi production at HERA*, Eur.Phys.J. **C46** (2006) 585–603, [`hep-ex/0510016`].

[111] **H1 Collaboration** Collaboration, F. Aaron et al., *Measurement of deeply virtual Compton scattering and its t-dependence at HERA*, Phys.Lett. **B659** (2008) 796–806, [`arXiv:0709.4114`].

[112] M. Diehl, T. Feldmann, R. Jakob, and P. Kroll, *Generalized parton distributions from nucleon form-factor data*, Eur.Phys.J. **C39** (2005) 1–39, [`hep-ph/0408173`].

[113] W. Vogelsang, *Q**2 evolution of spin dependent parton densities*, Acta Phys.Polon. **B29** (1998) 1189–1200, [`hep-ph/9805295`].

[114] J. Gaunt, *Double parton scattering in proton-proton collisions*. Cambridge University Thesis, 2012.

[115] A. Martin, W. Stirling, R. Thorne, and G. Watt, *Parton distributions for the LHC*, *Eur.Phys.J.* **C63** (2009) 189–285, [`arXiv:0901.0002`].

[116] M. Gluck, P. Jimenez-Delgado, and E. Reya, *Dynamical parton distributions of the nucleon and very small-x physics*, *Eur.Phys.J.* **C53** (2008) 355–366, [`arXiv:0709.0614`].

[117] J. Blümlein and H. Böttcher, *QCD analysis of polarized deep inelastic data and parton distributions*, *Nucl.Phys.* **B636** (2002) 225–263, [`hep-ph/0203155`].

[118] M. Botje, *QCDNUM: Fast QCD evolution and convolution*, *Comput.Phys.Commun.* **182** (2011) 490–532, [`arXiv:1005.1481`].

[119] **CMS Collaboration** Collaboration, V. Khachatryan et al., *Observation of Long-Range Near-Side Angular Correlations in Proton-Proton Collisions at the LHC*, *JHEP* **1009** (2010) 091, [`arXiv:1009.4122`].

[120] T. Kasemets and T. Sjostrand, *A Comparison of new MC-adapted Parton Densities*, *Eur.Phys.J.* **C69** (2010) 19–29, [`arXiv:1007.0897`].

[121] J. Pumplin, D. Stump, J. Huston, H. Lai, P. M. Nadolsky, et al., *New generation of parton distributions with uncertainties from global QCD analysis*, *JHEP* **0207** (2002) 012, [`hep-ph/0201195`].

[122] S. J. Brodsky, T. Huang, and G. Lepage, *The hadronic wave function in Quantum Chromodynamics*, .

[123] M. Diehl, T. Feldmann, R. Jakob, and P. Kroll, *Linking parton distributions to form-factors and Compton scattering*, *Eur.Phys.J.* **C8** (1999) 409–434, [`hep-ph/9811253`].

[124] X. Artru and M. Mekhfi, *Transversely polarized parton densities, their evolution and their measurement*, *Z.Phys.* **C45** (1990) 669.